THE MICROTUBULE ASSOCIATED PROTEIN TAU RENDERS BREAST CANCER CELLS TNF-ALPHA RESISTANT BY INHIBITING TNF-RECEPTOR SIGNALING

By

Shawon Debnath

A doctoral dissertation submitted to the Graduate Faculty in Biochemistry in partial fulfillment with the requirements for the degree of Doctor of Philosophy, Doctoral Program in Biochemistry, The City University of New York.

2013

This manuscript has been read and accepted for the Graduate Faculty in Biochemistry in satisfaction of the dissertation requirement for the degree of Doctor of Philosophy.

Date

Chair of Examining Committee
Dr, Jimmie E. Fata, College of Staten Island

Date

Executive Officer

Dr. Edward J. Kennelly

Dr. Jimmie E. Fata, College of Staten Island

Dr. Alejandra Alonso, College of Staten Island

Dr. Probal Banerjee, College of Staten Island

Dr. Frida Kleiman, Hunter College

Dr. Jill Bargonetti, Hunter College

Supervising Committee

The City University of New York

THE MICROTUBULE ASSOCIATED PROTEIN TAU RENDERS BREAST CANCER CELLS TNFα RESISTANT BY INHIBITING TNF-RECEPTOR SIGNALING.

By Shawon Debnath

Advisor: Dr. Jimmie E. Fata

Abstract:

The pro-inflammatory cytokine Tumor Necrosis Factor-alpha (TNFα) is often found in elevated concentration within the microenvironment of breast tumors. A number of findings have now established that TNFα can exert opposing effects on tumor cells - acting either as an anti-cancer agent or as a promoter of tumor progression. To date, mechanisms underlying these divergent outcomes have not been elucidated. Here, we demonstrate that tau, classically considered as a microtubule-associated protein, plays a key role to determine whether cancer cells respond negatively (apoptosis) or positively (proliferation) to TNFα exposure. Using RNAi knockdown experiments we show that up-regulation of tau protein in breast cancer cells is necessary for the acquisition of resistance to TNFα-mediated cytotoxicity. In contrast, an analysis of generated stable cell lines overexpressing full-length tau indicates that tau can inhibit TNFα-induced caspase activation and NFκB nuclear translocation. Site-directed mutagenesis has revealed that the N-terminal portion of tau, which does not bind to tubulin, is sufficient for this inhibition of TNFα signaling. Finally, mechanistic studies have uncovered that tau inhibits TNF-receptor trimerization and receptor clustering thereby blocking subsequent signaling. Taken together, we conclude that acquisition of TNFα resistance requires a previously undescribed mechanism involving up-regulation of tau, which in turn inhibits receptor trimerization and thus attenuates TNFα downstream signaling in tumor cells.

Acknowledgments:

To Dr. Jimmie E. Fata, thank you for the incredible, relentless advice and support throughout all these years. You are the most humble, honest man with unflinching character I have ever known. I couldn't have asked for a better mentor than you.

To Dr. Alejandra Alonso, it wouldn't have been possible without your help. You are an amazing person with great qualities.

To Edmund Charles Jenkins Jr, you have been always there for me whenever I needed you. You are a true friend and a great human being.

To Sajini Gundry and Stephen Gundry, you were always by my side in both good and bad times.

To Peter Hannon and Samantha A. Ni, you have been brilliant and amazing all this time. I am proud to have you.

To Gustavo Basurto , Diana Ivette Aparacio and Shatarupa Sinha, you brought smile in time of need. I wish you all continued success.

To Chong Sun, you always provided an opportunity to relax and enjoy.

To our current and former lab members, you have helped to build up a great lab environment. I thank you all for the sweet memories that we have shared together.

To Dr. Probal Banerjee and Dr. Krishnaswami Raja, you helped me begin my journey in this country.

To Dr. Fred Naider, I thank you for supporting me in those difficult times.

To the committee members, co-authors and reviewers of this work, your contributions and insightful criticism have strengthened our findings.

Dedication:

I would like to dedicate this work to:

My parents, Basanti Debnath and Bijoy Kishore Debnath; your love, dedication and perseverance have helped me achieve what I have today.

My husband, Mayukh Banik;

You are the strength and love of my life.

My brother, Shantanu Debnath;

You are the most precious gift that I am bestowed with.

My grandmother late Namita Biswas;

I wish you were with me to see your dream come true.

My uncle Jyotish C. Shome, my teacher Debasish Barman, Shovan Chakroborty;

With full faith in me, you have waited long to see me successful.

My professor Dr. Gopal Bhattacharya, Dr. Nirmal K. Sarkar, and Dr. Trilochan Midya;

Your guidance and support has helped to pursue my dreams.

रागद्वेषविमुक्तैस्तु विषयानिन्द्रियैश्चरन् ।
आत्मवश्यैर्विधेयात्मा प्रसादमधिगच्छति ॥ ६४ ॥

Table of Contents

List of Figures:

List of Abbreviations:

μg— Microgram

μm — Micrometer

μM — Micromolar

Bcl-2 — B-cell lymphoma 2

BSA — Bovine Serum Albumin

CHX — Cycloheximide

DAPI — 4',6-diamidino-2-phenylindole

DMEM — Dulbecco's Modified Eagle Medium

DMSO — Dimethyl sulfoxide

ER — Estrogen Receptor

FADD — Fas Associated Death Domain

FCS — Fetal Calf Serum

IC_{50} — Inhibitory Concentration for 50% of a population

MAPK — Mitogen Activated Protein Kinase

mRNA — messenger RNA

MTBD — Microtubule Binding Domain

MTT — (3-(4,5-Dimethylthiazol-2-yl)-2,5-diphenyltetrazolium bromide

NFκB — Nuclear Factor kappa B

PAMAM — Poly amido amine

PBS — Phosphate Buffer Saline

pH3 — phospho histone H3.

SDS-PAGE — Sodium dodecyl sulphate polyacrylamide gel electrophoresis

SEM — Standard error mean

siRNA — small interfering ribonucleic acid

TNFα — Tumor Necrosis Factor alpha

TNFR1 — Tumor Necrosis Factor Receptor type 1

TRADD — TNFR1 Associated Death Domain

Preamble:

The parenchyma of normal breast tissue consists of an epithelial ductal network terminating in epithelial glandular compartments. Ductal epithelial cells provide a conduit for milk production, which occurs in the glandular compartment, while a second cell type, the myoepithelial cells, encapsulate the epithelial cells and aid in milk movement by contraction (Hennighausen and Robinson, 2005). The structure and function of these cells and the tissue in general is dependent on cell polarity, cell-cell contact and attachment with underlying basement membrane (Bissell and Peretson, 2002; O'Brien and Mostov, 2002; Rodriguez and Nelson, 1989). Surrounding the parenchyma is a stromal compartment rich in adipose, immune cells, fibroblasts, blood and lymph vessels and extracellular matrix (Hennighausen and Robinson, 2005). Throughout evolution the primary function of the breast is to produce milk for newborn suckling young.

Unfortunately the female breast is a common site for the development of cancer. In the USA, breast cancer is the second leading cause of cancer death in women with the lifetime risk of developing breast cancer being 1 in 8 (12%). The etiology of most types of breast cancers is unknown. However, several risk factors include age, family history of breast cancer, childbirth at a delayed age, prolonged hormone replacement therapy and genetic mutations such as BRCA1/2 (Carlson et al., 2009). Common lines of treatments for breast cancer include surgery, hormone therapy, chemotherapy and radiation.

A growing body of evidence has indicated that inflammation plays an important role in breast cancer progression (Cole, 2009). For instance, it has been well documented that pro-inflammatory cytokines activate stromal cells such as vascular endothelial cells, tumor-associated macrophages (TAMs) and fibroblasts present in the tumor microenvironment, and in

turn promote tumor growth and metastasis (Coussens and Werb, 2002; Chiang and Massague, 2008; Mantovani et al., 2008). TAMs are the major component of the inflammatory infiltrate that produce several chemokines and cytokines including tumor necrosis factor alpha (TNFα) (Coussens and Werb, 2002). Previous investigations into the role of tumor necrosis factor (TNF) cytokines in mammary cell biology and breast cancer have led to a number of seminal papers in the field (Fata et al., Cell 2001, Jones et al., Nature, 2006 and Schramek et al., Nature 2010). In this thesis, we continue to recognize the importance of these cytokines in cancer by investigating new mechanisms of how breast cancer cells acquire resistance to the cytotoxic effects of TNFα.

TNFα is the key mediator of inflammation and is found in elevated levels within the microenvironment of breast tumors (Balkwill and Mantovani, 2001). TNFα exerts various biological functions and within tumor tissue it has been shown to act both as a cytotoxic agent and as a tumor promoter (Aggarwal et al., 2012). These paradoxical outcomes exerted on tumor tissue by TNFα is believed to be context dependant, however, little is known about the mechanisms that determines these opposite outcomes (Guadagni et al., 2007). In this thesis, we have set up a quest to determine what factor(s) regulate and how breast cancer cells respond to TNFα and subsequent TNFα signaling.

Our hypothesis was that the microtubule associated protein tau could affect TNFα signaling in breast cancer cells. Tau is a neuronal protein, abundantly expressed in the axons of the central nervous system and plays a critical role in axonal development (Morris et al., 2011). At the time of developing this hypothesis there was little evidence to suggest a relationship between tau and TNFα. What we did know was that Tau protein is often ectopically expressed in breast cancer (Bhat and Setaluri, 2007; Rouzier et al., 2005) and it has been shown to promote

metastasis (Matrone et al., 2010). Furthermore, tau expression can be regulated by both estrogen and estrogen receptor (Andre et al., 2007; Frasor et al., 2004; Ikeda et al., 2010) it has clinical importance as a marker determining Paclitaxel sensitivity in breast cancer (Rouzier et al., 2005; Tanaka et al., 2009; Wagner et al., 2005). Our hypothesis was also initiated and developed around the collaborative efforts of the Fata lab (breast cancer) and Alonso lab (tau) both of which have contributed significantly to the development and success of this project.

In conclusion, this thesis focuses on how breast cancer cells acquire resistance to the cytokine TNFα and elucidates tau as a novel mediator of TNFα signaling.

References:

Aggarwal, B. B., et al., 2012. Historical perspectives on tumor necrosis factor and its superfamily: 25 years later, a golden journey. Blood. 119, 651-65.

Andre, F., et al., 2007. Microtubule-associated protein-tau is a bifunctional predictor of endocrine sensitivity and chemotherapy resistance in estrogen receptor-positive breast cancer. Clin Cancer Res. 13, 2061-7.

Balkwill, F., Mantovani, A., 2001. Inflammation and cancer: back to Virchow? Lancet. 357, 539-45.

Bhat, K. M., Setaluri, V., 2007. Microtubule-associated proteins as targets in cancer chemotherapy. Clin Cancer Res. 13, 2849-54.

Bissell, M. J., et al., 2002. The organizing principle: microenvironmental influences in the normal and malignantbreast. Differentiation. 70, 537–546.

Carlson, R. W., et al., 2009. Breast cancer. J Natl Compr Canc Netw. 7, 122-192.

Cole, S. W., 2009. Chronic inflammation and breast cancer recurrence. J Clinical Oncology. 27(21), 3418-19.

Coussens, L. M., Werb, Z., 2002. Inflammation and cancer. Nature. 420, 860-7.

Fata, J. E., et al., 2000. The osteoclast differentiation factor osteoprotegerin-ligand is essential for mammary gland development. Cell. 103 (1). 41-50.

Frasor, J., et al., 2004. Selective estrogen receptor modulators: discrimination of agonistic versus antagonistic activities by gene expression profiling in breast cancer cells. Cancer Res. 64, 1522-33.

Guadagni, F., et al., 2007. Review. TNF/VEGF cross-talk in chronic inflammation-related cancer initiation and progression: an early target in anticancer therapeutic strategy. In Vivo. 21, 147-61.

Henninghausen , L., Robinson , G. W., 2005. Information networks in the mammary gland. Nature. 6, 715-25.

Ikeda, H., et al., 2010. The estrogen receptor influences microtubule-associated protein tau (MAPT) expression and the selective estrogen receptor inhibitor fulvestrant downregulates MAPT and increases the sensitivity to taxane in breast cancer cells. Breast Cancer Res. 12, R43.

Jones, D. H., et al., 2006. Regulation of cancer cell migration and bone metastasis by RANKL. Nature. 440(7084). 692-6.

Matrone, M. A., et al., 2010. Metastatic breast tumors express increased tau, which promotes microtentacle formation and the reattachment of detached breast tumor cells. Oncogene. 29, 3217-27.

Mantovani, A., et al., 2008. Cancer-related inflammation. Nature. 454, 436-44.

O'Brien, L. E., et al.,2002. Building epithelial architecture: insights from three- dimensional culture models. Nature Rev Mol Cell Biol. 3, 531–37.

Rodriguez-Boulan, E., Nelson, W. J., 1989.Morphogenesis of the polarized epithelial cell phenotype. Science. 245, 718–25.

Rouzier, R., et al., 2005. Microtubule-associated protein tau: a marker of paclitaxel sensitivity in breast cancer. Proc Natl Acad Sci U S A. 102, 8315-20.

Schramek, D., et al., 2010. Osteoclast differentiation factor RANKL controls development of proestin-driven mammary cancer. Nature. 468(7320). 98-102.
Tanaka, S., et al., 2009. Tau expression and efficacy of paclitaxel treatment in metastatic breast cancer. Cancer Chemother Pharmacol. 64, 341-6.
Wagner, P., et al., 2005. Microtubule Associated Protein (MAP)-Tau: a novel mediator of paclitaxel sensitivity in vitro and in vivo. Cell Cycle. 4, 1149-52.

Chapter I

Tau renders breast cancer cells TNFα resistant by inhibiting TNF-receptor signaling.

Introduction:

In 1863, Rudolf Virchow hypothesized a connection between the site of chronic inflammation and origin of cancer. Inflammation is now well accepted as an enabling characteristic that contributes to core hallmark features associated with the promotion of tumorigenesis (Hanahan and Weinberg, 2011). Tumors have been characterized as "wounds that fail to repair" (Dvorak, 1986), since, they harbor many of the tissue characteristics found during wound healing. These include, in part, an infiltration of inflammatory cells, acceleration of cell proliferation, and an environment rich in inflammatory cytokines. Over the years, evidence has indicated that inflammation may be the cause of certain cancers (Berasain et al., 2009), while other findings suggest that the inflammatory signaling pathways are generally downstream of oncogenic mutations (Mantovani et al., 2008). In the majority of cases, cancer itself causes and progresses through inflammation. The tumor microenvironment, largely choreographed by inflammatory cells, is thought to augment neoplastic growth through sustained proliferation, survival and migration (Coussens and Werb, 2002). Activated tumor-associated macrophages (TAMs) are a major component of the inflammatory infiltrate of almost all tumors (Mantovani et al., 1992) and they are known to actively produce potent angiogenic growth factors, proteases and cytokines like Tumor Necrosis Factor alpha (TNFα) (Torisu et al., 2000). How tumor cells respond to TNFα and the factors that affect TNFα signaling will be addressed within this thesis.

TNFα signaling

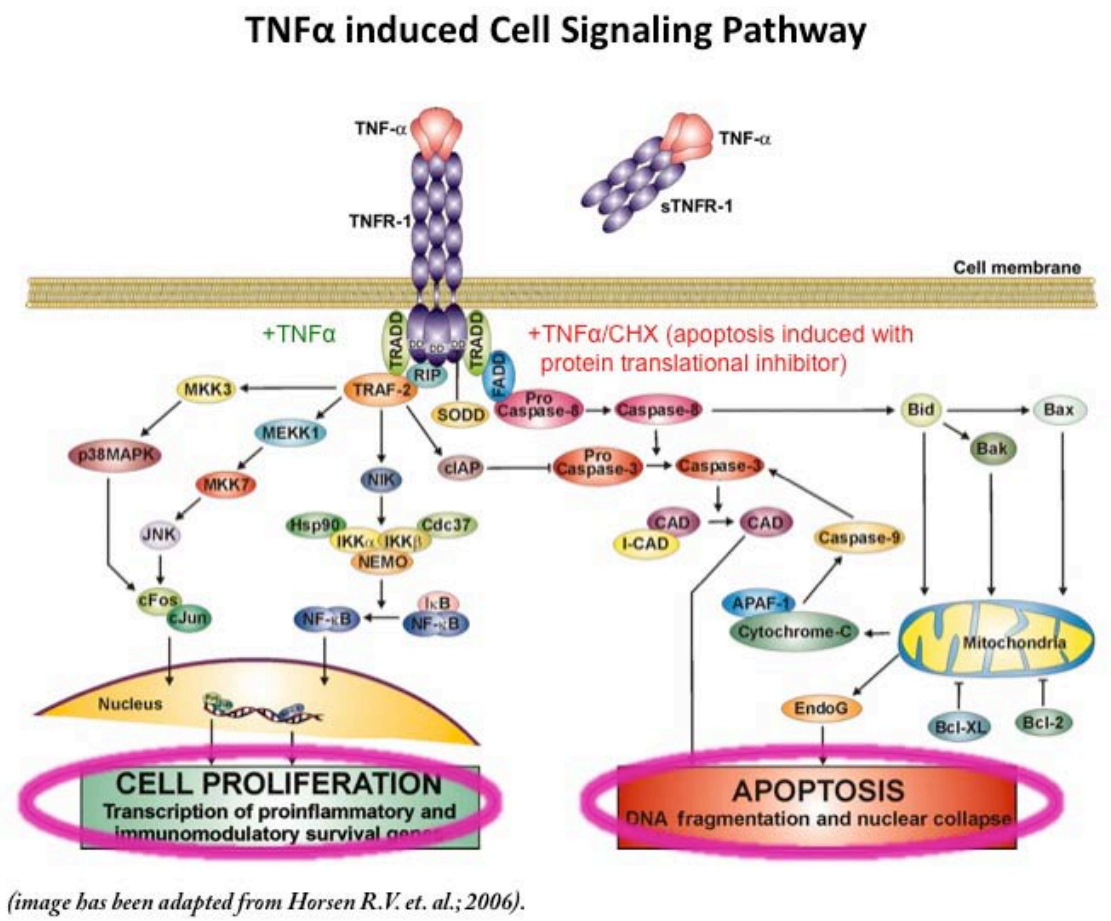

(image has been adapted from Horsen R.V. et. al.; 2006).

Figure 1: TNFα signaling pathway

TNFα is a 17-kDa protein mapped to chromosome 6 (Muller et al., 1987) and binds as a homotrimer to preassembled (Chan et al., 2000) TNF receptors type 1 and 2 (Baud and Karin, 2001; Locksley et al., 2001) that causes the receptors to trimerize (Banner et al., 1993). Unlike TNFR-2, which is expressed mainly by immune cells, TNFR-1 is present in all cell types (Aggarwal, 2003). The presence of death domains (DDs) in the cytoplasmic tail of only TNFR-1 makes it an important member of the death receptor family (Tartaglia and Goeddel, 1992). The

cytotoxicity of TNFα is mediated by TNFR-1 by inducing cell apoptosis and programmed necrosis (Tartaglia et al., 1993). The trimerized state of the receptor binds TRADD (TNFR-associated death domain) to the DDs (Hsu et al., 1995). This can actively recruit adaptors like receptor interacting protein (RIP) (Hsu et al., 1996a), TNFR-associated factor 2 (TRAF-2) (Hsu et al., 1996b) leading to the activation of NFkB and JNK prosurvival pathways (Hsu et al., 1995; Senftleben et al., 2001) or Fas-associated death domain (FADD) that leads to apoptosis (Hsu et al., 1996b; Rath and Aggarwal, 1999) (refer to the above image; in our study we have induced cell apoptosis with administration of cycloheximide (CHX) and TNFα). Regulation of the death and survival pathway is critically important to understand, since an unregulated sustained TNFα production is associated with a variety of diseases (Balkwill, 2006).

X-ray crystallographic studies show that the trimeric form of TNFα is preserved in the ligand-receptor complex (Banner et al., 1993; Hymowitz et al., 1999; Mongkolsapaya et al., 1999). Upon ligand binding, TNF-receptors are thought to either trimerize from monomeric form (Chan, 2007) or may be in pre-assembled receptor complexes (as oligomers) prior to trimerization (Chan et al., 2000b). Oligomerization of Epidermal Growth Factor (EGF) receptor has been shown to increase ligand binding affinity (Ozcan et al., 2006). For cytokine receptors, oligomerization of the receptor subunits has been shown to possess an additional effect to alter ligand specificity and is a pre-requisite to mediate receptor function (Leonard, 2001).

TNF receptors contain a conserved domain known as pre-ligand assembly domain (PLAD), which is present in the first extracellular cystein rich domain of the receptor(Locksley et al., 2001). PLAD mediates homotypic ligand–independent assembly of the receptor complexes (Chan et al., 2000a; Papoff et al., 1999; Siegel et al., 2000b) and is physically distinct from the ligand-binding domain. In absence of the ligand, TNFR1 adopts parallel dimeric conformation

(Naismith et al., 1996a; Naismith et al., 1995; Naismith et al., 1996b). When bound to ligand, the receptor undergoes a conformational change (Chan et al., 2001), which apparently triggers the signaling pathway. Several studies have shown that PLAD region is highly critical for proper TNFα signaling (Siegel et al., 2000a).

Biological roles of TNFα

The multifunctional cytokine TNFα is the key mediator of inflammation that exerts multiple physiological and pathological outcomes (Aggarwal et al., 2012). It plays a paradoxical role both as a tumor promoter and tumor suppressor (Guadagni et al., 2007), where the mechanisms determining these different outcomes have yet to be fully resolved. These different outcomes are observed when TNFα concentrations are varied. For instance, local administration of high doses of TNFα exerts powerful anticancer activity by inducing cellular apoptosis, whereas chronic endogenous secretion at lower concentrations has been shown to contribute to tissue remodeling, stromal cell activation, angiogenesis, and tumor cell proliferation (Balkwill and Mantovani, 2001). TNFα concentration, therefore, appears to be a critical factor in driving either tumor cell death (high concentration) or cell proliferation (low concentration).

TNFα acts as a key downstream mediator of inflammation and regulates a cascade of chemokines, cytokines, MMPs and angiogenic factors to promote tumor formation (Balkwill, 2002). High levels of TNFα have been detected in the malignant and stromal cells of various types of cancer such as ovarian, prostate, breast, bladder and colorectal (Balkwill and Mantovani, 2001; Burke et al., 1996; Leek et al., 1998). Elevated level of TNFα is a micro-environmental hallmark of many solid tumors such as breast cancer, where it is largely derived from tumor associated immune cells (Balkwill and Mantovani, 2001). Historically, administration of TNFα

was considered as a promising antitumor-therapy. However, early clinical trials to use TNFα for cancer biotherapy failed because of acute toxicity and acquisition of tumor cell resistance (Balkwill, 2009).

Acquiring resistance to TNFα

In assessing TNFα as an effective anti-cancer agent, resistance became a prominent problem that has yet to be remedied (Balkwill, 2009). A number of studies indicate that both upstream and downstream factors of TNF receptor activation may participate in providing TNFα resistance to tumor cells. For instance, decreases in TNFR1 (TNF receptor type I) both at the level of transcription and translation are observed in acquired TNFα-resistance in MCF7 cells (Antoon et al., 2012). Factors like microtubule stability, lipid raft organization can alter TNFα signaling and may play a role in acquiring resistance (Legler et al., 2003; Shivanna and Srinivas, 2009). Downstream of TNF receptor activation, reduced TRADD (TNFR-1 associated death domain) expression can promote cancer progression and has been associated with TNFα resistance in prostate cancer (Wang et al., 2009). The pro-survival factor NFκB, can also interfere at multiple levels with TNFα-induced apoptotic signals and its specific inhibition has been shown to increase sensitivity of tumors to TNFα (Beg and Baltimore, 1996; Magne et al., 2006). Further, the Bcl-2 gene can prevent TNFα-induced apoptosis and over-expression of anti-apoptotic proteins of this family like Bcl-2 and $Bclx_L$ can contribute to chemoresistance (Krajewski et al., 1999). Evidence indicates that predominant knock-down of $Bclx_L$ drives TNFα mediated apoptosis in pancreatic cancer cells (Bai et al., 2005), while colon carcinoma cells that are deficient in the pro-apoptotic protein Bax have been shown to become resistant to TNFα-induced cell death (LeBlanc et al., 2002).

Although, a number of findings have indicated factors that can attenuate or inhibit TNFα signaling, the majority of these factors have not been shown to be directly responsible for tumor cells acquiring resistance. Here, we investigated how breast cancer cells acquire TNFα resistance and have uncovered the novel microtubule associated protein tau as a critical regulator of this process. This study represents the first indication that tau expression in cancer cells can be a deciding factor as to whether these cells succumb to TNFα-induced cytotoxicity or continue to proliferate in a TNFα-rich microenvironment.

Tau protein

Tau protein is predominantly expressed in the axons of the central and peripheral nervous system and has been classically characterized in neurons (Zhou et al., 2008, (Trojanowski et al., 1989). It is an important neuronal protein, which plays a critical role in axon development (Zhou et al., 2008). Besides neurons, tau is widely expressed in other tissues like heart, skeletal muscle, lung, kidney, testes, (Gu et al., 1996) and normal human breast epithelial cells (Rouzier et al., 2005). The human tau gene mapped to chromosome 17q21 is 100 kilobases long and contains 16 exons. Alternate splicing among exons 2, 3 and 10 gives rise to six isoforms of tau (Zhou et al., 2008). Exons 9, 10, 11, 12 code for the four microtubule binding regions and they are located at the carboxy-terminal domain of the protein (Andreadis et al., 1992; Crowther et al., 1989; Goedert et al., 1989). Tau protein, which was co-purified with the cytoskeletal element tubulin, promotes tubulin polymerization and stabilizes microtubules (Cleveland et al., 1977; Drechsel et al., 1992; Fellous et al., 1977). However, phosphorylation of this protein at multiple sites (Thr^{231}, Ser^{262}, Thr^{231}/Ser^{235}, Ser^{396}/Ser^{404} residues) (Biernat et al., 1993; Cho and Johnson, 2004; Ding et al., 2006) mediated by microtubule affinity regulating kinases (p38, GSK3β) reduces its affinity for tubulin (Cho and Johnson, 2003; Cho and Johnson, 2004; Reynolds et al., 1997;

Stoothoff and Johnson, 2005). Tau, when hyperphosphorylated, undergoes self-assembly forming insoluble tangles of paired helical filaments and straight filaments which is a hallmark of several neurodegenerative diseases like frontotemporal dementia with parkinsonism linked to chromosome 17 (FTDP-17), Alzheimer's and progressive supranuclear palsy (PSP) (Abraha et al., 2000; Alonso et al., 2001; Alonso et al., 1996; Alonso et al., 2008; Alonso et al., 2010; Ferrari et al., 2003; Grundke-Iqbal et al., 1986; Kondo et al., 1988; Lee et al., 1991; Lee et al., 2001; Matsumura et al., 1999; Nukina and Ihara, 1986; Vogelsberg-Ragaglia et al., 2000).

Comprehensive research has been done focusing on tau phosphorylation and its aggregation. Tau phosphorylation is a normal event observed in fetal brain as well as in adult brain without evoking signs of toxicity (Matsuo et al., 1994; Yu et al., 2009). Phosphorylation of tau gets elevated in response to various stressors like trauma, hypothermia, hypoxia and glucose deprivation (Morris et al., 2011). Data shows that hyperphosphorylated tau in Alzheimer's disease (AD) is able to disassemble microtubules and sequester normal tau into tangles of large filaments which leads to neurodegeneration (Alonso et al., 1996). Evidence indicates that hyperphosphorylation in tau, as well as, its redistribution can be induced when exposed to aqueous extract of neurotoxic Aβ oligomers from AD brains (De Felice et al., 2008; Zempel et al., 2010). Data from *in vivo* study insinuates that neurotoxicity may be caused by tau phosphorylation in a combinatorial manner, which leads to conformational change and abnormal tau folding, rather than through individual modifications of the phosphorylation sites (Steinhilb et al., 2007). This data is further supported when combined phosphorylation of tau at Thr 212, Thr 231, and Ser 262 is shown to trigger caspase-3 activation in CHO cells whereas single phosphorylation has negligible effect on tau activity (Alonso et al., 2010). Tau phosphorylation is also noticed in cancer cells. The prostate cancer ALVA-NEO cell line has been shown to

express tau phosphorylation on several sites (Ser396/Ser404, Ser262/Ser396, Thr231, Tyr18) resembling several modifications associated with AD brain tau (Souter and Lee, 2009).

Although, tau has been heavily investigated in neurons, little is known about its functional significance outside neuronal system. Recent evidence has associated tau as a predictor of chemotherapy sensitivity to Paclitaxel in breast cancer cell lines (Rouzier et al., 2005; Smoter et al., 2011; Tanaka et al., 2009; Wagner et al., 2005). Paclitaxel is a frontline anticancer drug used to treat ER- (estrogen receptor negative) as well as metastatic breast cancer. It binds to the inner surface of tubulin and inhibits spindle microtubule dynamics, leading to cell cycle arrest in G2/M phase followed by apoptosis (McGrogan et al., 2008; Yvon et al., 1999). Since, tau is able to bind to both the outer and inner surface of tubulin to stabilize microtubules, it is thought to compete with Paclitaxel thereby interfering with its action (Kar et al., 2003; Santarella et al., 2004). Further, tau enrichment in metastatic breast tumors has also been shown to promote micro-tentacle formation facilitating tumors to metastasize (Matrone et al., 2010). The prognostic value of tau expression in breast cancer is currently undergoing.

N and C-terminal Tau domains

Tau protein structure is classified into 4 regions – N-terminal projection region, proline rich region, microtubule binding domains (MTBD) and C-terminal region (Mandelkow et al., 1996). Physiological tau exists in an intrinsically disordered structure and the protein is highly regulated through a variety of extensive post-translational modification (phosphorylation, acetylation, glycation, nitration) (Alonso et al., 2008; Morris et al., 2011).

Tau binds to the outside as well as to the inside of microtubules with its N and C-terminal regions flanking outwards (Kar et al., 2003; Santarella et al., 2004). Tau binding to

microtubules is dependent on the MTBD and its adjacent regions (Gustke et al., 1994). The tandem repeat sequences present within the MTBD contain a net positive charge that interacts with negative charge residues of tubulin and facilitates tau binding with microtubules (Kar et al., 2003; Morris et al., 2011). Tau association with microtubules is regulated through phosphorylation. Findings have indicated that phosphorylation of tau in or around MTBD neutralizes the positive charge and induces conformational change in MTBD that impairs its binding with microtubules (Fischer et al., 2009; Jho et al., 2010). Phosphorylated tau is thought to detach from microtubules and accumulate in neuronal cell bodies forming insoluble filaments of neurofibrillary tangles (Morris et al., 2011; von Bergen et al., 2005). Data shows that tau hyperphosphorylation promotes paired helical filament (PHF) and straight filament formation and the presence of MTBD / repeat region is sufficient to induce self-assembly into PHF (Alonso et al., 2001). Furthermore, studies also highlight the presence of two hexapeptides (PHF6 VQIVYK) in the second and third repeat of MTBD, which is crucial for PHF formation. Missense mutation within this hexapeptide motifs, (PHF6 VQIVYK to PHF6* VQIINK) triggers conformational change in tau, from random coil to beta sheet structure and results in tau aggregation (von Bergen et al., 2005; von Bergen et al., 2001). Emerging new insights into this field, illustrates that tau can also promote microtubule stability independent of microtubule binding. *In vivo* studies indicate that tau directly interacts with and inhibits histone deacetylase 6 (HDAC6), which increases tubulin acetylation (Perez et al., 2009) and decreases microtubule stability.

Aside from affecting tubulin dynamics, several studies have also highlighted the role of tau in signal transduction. In contrast to the C-terminus region, which harbors the MTBDs, the N-terminal region of tau has been shown to associate with the plasma membrane where it is a

feasible part of the membrane associated complex (Brandt et al., 1995; Maas et al., 2000). The proline rich sequences of the N-terminal region of tau have been shown to interact with SH3 domains (SH3 recognizes PXXP motifs) of fyn and src non-receptor tyrosine kinases (Lee et al., 1998). There are seven PXXP motifs present in tau which either contain or are in close proximity with several well known phosphorylation sites (Augustinack et al., 2002; Biernat et al., 1992). Phosphorylation of these sites in or around the proline rich domain have been shown to regulate tau interaction with SH3 domains of several proteins like phospholipase Cγ1, Grb2, PI3 kinase, suggesting a potential role of tau in signal transduction (Reynolds et al., 2008). Studies in PC12 cells demonstrates that in response to nerve growth factor (NGF) and epidermal growth factor (EGF), tau promotes activation of transcription factor AP-1 through activation of MAPK pathway. Phosphorylation of tau at 231 in response to NGF or EGF is necessary to activate MAPK signaling and is independent of its binding with microtubules (Leugers and Lee, 2010). Tau mediated enhancement of growth factor signaling may explain why tau is over-expressed in several types of chemotherapy resistant cancer cells (Jimeno et al., 2007; Mimori et al., 2006; Rouzier et al., 2005; Souter and Lee, 2009).

Materials and methods:

Cell lines and culture: Human breast cancer cell lines MCF7 and SkBr3 and the rat pheochromocytoma cells (PC12) were obtained from American Type Culture Collection (ATCC). MCF7 cells were cultured in basal media (High Glucose Dulbecco's Modified Eagle's Medium (Lonza), 10 units/ml Penicillin and 10 ug/ml Streptomycin (Hyclone)) with 10% (v/v) fetal calf serum (FCS). SkBr3 cells were cultured in DMEM/F-12 (1:1) (Invitrogen) supplemented with 10% (v/v) FCS. Both cell lines were maintained at 37°C in with 5% CO_2 in 10cm culture dishes (BD Bioscienes). Media was changed regularly at 2-3 day intervals. Cells were passaged with 0.25% Trypsin (Cellgro) once they reached a confluency of 70-80%.

PC12 cells were maintained in RPMI-1640 (Hyclone) medium containing 10% horse serum (Sigma), 5% FBS (Hyclone) and 1x Penicillin / Streptomycin (Gibco) in 75 cm^2 flask (Corning Incorporated). Cells were cultured for 2 days on Collagen Type I (BD Biosciences # 354236) treated 8 well plates (BD Biosciences) prior to stimulation with 50 µg/ml of Nerve growth factor (mNGF 2.5s Grade II N-100 Alomone labs) for an additional 2 days to stimulate differentiation prior to experimentation.

TNFα selection of MCF7 cells: Wild type MCF7 cells were cultured in 12 well plates (BD Falcon) in the presence of human recombinant tumor necrosis factor alpha (TNFα) (Calbiochem # 654205). TNFα was diluted in basal media containing 5% FCS. MCF7 cells were initially grown in the presence of TNFα (2.5ng/ml) and passaged twice before increasing the TNFα concentration to 5, 7 and finally 10ng/ml, passaging twice at each concentration. MCF7 cells grown in the absence of TNFα under identical conditions served as a control. Basal media containing 5% FCS and TNFα was replaced every alternate day. Cells were passaged with 0.25%

trypsin at 70% confluence. This processes spanned 10 weeks and was conducted prior to any experimental analysis of TNFα selected MCF7 cells.

Site-directed mutagenesis: Primers were designed and ordered from the Midland certified reagent company. Site-directed mutagenesis was conducted according to the instructional guideline provided by Stratagene. Stratagene Quick change Lightning Site-directed Mutagenesis kit (Catalog # 210518) was used to perform site-directed mutation in tau gene. Briefly both sense and anti-sense primers (125 ng each) were added to the sample reaction buffer containing 100 ng of the dsDNA plasmid (pEGFP-C1 containing full-length tau) and subjected to PCR. The parental strand was briefly digested with 2μl Dpn I restriction enzyme for 5mins at 37°C. Bacterial transformation with the synthesized DNA construct was performed in X-Gold ultra competent *Escherichia coli* cells in NZY^{+} broth. The transformed cells were plated in Kanamycin treated LB plates, incubated at 37°C and colonies were allowed to develop. Plasmid isolation was performed and the constructs were sequenced by GENEWIZ, Inc.

Stable transfection of Tau2N4R and Tau 2N constructs: MCF7 and SkBr3 cells were grown in a 6 well plate (BD Falcon) format and allowed to attain 80% confluency. Cells (MCF7 or SkBr3) were then transfected with purified plasmid DNA pEGFP-C1 (Clontech # 6084-1) alone (GFP MCF7) or containing either full length human Tau (amino acid residues 1-441) (GFP-Tau MCF7 and GFP-Tau SkBr3) or Tau 2N (N-terminal domain; amino acid residues 1-242) (GFP-Tau2N MCF7) constructs. Transfection was accomplished following the standard Lipofectamine^{TM}2000 (Invitrogen) transfection protocol. The constructs were sequenced by GENEWIZ, Inc. 24 hrs after transfection, cells containing the plasmid were selected with G418 antibiotic (Sigma) at 400 ug /ml for 2 weeks, then maintained at 200 ug /ml. Media containing

G418 was replaced every 2-3 days. PC12 cells were stably transfected with a human Tau construct that did not contain a GFP tag.

Small interfering RNA (siRNA) mediated Tau knock down: TNFα selected MCF7 cells were plated in 12 well plates (BD Falcon) for 48 hrs and allowed to attain a confluency of 35% prior to siRNA transfection. Tau expression was transiently knocked down in cells using 0, 40, 80 or 120 picomolar of predesigned MAPT siRNA (Ambion, Life technologies # 4392420) using the Lipofectamine ^{TM} 2000 (Invitrogen) siRNA transfection protocol. Cells were transfected with scrambled siRNA (Ambion, Life technologies # 4390843) to serve as a negative control. Basal media containing 2% FCS was added back to the culture after 24 hrs of transfection. The presence of Tau protein was measured by immunoblot (described below) 24 hrs later (48hrs after transfection). Protein was extracted using NP40 lysis buffer (described below). The blot was probed with mouse DA9 antibody (1:2000); a generous gift from Dr. Peter Davis from Albert Einstein's College, School of Medicine) against Tau. Anti-β-actin rabbit polyclonal antibody (Cell signaling # 4967) was used a loading control.

MCF7 GFP and GFP-Tau2N cells were plated in 12 well plates (BD Falcon) for 48 hrs and allowed to attain a confluency of 35% prior to siRNA transfection. Tau expression was transiently knocked down in cells using 0 or 120 picomolar of predesigned MAPT siRNA (Ambion, Life technologies # 4392420) using the Lipofectamine ^{TM} 2000 (Invitrogen) siRNA transfection protocol. Basal media containing 2% FCS was added back to the culture after 24 hrs of transfection. The presence of tau protein was measured by immunoblot 24 hrs later (48hrs after transfection). Protein was extracted using NP40 lysis buffer (described below). The blot was probed with mouse monoclonal Tau13 antibody (1:5000). Anti-β-actin rabbit polyclonal antibody (Cell signaling # 4967) was used a loading control.

Immunoblotting: Protein was extracted from cells by lysis with ice-cold NP40 lysis buffer (50mM tris-Hcl, pH 8.0; 150mM Nacl; 5mM EDTA; 0.5% NP40; 1mM NaF; 1.25mM Na_3VO_4 and 1X protease inhibitor cocktail (Calbiochem)) and quantified with the DC Protein assay (Bio-Rad). Equal amounts of protein were resolved by SDS-PAGE under reducing conditions with the XCell II Blot module from Invitrogen and then transferred to a nitrocellulose membrane (blot) (Bio-Rad) for 1.5 hrs at 100 mAmps. Blots were then rinsed with water and blocked with 2% milk in TTBS (Tris buffered saline (TBS) plus 0.05% Tween 20) for 1-2 hrs before being probed with primary antibody overnight at 4°C. Primary antibodies were diluted in 5% bovine serum albumin (BSA) w/v in TTBS. Blots were then washed (once with TTBS and twice with TBS) and probed with the species appropriate HRP conjugated secondary antibody (Cell Signaling) (1:2000) for 3 hrs before undergoing another wash series. Secondary antibodies were diluted in 2% milk in TTBS. Blots were developed using the Bio-Rad Immun-Star™ HRP substrate kit, and imaged with a FC2 Multi Imager II by Alpha Innotech. Bands were quantified using FluoChem HD2 software (Alpha Innotech) and processed in Adobe Photoshop.

Immunoblot analysis of transfected PC12 and TNFα selected MCF7 cells: Differentiated PC12 cells (see above) were extracted and lysed with ice cold NP40 lysis buffer. Equal amounts of protein were resolved by 10% SDS-PAGE (see Immunoblotting). The blot was probed with mouse DA9 antibody (1:2000) against Tau and again probed with anti-β-actin rabbit polyclonal antibody (Cell signaling # 4967) (1:2000) as a loading control. Protein extracts of MCF7 TNFα selected and non-selected cells were similarly made with NP40 lysis buffer and resolved by 10% SDS-PAGE. This blot was probed with anti-E-cadherin (Milipore # 04-1103; rabbit monoclonal 1:5000) and again probed with anti-Tubulin (Milipore # 05-829; mouse monoclonal 1:1000) as a loading control.

Tau protein estimation following TNFα/CHX addition: GFP and GFP-Tau2N MCF7 cells were plated at equal density in 12 well plate and allowed to grow for 2-3 days. Cells were washed twice and exposed to TNFα (50 ng/ml) and CHX (15ug/ml) diluted in 2% FCS supplemented medium for 6 hrs. Cells were extracted on ice with NP40 lysis mix, quantified and resolved in 10% SDS-PAGE as previously described. Endogenous tau and GFP-Tau2N were detected with Tau13 mouse monoclonal antibody (1:5000) and 134d rabbit polyclonal antibody (1:5000). Actin was used as loading control (1:2000).

Microtubule Binding assay (MtBA): GFP and GFP-Tau MCF7 cells were seeded at a density of 100×10^3 cells/well in a 4 well glass chamber slide (BD Falcon) and cultured for 24 hrs at 37°C with 5% CO_2. Cells were washed twice with basal medium prior to any treatment. Cells were then subjected to ± TNFα (50ng/ml) (Calbiochem # 654205) and cycloheximide (CHX; 15 µg/ml) (Chem Service # PS-1002) in basal media with 2% FCS for 8-10 hrs. Cells were washed with warm (37°C) phosphate buffered saline (PBS) (Fisher Scientific) at room temperature (RT) and harvested with RAB buffer (100mM MES, pH 6.8; 0.5 mM $MgSO_4$; 1mM EGTA; 2mM DTT; 0.1% Triton X-100) containing freshly added Taxol (20µM) (Acros Organics), GTP (2mM) (Cytoskeleton # BST06), Na_3VO_4 (1.25 mM), NaF (1mM), and a protease inhibitor cocktail (Calbiochem) strictly maintained at 37°C. The cell extract was homogenized in a Dounce homogenizer with 15 strokes and centrifuged at 50,000 g (CentrifugeTL-100 Beckman) for 20 mins at 30°C. The pellet was separated from the supernatant and resuspended in volume equal to that of the supernatant. The pellet suspension was then briefly (3-5 sec) sonicated (Sonic Dismembrator Model 100, Fisher scientific). Protein was quantified using the DC Protein assay (Bio-Rad). 20-25 µg of protein was resolved by 10% SDS-PAGE. Immunoblotting was performed as described above (see Immunoblotting). The mouse monoclonal DA9 antibody

(1:2000) was used for Tau detection. Tubulin was detected with DM1A mouse monoclonal antibody (1:1000) (Milipore, 05-829). Microtubule stability was determined by measuring the ratio of insoluble to soluble tubulin.

MtBA of taxol stabilized, TNFα selected, and GFP-Tau2N MCF7 cells: MCF7 cells were seeded at a density of 200×10^3 cells/well and cultured in a 12 well plate (BD Falcon) for 24 hrs. Cells were exposed to taxol (20μM, 10μM, 5μM, 1μM or 0.5 μM) in basal media containing 2% FCS for 1 hr, then washed twice with PBS at RT. The MtBA was performed as described above (see microtubule binding assay). To determine the effect of TNFα selection on Tau expression, MCF7 cells that either had or had not undergone selection with TNFα were seeded at a density of 5000 cells/well in a 4 well glass chamber slide (BD Falcon) and cultured for 5-6 days in the complete absence of TNFα. MtBA was performed to detect Tau protein in the soluble and insoluble factions. This was done to determine if either fraction showed increased levels of Tau protein in response to TNFα selection. The blot was probed for Tau with DA9 mouse monoclonal antibody (see microtubule binding assay) (1:2000) and was again probed with anti-β-actin rabbit polyclonal antibody (see microtubule binding assay) (1:2000) as a loading control. The MtBA was also performed with stably transfected GFP-Tau2N MCF7 cells grown in 4 well glass chamber slides as described above. Tau was detected with rabbit monoclonal 134d antibody (1:5000) (generous gift from the lab of Dr. Khalid Iqbal, Institute of Basic Research) and tubulin was detected as described above (see microtubule binding assay).

Cell proliferation assay: Equal densities of GFP and GFP-Tau MCF7 cells were seeded in 12 well plates (BD Falcon) and incubated until fully adhered (flattened). The cells were serum starved with basal media containing 0.5% FCS for 24 hrs prior to TNFα exposure. Cells were exposed to TNFα (10ng/ml) in basal media containing 2% FCS. This media was replaced every

24 hrs. Cells were lysed on ice with NP40 lysis buffer (see Immunoblotting) after 24, 48 or 72 hrs of TNFα treatment. Protein was quantified using the DC Protein assay (Bio-Rad). Immunoblotting was performed as described above. Proteins were resolved by SDS-PAGE (12% gel) and transferred to nitrocellulose membrane for 1 hr at 100 mAmps of current. Blots were probed for phosphorylated histone H3, a marker of cellular proliferation, with anti-phospho Histone-H3 (Ser 10) (Milipore # 06-570) (1:1000). Anti-Glyceraldehyde 3-phosphate dehydrogenase (GAPDH; Cell Signaling # 5174) antibody was used as a loading control. The quantified data represents the ratio between phospho Histone-H3 and GAPDH. Values were made relative to their respective controls (GFP or GFP-Tau MCF7 cell without TNFα exposure). Total amount of Histone H3 was measured with rabbit polyclonal antibody at 1:1000 (Cell signaling # 9715) and β-actin was used as the loading control.

Cell fractionation and immunoblotting for NFκB: GFP, GFP-Tau, and GFP-Tau2N MCF7 cells of equal density were seeded in a 6 well plate (BD Falcon) and allowed to flatten. They were washed twice with basal media and exposed to TNFα (50ng/ml) in basal media with 2% FCS medium. Cells were extracted at 0, 30 or 60 mins following TNFα exposure, and fractionated with sub-cellular fractionation buffer at 4°C (Jenkins et al., 2012). Briefly, cells were washed once with ice cold PBS (Fisher Scientific) and extracted with sub-cellular fractionation buffer (250 mM sucrose; 20 mM HEPES, pH 7.4; 10mM Nacl; 1.5mM $Mgcl_2$; 1mM EDTA; 1mM EGTA) with freshly added 1mM DTT, 1.25mM Na_3VO_4, 1mM NaF, Protease inhibitor cocktail (Calbiochem) at 4°C. The cell lysate was passed through 25G needle for 10 times and left on ice for 20 mins followed by brief centrifugation at 720G (Biofuge Pico, Thailand) for 5 mins. The obtained nuclear pellet was separated from the supernatant and washed with fractionation buffer. The pellet was dispersed and passed through 25G needle for several times and centrifuged at

720G for 10 mins. This was repeated twice and finally the nuclear pellet was suspended in an equal volume of the supernatant in nuclear buffer (cell fractionation buffer with 10% glycerol and 0.1% SDS). The pellet was briefly sonicated (Sonic Dismembrator Model 100, Fisher scientific) for 3 secs on ice. Immunoblotting was performed on both the nuclear and cytoplasmic fractions (10% SDS-PAGE) (see immunoblotting). Blots were probed with anti-NFκB p65 rabbit monoclonal antibody (Cell Signaling # 4764) (1:1000). The blots with nuclear extracts were probed with anti-PCNA mouse monoclonal antibody (Cell Signaling # 2586) (1:2000)) or anti-nuclear lamin A/C mouse monoclonal antibody (Cell signaling # 4777; 1:2000). The cytoplasmic blots were probed with DM1A mouse monoclonal (Milipore, 05-829) (1:1000) or anti-β-actin rabbit polyclonal antibody (Cell signaling # 4967) (1:2000) as loading controls.

Membrane receptor cross-linking: GFP and GFP-Tau MCF7 cells were grown in a 6 well plate (BD Falcon) for 48 hrs. They were washed three times with basal media and incubated with or without TNFα (50ng/ml) in basal media with 2% FCS for 1 hour with occasional stirring. Cells were washed twice with PBS. Membrane receptor cross-linking with 3,3'-dithiobis[sulfosuccinimidylpropionate] (DTSSP) (Thermo Scientific # 21578) was performed as previously described (Chan et al., 2000). Briefly, cells were treated with 2mM solution with DTSSP for 30 mins and the reaction was quenched with on ice with 20 mM tris-Cl (pH-7.5) for 15 mins. Cells were lysed with lysis buffer containing 150mM Nacl, 20mM tris-Cl, 1mM EDTA, 1mM NaF, 1.25mM Na_3VO_4 and 1X protease inhibitor cocktail (Calbiochem). Immunoblotting was performed with equal amounts of cell lysate and resolved by gel electrophoresis under non-reducing (no β-mercaptoethanol) conditions (see immunoblotting). The blot was probed with rabbit monoclonal anti-TNFR1 (C25C1) antibody (Cell Signaling # 3736) (1:1000). The data represents the average of three independent experiments.

MTT assays: Equal densities of GFP and GFP-Tau MCF7 cells were seeded in a 96 well plate (BD Falcon) and cultured for 24hrs at 37°C with 5% CO_2. Cells were washed twice with basal media and exposed to TNFα (50, 25, 10 or 5ng/ml) in basal media with 2% FCS for 96 hrs. This media was replaced after 48 hrs. The (3-(4,5-Dimethylthiazol-2-yl)-2,5-diphenyltetrazolium bromide (MTT) assay was performed after 96 hrs according to the MTT based *in vitro* Toxicology assay kit (Sigma, TOX-1). Absorbance at 570 nm and 690nm was recorded by a Spectra Max 340 PC microplate spectrophotometer (Molecular Device, CA). To assess the effect of TNFα on MCF7 cells that either had or had not been selected for TNFα resistance, selected and non-selected MCF7 cells were grown for 48 hrs in a 96 well plate at equal density as described above. Cells were treated with TNFα (0, 5, 10, 25, 50ng/mL) in basal media with 2% FCS. The MTT assay was conducted after 96 hrs. PC12 cells transfected with the empty plasmid (vehicle (vh) control) or plasmid containing full length Tau (see stable transfection of Tau2N4R and Tau2N constructs) were seeded at equal densities in Collagen Type I treated 96 well plates and allowed to differentiate with 50 µg/ml of NGF as mentioned (see cell lines and cell culture). The differentiated cells were exposed to TNFα (0, 5, 10, 25, 50ng/mL) and the MTT assay was performed after 96 hrs. The MTT results represent an average of three independent experiments, and each conducted in triplicate.

Immunocytochemistry: The immunocytochemistry procedure common to all antibodies discussed below is as follows: after fixation, cells were rinsed with warm (37°C) PBS at room temperature (RT) for 10 mins, blocked with immunoblocker buffer solution (2% BSA, 10% horse serum, 0.5% Triton X-100 in PBS) for 1-2 hrs at room temperature (RT) and incubated overnight at 4°C with primary antibody. Cells were then washed (once with PBS+0.5% TritonX-100 for 5 min and twice with PBS for 5 min each) and incubated for 1-2 hrs with a

species appropriate Alexa Fluor conjugated secondary antibody (Invitrogen; 1:2000 dilution). All primary and secondary antibody dilutions were made in immunoblocker buffer. Finally, nuclei either were or were not counterstained with 4',6-diamidino-2-phenylindole (DAPI; 400nM) for 5 mins before being washed again and imaged.

Microtubules: GFP-Tau and GFP-Tau2N MCF7 cells were seeded at a density of 10×10^3 cells/well in a 8 well chamber (BD Falcon) and were cultured for 2 days before being fixed with pre-chilled (-20°C) Cytoskelfix^{TM} cell fixative (Cytoskeleton # CSK01) for 4 mins at -20°C. Tubulin was detected with mouse monoclonal DM1A antibody (Milipore, 05-829) (1:200) and Alexa Fluor 594 goat anti-mouse IgG secondary antibody (Invitrogen). Microtubules for Skbr3 cells were similarly fixed and co-immunostained for both tubulin and tau.

Tau detection: GFP-Tau MCF7 cells were analyzed for total GFP-Tau by fixing cells with 4% paraformaldehyde for 15 mins at RT. The microtubule bound insoluble GFP-Tau component was detected by fixing with pre-chilled methanol at -20°C for 6 mins. Endogenous Tau in untransfected MCF7 cells was detected by fixing cells with 4% paraformaldehyde for 15 mins at RT, then treating with chilled (-20°C) methanol for 6 mins at -20°C. Tau was detected with mouse DA9 antibody (1:500) and Alexa fluor 594 goat anti-mouse IgG secondary antibody (Invitrogen).

Cleaved Caspase-3 detection: Cell apoptosis was visualized by immunocytochemistry for cleaved (active) caspase-3. Cells were seeded at density of 50×10^3 cells/well in an 8 well chamber (BD Falcon) in basal media with 10% FCS for 24hours. Cells were then rinsed twice with basal media alone and exposed to TNFα (50ng/ml) and cycloheximide (CHX; 15μg/ml) in basal media with 2% FCS for 6 hrs. Cells were the fixed with 4% paraformaldehyde for 15 mins at RT and immunostained as described above. Cleaved caspase-3 was detected with anti-cleaved

caspase-3 (D175) rabbit polyclonal antibody (Cell Signaling # 9661) (1:200) and Alexa Fluor 594 goat anti-rabbit IgG secondary antibody (Invitrogen) (1:2000). Nuclei were counterstained with DAPI for 5 mins. In order to show that microtubule stabilization alone does not protect against apoptosis, MCF7 cells were pretreated with a sublethal concentration of taxol (1μM) for 1 hr in basal media with 2% FCS, then washed with PBS and exposed to TNFα/CHX for 6 hrs. Immunocytochemistry for cleaved caspase-3 was performed as described above. Cells treated with taxol (1μM) alone did not show caspase activation after 6 hrs of exposure and served as the control for the experiment.

NFκB activation: GFP, GFP-Tau, and GFP-Tau2N MCF7 cells were fixed with 4% paraformaldehyde for 15 mins at RT after 0 and 60 mins of treatment with TNFα (50ng/ml) in basal media containing 2% FCS. Immunocytochemistry was performed as described above. NFκB was detected with anti-NFκB p65 rabbit monoclonal antibody (Cell Signaling # 4764) (1:50) and Alexa Fluor 594 goat anti-rabbit IgG secondary antibody (Invitrogen). Nuclei were counterstained with DAPI (400nM) for 5 min. MCF7 wild type cells were treated for an hour with 1μM taxol, washed twice with plain media and treated with TNFα (50ng/ml) for 30 mins. Cells were then immunostained to detect NFκB as described.

Receptor staining: GFP and GFP-Tau2N MCF7 cells were plated in 8 well chamber slides (BD Falcon) and allowed to fully adhere (flatten). Cells were washed three times with basal media then incubated with TNFα (50ng/ml) in basal media with 2% FCS for 1 hour. Cells were the fixed with 4% paraformaldehyde for 7 mins at RT, washed three times with PBS, blocked for an hour with blocking buffer (2% BSA in PBS + 0.1% Tween 20). TNFR1 (Santa Cruz # 8436) mouse monoclonal antibody was diluted to 1:50 times in the blocking buffer and cells were incubated overnight with the primary antibody. Cells were washed thrice with PBS and

incubated with Alexa fluor 594 goat anti-mouse IgG secondary antibody for 2 hrs with gentle shaking. Nuclei were counterstained with DAPI (400nM).

Live Cell imaging and image acquisition: GFP and GFP-Tau MCF7 cells were grown in 8 well chamber slides and treated with or without TNFα/CHX. Live cell imaging was performed immediately after exposure. Bright field images for live video-microscopy were captured at 30 mins interval for 10 hrs in a fully enclosed fluorescent microscope (Zeiss Axio Observer; Zeiss, Göttingen Germany) with humidity, CO_2, and temperature control. All immunocytochemistry slides were imaged with this microscope and processed later with Image J software.

Measurement of Caspase 3/7 activity: GFP and GFP-Tau MC F7 cells were seeded at equal densities of 250×10^3 cells/well in a 6 well plate (BD Falcon) for 48 hrs at 37°C with 5% CO_2. Cells were rinsed twice with basal media before being exposed to TNFα (50ng/ml) and CHX (15 ug/ml) in basal media with 2% FCS for 0, 3, or 6 hrs. Cell extraction procedure performed using the Sensolyte^{TM} Homogenous Rh 110 Caspase-3/7 assay kit (Ana Spec # 71141) according the manufacturer's specifications. Samples were stored at -80°C prior to use. All components were thawed gently to room temperature before use. Fresh caspase-3/7 substrate solution was prepared at the time of the assay. 150 µl of each sample was dispensed per well in a 96 well plate and 50 µl substrate solution was added, mixed thoroughly and incubated for 1 hr in a shaker protected from light. Fluorescence intensity was measured by an FL×800 Fluorescence reader (BIO-TEK Instruments, Vermont) at Excitation / Emission wavelengths of 496 / 520nm. The data reflects net caspase-3/7 activation relative to time zero, and is an average of three independent experiments. GFP-Tau 2N MCF7 cells were similarly treated with TNFα / CHX for 0, 4 or 6 hrs and caspase activation was determined as discussed. This procedure was also performed for MCF7 cell that either had or had not undergone TNFα selection. Cells were grown in a 6 well

plate in complete absence of TNFα and allowed to attain 35% confluency. Cells were then transiently transfected with scrambled siRNA and MAPT siRNA (120 pmol siRNA/well) as discussed above (see siRNA mediated tau knockdown and TNFα selection of MCF7 cells). Cells were treated with TNFα (50ng/ml) / CHX (15 µg/ml) (0, 3, 6 or 8 hrs) after 48 hrs of transfection and caspase 3/7 activity was measure as discussed above.

Statistics: Statistical analysis was performed with GraphPad Prism (Version 5) software. We performed unpaired t-test (2 tail) and one-way analysis of variance (ANOVA), with Tukey post analysis where appropriate. Statistical significance was achieved when $p < 0.05$.

Results:

TNFα selection in MCF7 cells

Tumor necrosis factor-alpha (TNFα) is a soluble pro-inflammatory cytokine often found elevated in solid tumors including breast cancer. At elevated levels TNFα upon binding to its receptor (TNFR1) is known to elicit an apoptotic response in cancer cells regardless of their p53 status, which makes it an attractive possible therapeutic. Although, TNFα is still being investigated as an anti-cancer agent, a number of studies have shown that tumor cells, through unresolved mechanisms, become resistant to the cytotoxic effects of TNFα. Here, a model is developed to investigate how cancer cells fail to respond to the cytotoxic effect of this cytokine. The hypothesis was that tau, a microtubule associated protein, played a role in how tumor cells respond to TNFα. This assumption was based on the facts that tau is often ectopically expressed in breast cancer cells. Additionally, tau expression is linked with Paclitaxel resistance in breast cancer, and microtubules are known to regulate TNFR1 function. Using the human breast cancer cell line MCF7, it is shown that when these cells acquire TNFα resistance, they up-regulate the expression of microtubule associated protein tau. To indicate that tau is necessary for TNFα resistance, it is found that a specific knockdown of tau renders TNFα-resistant cancer cells susceptible to TNFα-induced cell death. The following finding indicates that tau expression in breast cancer cells can be a deciding factor to determine TNFα sensitivity.

Prolonged exposure to TNFα causes upregulation of tau protein in MCF7 cells.

Although the prevalence of resistance to TNFα-induced cytotoxicity in tumor cells has been well documented (Aggarwal et al., 2012; Balkwill, 2009; Sugarman et al., 1985), the precise mechanism(s) mediating TNFα resistance remains largely undetermined. Previous reports indicated that microtubule stability can suppress TNFα signaling (Shivanna and Srinivas, 2009) and may interfere with the TNFR intracellular domain (Jackman et al., 2009). These findings led us to ask whether tau, a microtubule stabilizing protein, could also contribute to the regulation of TNFα signaling. Tau has been classically defined to be associated with microtubules and its abnormal phosphorylation has been implicated as a critical event during the pathogenesis of Alzheimer's (Ballatore et al., 2007). Aside from microtubule binding, it also participates in signal transduction (Lee et al., 1998), alters actin rearrangement (Sharma et al., 2007) and can form cellular aggregates to induce pathological neurodegenerative tauopothies (Alonso et al., 2008). Tau has been recently found ectopically expressed in breast tumors (Bhat and Setaluri, 2007; Rouzier et al., 2005) where it provides resistance against cancer therapies such as paclitaxel (Rouzier et al., 2005; Tanaka et al., 2009; Wagner et al., 2005). Here, it is first explored whether acquisition of TNFα-resistance in breast cancer cells was associated with increased levels of tau. The results indicate that continual exposure to TNFα for 10 weeks selected for a subpopulation of MCF7 cells that exhibited TNFα-resistance (Figure 2A) as determined by MTT assay. Cell apoptosis was evident during the initial selection process (1-3 weeks). However, cell death diminished around 4 to 5 weeks of TNFα exposure and the cells became completely resistant around 10 weeks of selection without any evidence of cytotoxicity (Figure 2A). Further, the selected cells displayed open colony morphology, diminished cellular

attachment (Figure 3A) and an epithelial-mesenchymal transition (EMT) as determined by E-cadherin loss (Figure 3B). The protein levels of endogenous soluble tau (unbound to tubulin) and insoluble tau (bound to tubulin) were greater than 2-fold higher in TNFα-resistant tumor cells compared to TNFα-sensitive non-selected cells (Figure 2B and C).

MCF7 cells acquire TNFα resistance through upregulation of tau.

To determine whether tau up-regulation was necessary to confer TNFα resistance, siRNA mediated knockdown of MAPT (microtubule associated protein Tau) was performed in MCF7 selected cells. Data indicated that tau upregulation was necessary for TNFα-resistance since a specific knockdown of tau protein levels (tau protein reduced by 75%) by RNAi (Figure 2D) reverted these cells back to being sensitive to TNFα-induced apoptotic responses such as cell rounding and blebbing (Figure 2E); (TNFα -induced apoptosis was induced in the presence of the translational inhibitor cycloheximide (CHX)). Significant caspase activation was evident when tau was knocked down in the selected cells (Fig 2F). These findings indicated that in MCF7 breast cancer cell line, the acquisition of tumor cell resistance to TNFα-induced cytotoxicity requires an upregulation of tau protein levels.

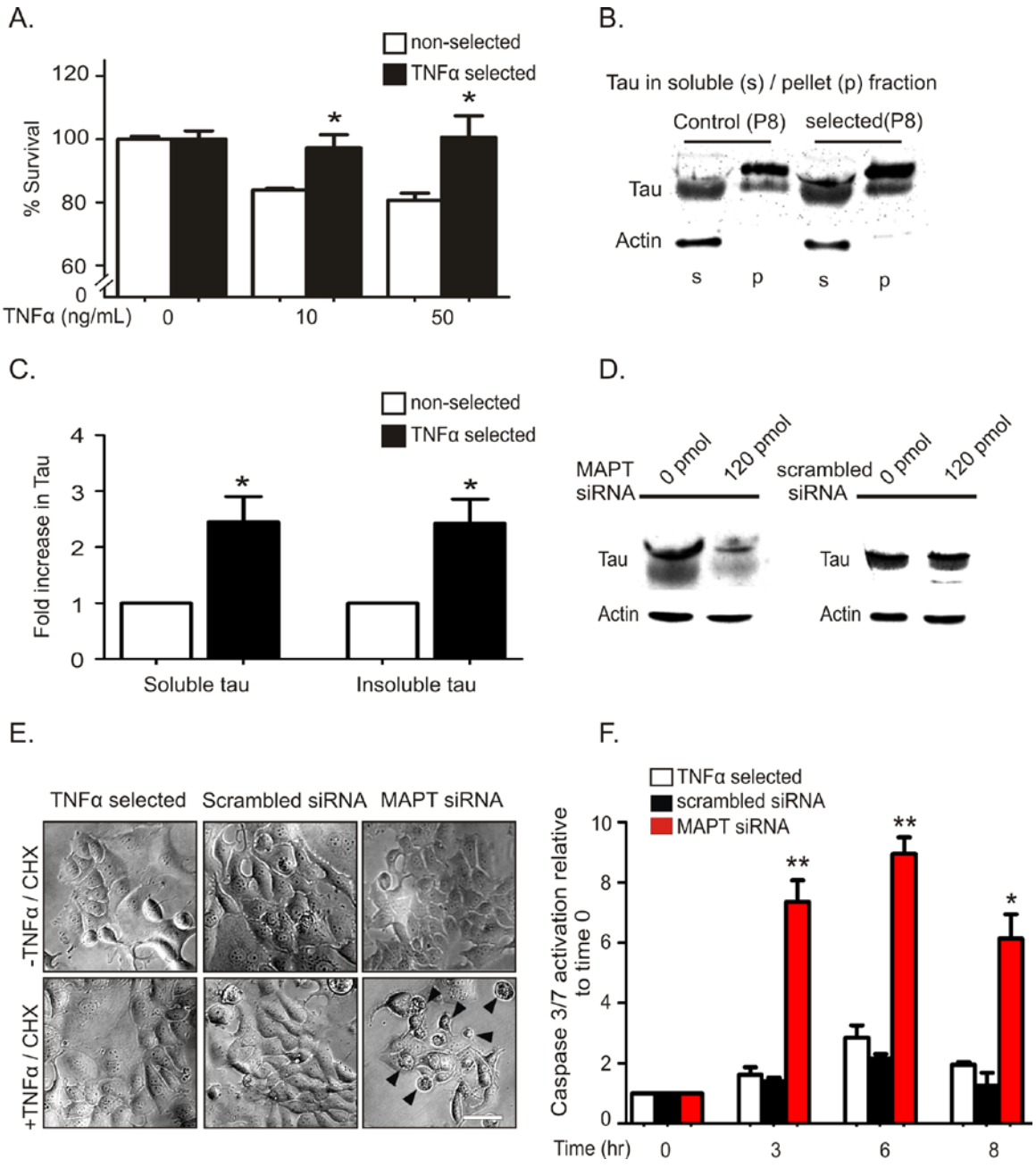

Figure 2: Acquired resistance to TNFα-induced cytotoxicity requires upregulation of tau protein. (A) MTT results (mean±SEM; n=3) from MCF7 cells exposed to 0, 10 or 50 ng/ml TNFα for 96 hrs. TNFα selected MCF7 cells show significant resistance to TNFα induced cytotoxicity at 10 and 50 ng/ml (*$p<0.05$; Student's t-test). (B) Microtubule binding assay (MtBA) of tau in soluble (s) and insoluble (p) protein fractions of MCF7 cells that either had (selected) or had not (control) undergone TNFα selection for eight passages (P8). Actin remains in the soluble compartment in this assay and serves as a loading control. (C) Quantification of panel B shows that selected cells have increased levels of tau in the soluble and insoluble cell fractions (*$p<0.05$; means±SEM; n=2) (Student's t-test). (D) Immunoblot analysis of siRNA (0, 120 pmol) mediated knockdown of microtubule associated protein tau (MAPT) in TNFα-selected

MCF7 cells. (E) TNFα selected MCF7 cells before (top row) and after (bottom row) exposure to TNFα (50 ng/ml)/CHX (15 µg/ml). The middle and right columns were transfected with scrambled siRNA or MAPT siRNA respectively (arrows = dead cells). Scale bar 36 µm. (F) Caspase 3/7 activation (means±SEM; n=3) following TNFα/CHX treatment in TNFα selected MCF7 cells with MAPT siRNA or scrambled siRNA transfection. Significantly higher caspase activation is observed at 3 (**$p<0.005$), 6 (**$p<0.005$) and 8 hrs (*$p<0.05$) (ANOVA analysis) when tau was silenced with MAPT siRNA.

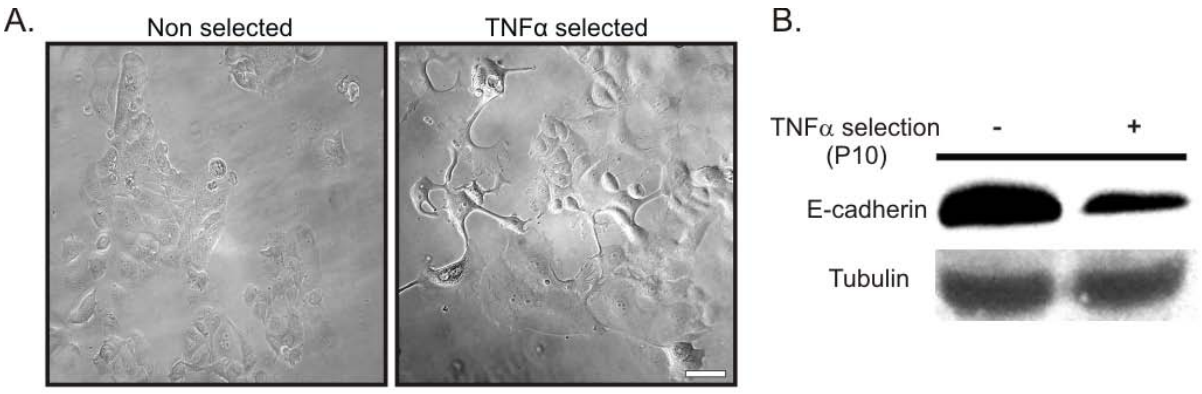

Figure 3: TNFα selected MCF7 cells. (A) Bright-field images of non-selected TNFα-sensitive and selected TNFα-resistant MCF7 cells. Scale bar 50 μm. (B) Immunoblot analysis of E-cadherin protein from non-selected and selected MCF7 cells (TNFα selection for 10 passages; P10). Results indicate reduction of E-cadherin protein in TNFα selected MCF7 cells. Tubulin used as a loading control.

Over-expression of GFP-Tau in cell lines

The microtubule associated protein tau has been heavily studied in neurons. But, little is known about its function in non-neuronal systems. Recent evidence indicates that tau expression is a predictive marker to determine sensitivity of several anti-mitotic drugs including Paclitaxel in breast, ovarian, pancreatic and prostate cancer. Resistance to Paclitaxel in breast cancer cells is provided through tau competing with Paclitaxel for binding with microtubules. In previous section, it has been shown that breast cancer cell line MCF7 acquires resistance to the multifunctional cytokine TNFα through significant up-regulation of tau protein. In this section, further work has been conducted for gaining a molecular insight into how tau mediates TNF-resistance. Based on previous findings, it is now hypothesized that tau overexpression can attenuate TNFα cytotoxicity. To address this hypothesis, GFP-tagged full-length human tau isoform is over-expressed in multiple cell lines. Here, the data shows, that over-expression of tau in human breast cancer cell lines and rat pheochromocytoma PC12 cells confer resistance to both TNFα induced cytotoxicity and cell apoptosis. Further, tau over-expression also attenuates TNFα-induced NFκB nuclear translocation in MCF7 cells. Based on reports, which indicate that microtubule stability alters TNFα signaling, it is also examined whether tau induced microtubule stabilization provides TNF-resistance. The data shows that microtubule stability may not be necessary to regulate TNFα signaling, since taxol stabilized microtubules fail to attenuate both NFκB and caspase activation. These following results suggest that tau expression is important to determine TNF- sensitivity of breast cancer cells and that it's binding to microtubules is not required in providing this resistance.

Over-expression of GFP-Tau inhibits TNFα induced cell cytotoxicity.

To elucidate the role of Tau in TNFα signaling, stable expression of GFP tagged full-length human tau isoform (GFP-Tau) was achieved in MCF7 breast cell line. Data indicated presence of endogenous tau protein in MCF7 cells (Figure 4A), which had an approximate molecular weight of 56 kDa and was predominantly present in the soluble (s) compared to the insoluble (p) fraction of the GFP transfected cells (Figure 4B, a). Over-expressed GFP-Tau displayed multiple Tau bands of higher molecular wt (˜100kDa) (Figure 4B, a) and was found to co-localize with microtubules (Figure 12D). Biochemical assay performed to determine microtubule stability in GFP-Tau cells, revealed increased immunoreactivity of tubulin in the pellet fraction (p) than the supernatant (s) (Figure 4B, b). The ratio of insoluble to soluble tubulin was significantly higher (about 8 fold) in GFP-Tau cells than control (Figure 4B, c). However, a significant fraction of the over-expressed tau isoform was detected in the soluble fraction (Figure 4B, a).

Based on previous finding, which shows, how tau up-regulation confers TNFα resistance, cell cytotoxicity is evaluated in MCF7 GFP-Tau cells when exposed to various concentration of TNFα (0, 5, 10, 25 and 50 ng/ml). After 96 hrs of exposure to toxic levels of TNFα (50 ng/ml), GFP-control cells were drastically diminished in cell number, exhibited extensive cell death (Figure 4C). In contrast, MCF7 cells with stable GFP-Tau expression exhibited no indication of cell loss or cell death. MTT result indicated that TNFα at concentrations of 25 and 50 ng/ml was significantly cytotoxic in GFP control cells (Figure 4D). TNFα addition however, failed to induce toxicity in the over-expressed GFP-Tau cells. It was also apparent that when GFP-control MCF7 cells were exposed to non-lethal doses of TNFα (10 ng/ml) for 72 hours they failed to proliferate. This was confirmed by a lack of cell number expansion as measured by a significant

down-regulation of the proliferative marker, phosphorylated histone H3 (phospho-H3) (Figure 4E a, b). In contrast, MCF7 cells expressing GFP-Tau continued to proliferate in the presence of non-lethal doses of TNFα (10 ng/ml) (Figure 4E a, b). Significant decrease in phosho-H3 level is also observed in MCF7 control cells at 24 and 48 hrs of TNFα treatment (10 ng/ml) (Figure 5) when compared to over-expressed GFP-Tau cells. When summarized, overexpression of tau in breast cancer cells impedes both the cytotoxic and cytostatic effects mediated by TNFα.

Over-expression of GFP-Tau inhibits TNFα induced cell apoptosis.

Live cell imaging was performed with MCF7 GFP cells exposed to TNFα (50 ng/ml) and cycloheximide (15 μg/ml) (CHX; protein translational inhibitor used to induce apoptosis). Data showed predominance of apoptotic hallmark features (Figure 6A). This was characterized by rounding up of adherent flattened cells followed by cell shrinkage, loss in membrane uniformity and membrane blebbing, which attained completion by the end of 10 hrs. On the contrary, MCF7 GFP-Tau cells under identical condition did not display such phenotypic alterations and maintained healthy flattened cell morphology (Fig 6A).

Apoptosis was confirmed in MCF7 GFP cells when they displayed caspase-3 activation post 6 hrs of addition of TNFα and CHX (Figure 6B). Data showed robust caspase activity with condensed nuclei in control (Fig 6B; top) in comparison to insignificant amount of activated caspase in MCF7 GFP-Tau cells (Fig 6B; middle). Caspase activity was also determined in another tau negative breast cancer cell line SkBr3 (Figure 7A and B). Stable tau overexpression in SkBr3 cells (Figure 7C and D) indicated inhibition of caspase-3 action in presence of TNFα and CHX (Figure 6B; bottom). To confirm that apoptosis was not a delayed event, GFP-Tau cells were further immunostained to detect cleaved caspase-3 after 18 hrs of exposure (Figure 8).

When quantified, data indicated significant increase in caspase activity in MCF7 GFP cells when compared to GFP-Tau cells at 6 hrs of TNFα/CHX addition (Fig 6C). To further investigate if tau mediated suppression of TNF-induced cytotoxicity was unique to cancer, we chose rat pheochromocytoma PC12 cells. Data showed that stable expression of full-length human tau isoform in PC12 cells (Figure 9A) significantly suppressed TNF-mediated cytotoxicity at 25 and 50 ng/ml of the cytokine (Figure 9B).

Tau has been previously identified as a substrate for caspases, where the resulting cleaved tau product is shown to induce neurofibrillary tangle formation (de Calignon et al., 2010; Fasulo et al., 2000). A significant loss of endogenous tau was noted in control cells that had extensive caspase activation (Figure 6D a, b) - this loss did not occur in cells over expressing GFP-Tau. It was therefore, concluded that tau over-expression was able to suppress TNFα induced apoptosis in breast cancer cells.

Tau over-expression suppresses NFkB nuclear translocation.

Once, the TNFα apoptotic pathway in cancer cells was elucidated, further investigation was conducted on the TNFα pro-survival pathway, which is elicited by NFkB activation in presence of this cytokine when administered alone. Data indicated that addition of TNFα (50 ng/ml) stimulated NFkB activation followed by its nuclear translocation in MCF7 GFP cells at 30 (Fig 10A, middle) and 60 mins (Figure 10A, bottom). TNFα addition in GFP-Tau cells however, did not contribute to detectable presence of nuclear NFkB (Figure 10B). Data of immunoblot assay performed with nuclear and cytoplasmic fractions of TNFα treated cells, further confirmed this result (Figure 10C and D). The amount of nuclear and cytoplasmic NFkB when quantified, displayed striking differences between control and GFP-Tau overexpressed cells. Significant

elevated amount of nuclear NFkB (about 2 fold) was detected in control at 30 and 60 mins of TNFα addition when compared to GFP-Tau fraction (Figure 10D, top). On the contrary, the amount of cytoplasmic NFkB was higher in GFP-Tau cells at the specified time points when compared to control (Figure 10D, bottom). Taken together, data indicated that over expression of GFP-Tau was also able to suppress TNFα induced nuclear NFkB translocation in MCF7 cells.

Taxol stabilized microtubules fails to inhibit TNFα signaling.

Reports indicate that microtubule stability can alter TNFα signaling (Jackman et al., 2009; Shivanna and Srinivas, 2009). Based on these findings, it was hypothesized that TNFα-resistance was mediated through stabilization of microtubules by tau. Using an alternative approach, it was asked whether stabilizing microtubules alone, independent of tau over-expression, could induce TNFα-resistance (Figure 11). Taxol drug was used to increase microtubule stability (Figure 11B) to similar levels found in our tau over-expression experiments (Figure 11C a, b). Cells with pre-stabilized microtubules (1μM taxol treated) remained TNFα-sensitive as measured by both caspase-3 activation (Figure 11D) and NFkB nuclear translocation (Figure 11E) indicating that increased microtubule stability alone could not mediate an increase in TNFα-resistance.

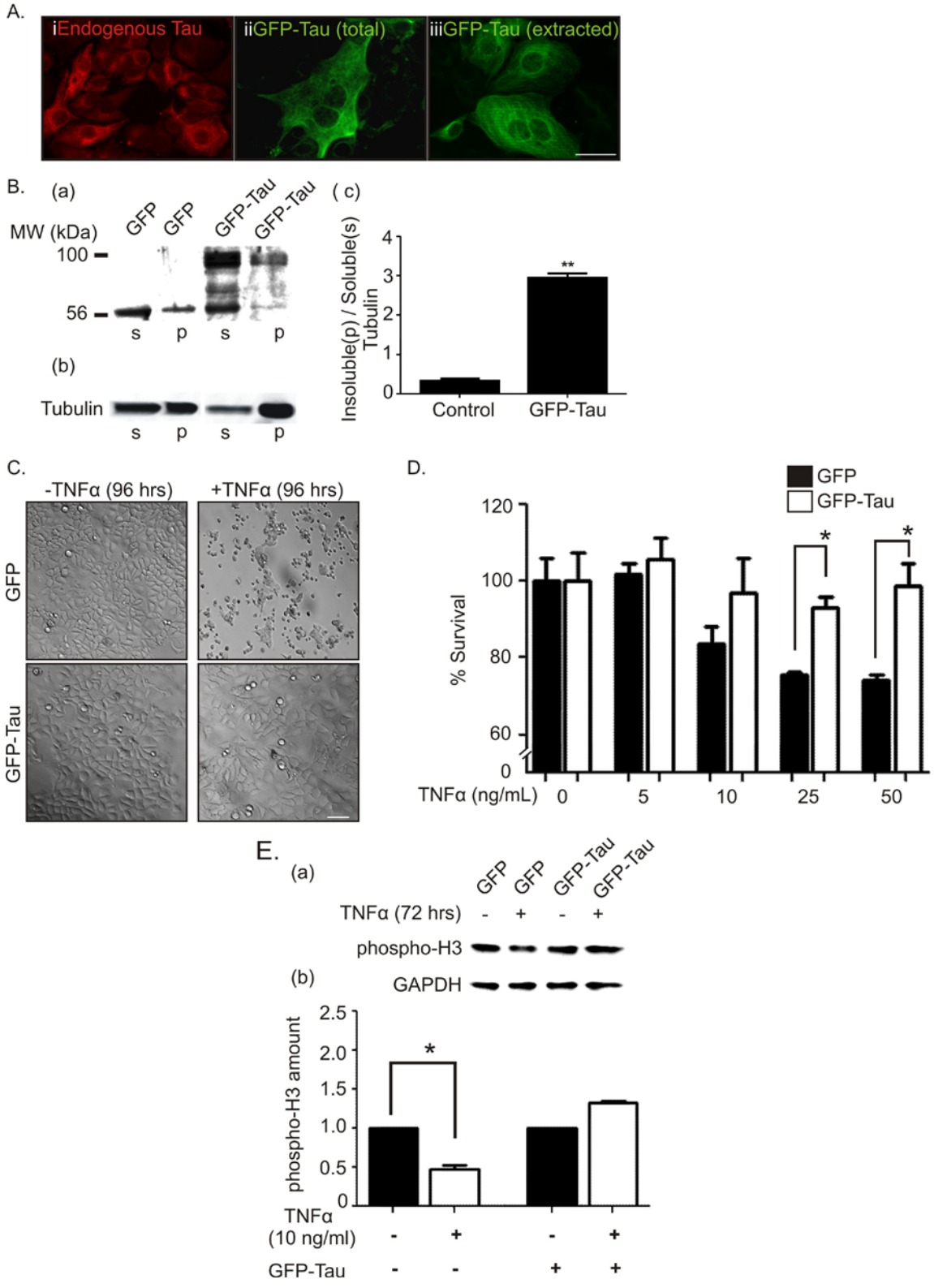

Figure 4: Over-expression of GFP-Tau suppresses TNFα-induced cell cytotoxicity. (A) Immunocytochemistry of endogenous tau in MCF7 cells (i), total GFP-Tau (ii) and insoluble

microtubule bound GFP-Tau (iii). Scale bar 25 μm. (B) Microtubule binding assay (MtBA) of tau (a) and tubulin (b) in soluble (s) and insoluble (p) fractions for both GFP and GFP-Tau MCF7 cells. Quantification of insoluble (p) to soluble tubulin (s) indicates significantly (**$p<0.005$) greater microtubule stability in GFP-Tau MCF7 cells (mean±SEM; n=3) (Student's t-test) (c). (C) Bright-field images of MCF7 cells stably transfected with GFP alone (top row) or GFP-Tau (bottom row) and exposed to TNFα (50ng/ml) for 96hrs. Scale bar 100μm. (D) MTT analysis (means±SEM; n=3) of GFP or GFP-Tau transfected MCF7 cells following 96hrs of treatment with TNFα (0, 5, 10, 25, or 50ng/ml). GFP-Tau confers significant resistance to TNFα induced cytotoxicity at 25 (*$p<0.05$) and 50ng/ml (*$p<0.05$; Student's t-test). (E) Cellular proliferation in both GFP and GFP-Tau MCF7 cells was measured by phosphorylated histone H3 (phospho-H3) by immunoblot in the presence or absence of TNFα (10ng/ml) for 72hrs (a). Quantification of phospho-H3 levels reveals GFP control cells show a significant (*$p<0.05$; Student's t-test) decrease in proliferation following TNFα exposure after 72hrs (mean±SEM; n=2) (b).

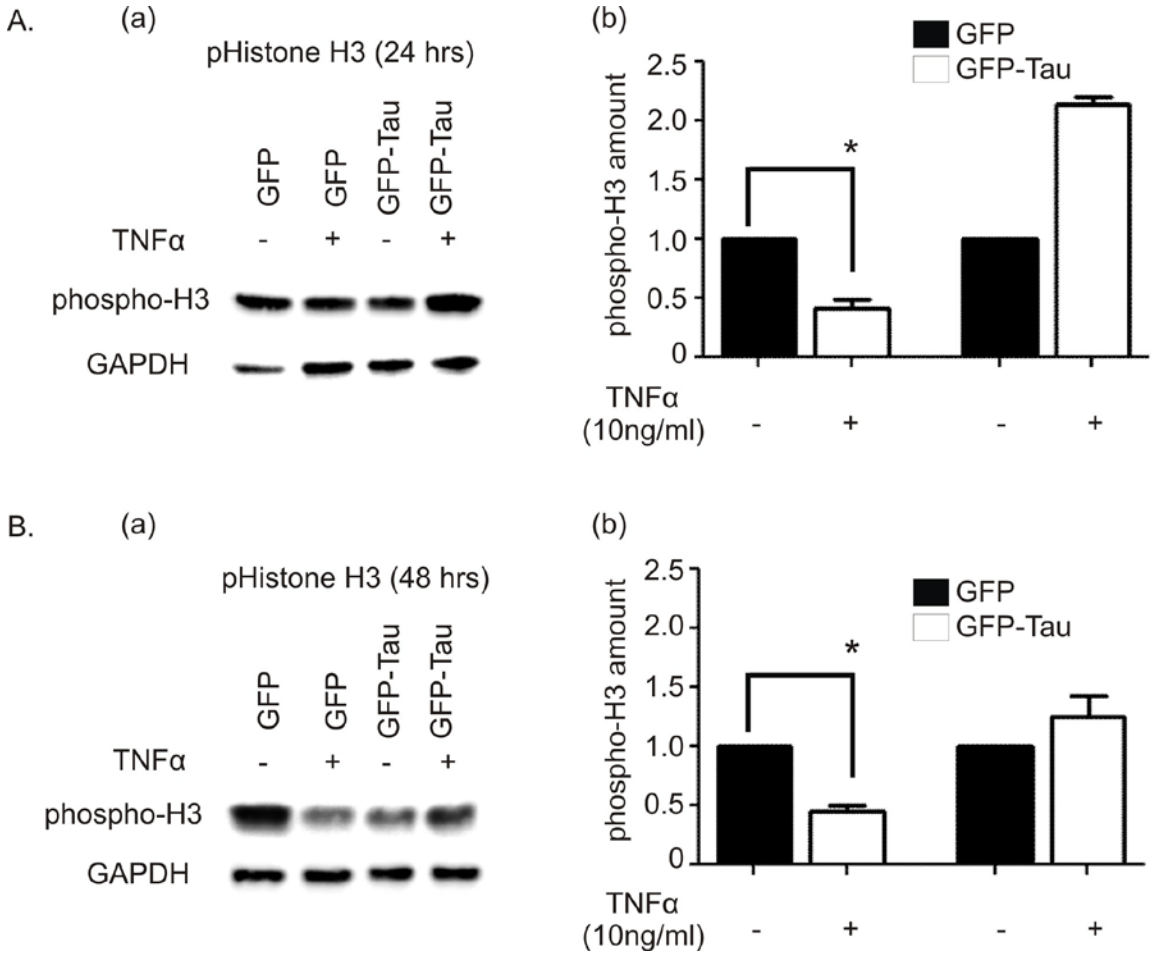

Figure 5: MCF7 cells with GFP-Tau overexpression continue to proliferate in presence of TNFα. WB was performed following treatment with TNFα (10ng/ml) after 24 (A, a) and 48 hrs (B, a) in control MCF7 GFP and GFP-Tau cells. Phospho histone H3 antibody (phospho-H3) used as marker for cell proliferation and GAPDH as loading control. The phospho-H3 amount was quantified based on WB data and made relative to respective controls (A, b and B, b). The data shows significant (means ± SEM; n=2) decrease in phosho-H3 amount in GFP cells with TNFα addition at 24 hrs (*$p<0.05$; Student's t-test) and 48 hrs (*$p<0.05$; Student's t-test). In contrast, GFP-Tau cells continue to proliferate in presence of TNFα.

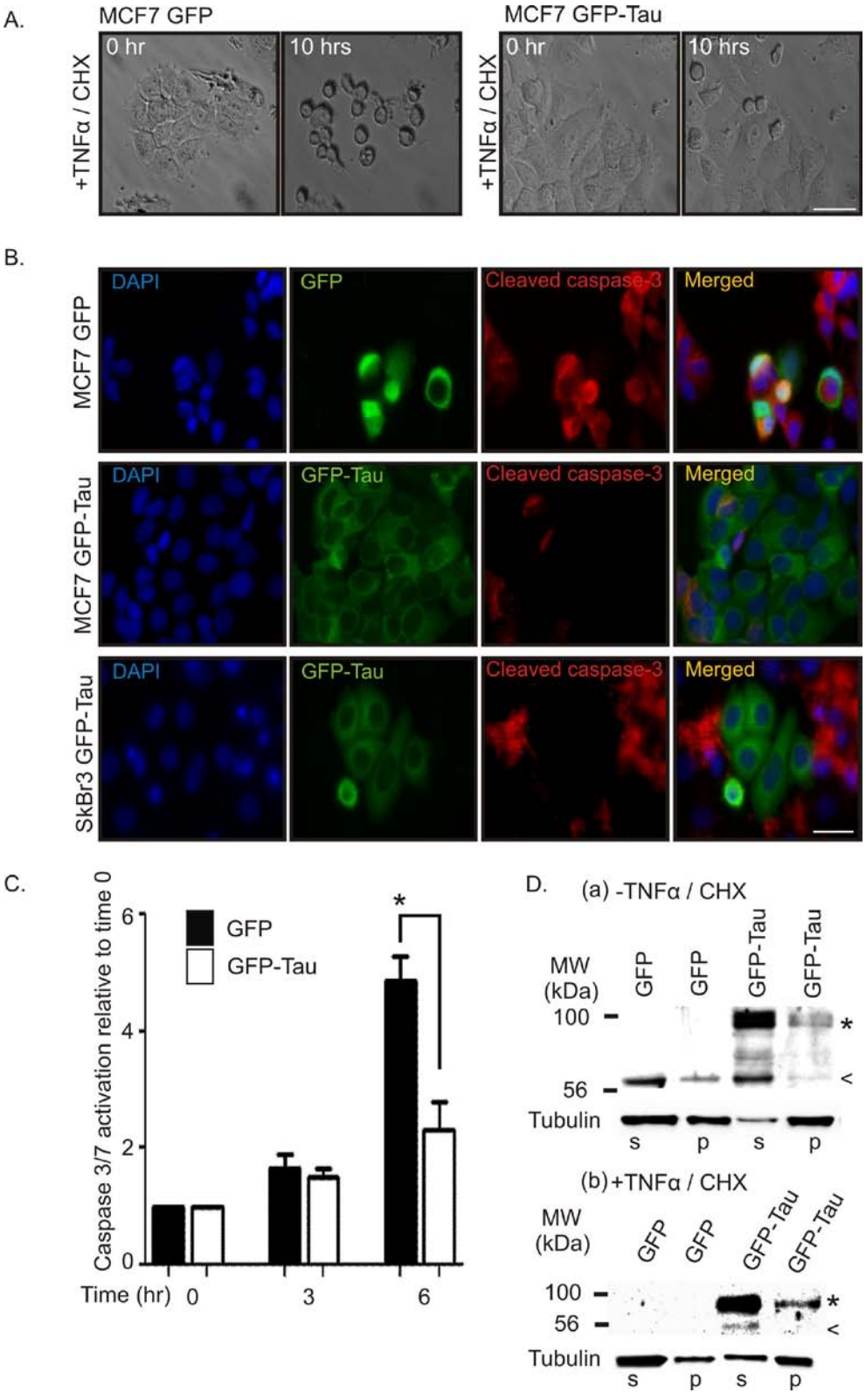

Figure 6: Over-expression of GFP-Tau suppresses TNFα-induced cell apoptosis. (A) Bright field images captured after exposing MCF7 GFP (left panel) and GFP-Tau cells (right panel)

with TNFα (50ng/ml) and Cycloheximide (CHX) (15ug/ml). The images represent the initial (0hr) and final time points (10hrs) of the performed live cell imaging. Scale bar 25 μm. Data provided by Jenkins E.C Jr. (B) Immunostaining done for cleaved caspase-3 following 6 hrs of treatment with TNFα / CHX in MCF7 GFP (top panel), MCF7 GFP-Tau (middle panel) and SkBr3 GFP-Tau (bottom panel; data provided by Peter Hannon) cells. Cleaved caspase-3 (red); GFP and GFP-Tau (green); 4', 6'- diamidino-2-phenylindole (DAPI) (blue); blue, green and red channels together as merged. Scale bar 30 um. (C) Quantification of caspase-3/7 activation reveals significantly less activation in GFP-Tau MCF7 cells (*$p<0.05$; Student's t-test) after 6 hrs of exposure to TNFα/CHX. Values are relative to time 0 (means±SEM; n=3). (D) Microtubule binding assay of tubulin and tau in soluble (s) and insoluble (p) fractions indicating the presence and amount of endogenous tau (~56kDa; <) and GFP-Tau (~100kDa; *) in both GFP and GFP-Tau transfected MCF7 cell lines without (a) or with (b) TNFα/CHX for 8-10 hrs.

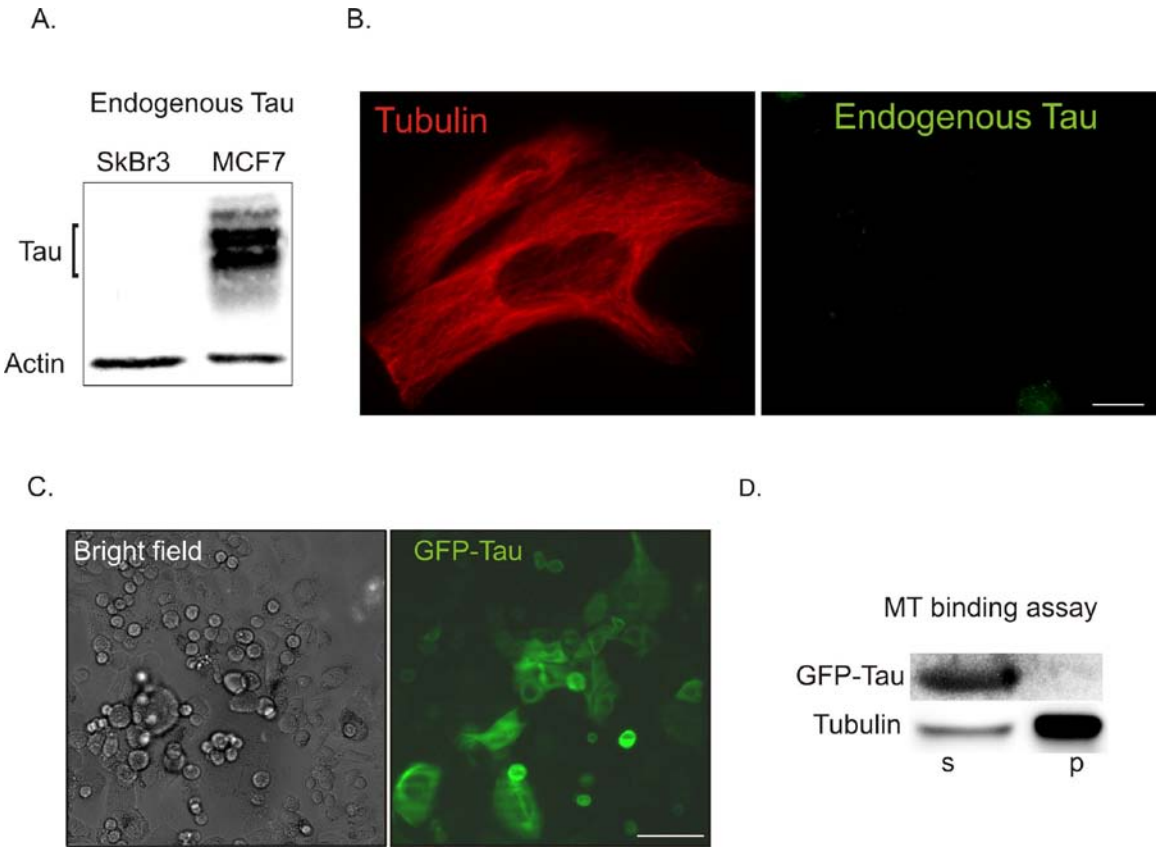

Figure 7: Tau expression in SkBr3 breast cancer cell line. (A) WB result indicates absence of endogenous tau protein in SkBr3 breast cancer cell line when probed with both DA9/134d antibodies. MCF7 used as a positive control; β-actin served as loading control. (B) Immunocytochemistry also confirms absence of endogenous tau in paraformaldehyde / methanol fixed SkBr3 cells. Tubulin (red), tau (green). Scale bar 12.5 µm .C) Bright field (left) and fluorescent (right) images of SkBr3 cells over-expressing GFP-Tau. Scale bar 50 µm. (C) Biochemical assay indicates presence of GFP-Tau in the soluble component (s) of the SkBr3 cells. Tubulin distribution shown in the soluble (s) and pellet (p) fractions of the cells.

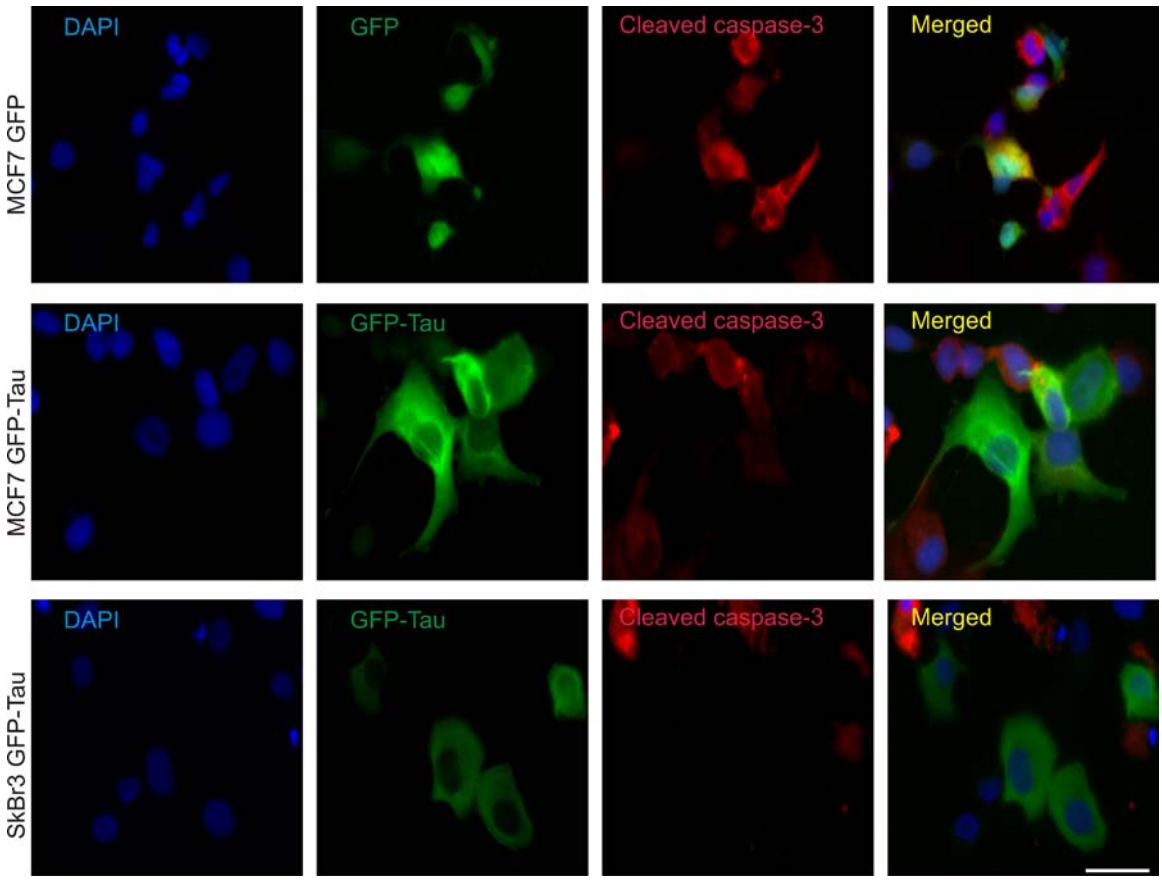

Figure 8: Caspase activation in human breast cancer cell lines after TNFα / CHX treatment. Immunostaining of cleaved caspase-3 in paraformaldehyde fixed cells after 18 hrs of treatment with TNFα (50 ng/ml) / CHX (15 µg/ml). MCF7 GFP (top panel), MCF7 GFP-Tau (middle panel) and SkBr3 GFP-Tau (bottom panel; data provided by Peter Hannon). DAPI (blue), GFP / GFP-Tau (green), cleaved caspase-3 (red), overlap of all channels as merged. Scale bar 25 µm.

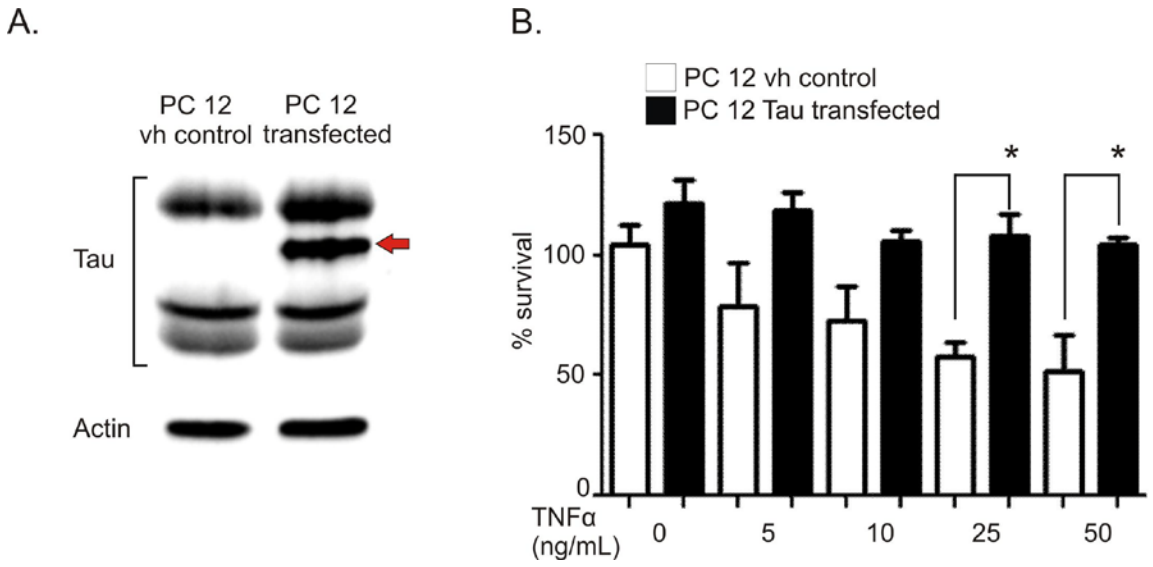

Figure 9: Over-expression of full-length human tau in PC12 cell line. (A) Immunoblot performed with PC12 cells that were stably transfected with either a vehicle control (vh control) or full-length human tau (transfected). The full-length human tau isoform is indicated with a red arrow. Multiple endogenous isoforms of tau are also visible. Actin used as a loading control. (B) MTT analysis (means ±SEM; n=3) of transfected PC12 cells exposed to TNFα (0, 5, 10, 25, or 50ng/ml) for 96 hrs. Results indicate that full-length tau expression (Tau transfected) confers significant resistance to TNFα induced cytotoxicity at 25 and 50ng/ml (*$p<0.05$; Student's t-test); this data is provided by Rodriguez N.N.

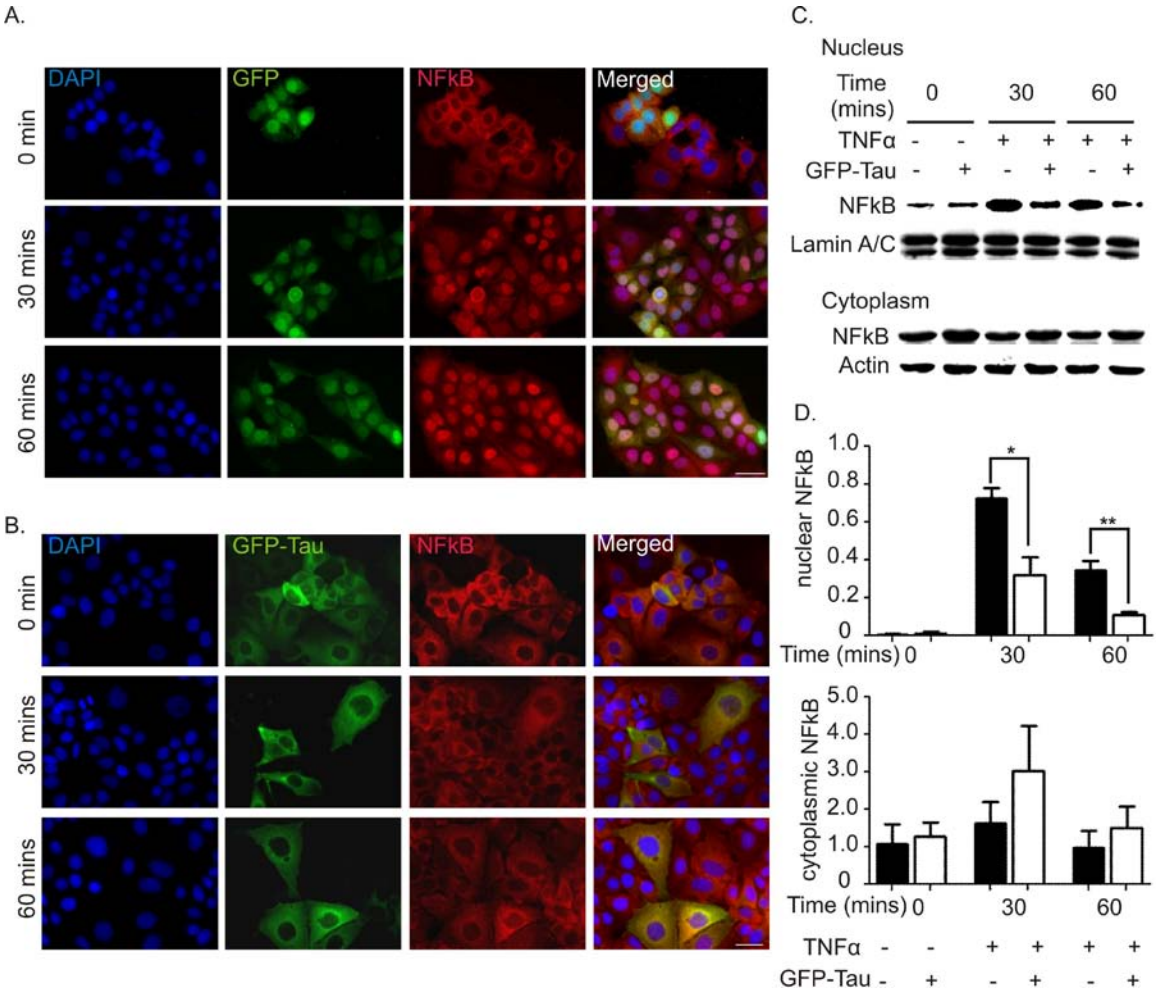

Figure 10: GFP-Tau over-expression suppresses NFκB nuclear translocation. (A) MCF7 GFP cells were immunostained for NFκB following addition of TNFα (50 ng/ml) at different time points of 0 (top panel), 30 (middle panel) and 60 mins (bottom panel). DAPI (blue), GFP (green), NFκB (red); overlap of all channels as shown as merged. Scale bar 25 um. Data shows, NFκB has cytoplasmic presence at time 0. TNFα induced NFκB activation causes its nuclear translocation at 30, and 60 mins in control cells. (B) NFκB immunostaining performed in MCF7 GFP-Tau cells after TNFα (50 ng/ml) treatment at 0 (top panel), 30 (middle panel) and 60 mins (bottom panel). Captured images represent predominance of NFκB in the cytoplasm of GFP-Tau cells at 30 and 60 mins of TNFα addition. Scale bar 25 µm. (C) Immunoblot performed with nuclear and cytoplasmic fractions of MCF7 cells and analyzed for NFκB following TNFα (50 ng/ml) addition. Both lamin A/C and PCNA (not shown) were used as a loading control for nuclear fraction and β-actin for cytoplasmic fraction. (D) Amount of NFκB present in the nucleus (top) (means ± SEM; n=3) and cytoplasm (bottom) (means ± SEM; n=3) was quantified from immunoblot results and were made relative to the loading controls (PCNA for nucleus; actin for cytoplasm). Significant NFκB nuclear translocation is observed in MCF7 control cells when compared to GFP-Tau cells at 30 mins (*$p<0.05$; Student's t-test) and 60 mins (**$p<0.005$; Student's t-test) with TNFα addition.

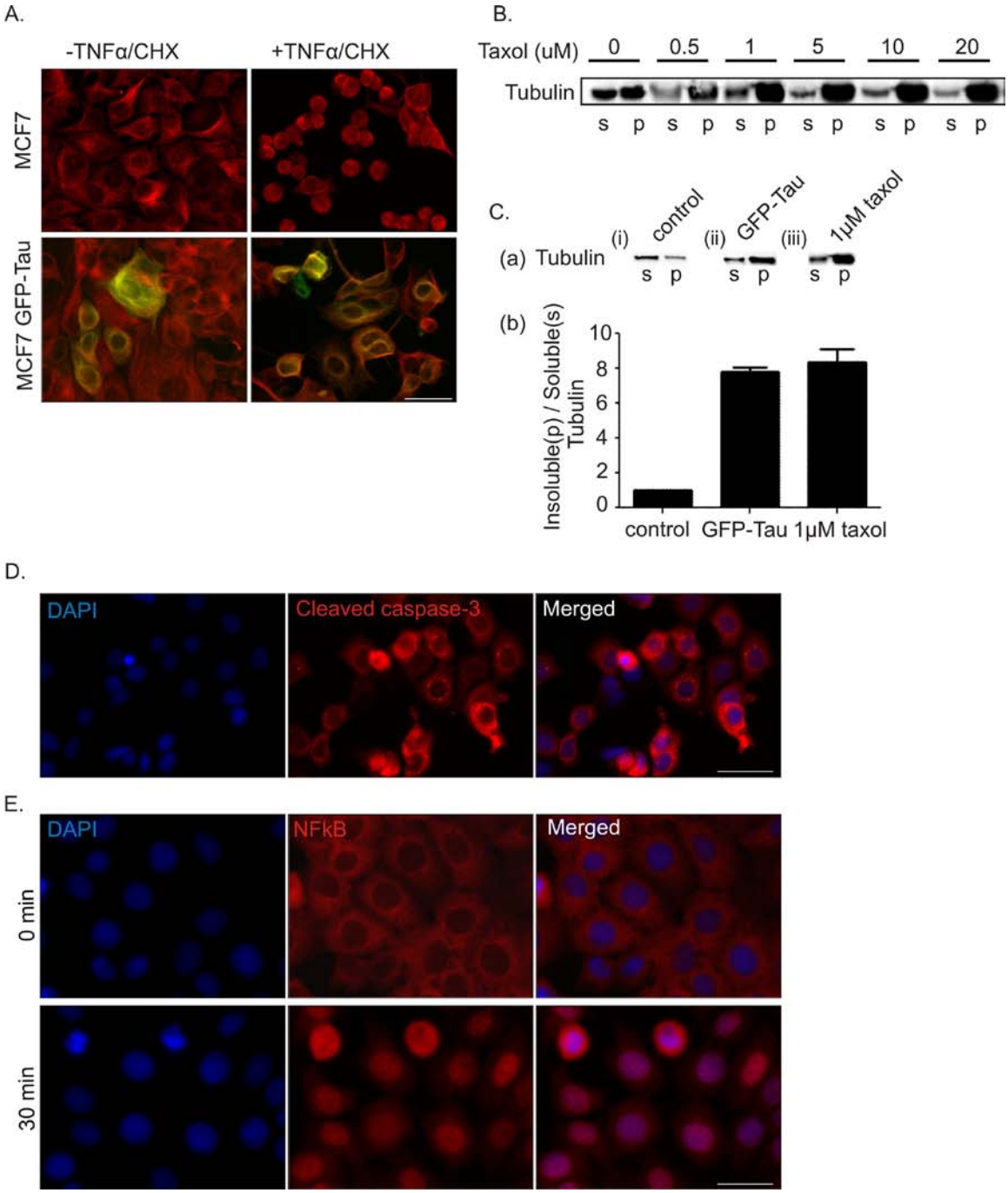

Figure 11: Taxol stabilized microtubules in MCF7 cells fail to suppress TNFα signaling. (A) Tubulin immunostaining performed in MCF7 control (top panel) and over-expressed GFP-Tau cell lines (bottom panel) in absence (left column) and presence (right column) of TNFα / CHX. Tubulin (red), GFP-Tau (green), red and green together as yellow / orange. Scale bar 50 μm. Images represent disrupted tubulin architecture in MCF7 control cells 6-8 hrs post TNFα / CHX addition. (B) Immunoblot results display the extent of microtubules stabilized under different concentration of taxol (0, 0.5, 1, 5, 10 and 20 μm) drug in MCF7 cells. Biochemical

assay performed by separating the soluble (s) and pellet (p) fractions of the cells after 1 hour of Taxol addition. (C) WB shows tubulin distribution in the s and p fractions of MCF7 control (i), GFP-Tau (ii), and 1 µM taxol stabilized (iii) cells (a). Quantification of stabilized microtubules (as fold increase) in MCF7 control, GFP-Tau and 1µM taxol stabilized cells (b). Data suggests that 1µM taxol stabilizes microtubules to a similar extent as that stabilized by the over-expressed GFP-Tau (means ± SEM, n=2 to 3). (D) Immunostaining result of cleaved caspase-3 in taxol (1µM) stabilized MCF7 cells after 6 hrs of exposure to TNFα / CHX. Taxol treated cells without TNFα/CHX addition had no caspase activation (data not shown). DAPI (blue), cleaved caspase-3 (red), blue and red channels together as merged image. Scale bar 50 µm. (E) NFκB immunostaining performed with taxol (1µM) stabilized MCF7 cells before (0 mins) (top panel) and after (30 mins) (bottom panel) TNFα (50 ng/ml) addition. DAPI (blue), NFκB (red), blue and red channels together as merged image. Scale bar 30 µm.

Over-expression of N-terminal Tau domain

Tau has been shown to play an important role in various signal transduction pathways, besides its classical role to stabilize microtubules. It has been previously shown that in MCF7 breast cancer cells tau up-regulation is necessary to acquire resistance to the cytokine TNFα. Further, it is also shown that tau overexpression confers resistance to TNFα induced cell cytotoxicity and apoptosis in breast cancer cells. These findings also indicate that taxol-induced microtubule stability alone cannot provide resistance to TNFα. Since, the C-terminus tau region contains the microtubule binding domains (MTBDs), that associate with and stabilize the microtubules, we hypothesized that loss of C-terminus will not impair tau mediated regulation of TNFα signaling. Therefore, through site-directed mutagenesis, the N-terminal domain of tau is generated that lacks all the MTBDs to explore its relationship with TNFα signaling. The following data indicates that tau binding to tubulin is not necessary to inhibit TNF-resistance, since; the N-terminal tau domain is sufficient to suppress both TNFα induced NFκB and caspase activation in MCF7 cells.

Expression of N-terminal tau domain in MCF7 cells.

The previous data confirmed that over-expression of full-length tau suppressed TNFα response in breast cancer cell lines. Further investigation was conducted to determine the mechanistic region of tau that is involved in regulation of TNFα signaling. The first approach was based on reports, which indicate that stabilized microtubules can alter TNFα signaling (Jackman et al., 2009; Shivanna and Srinivas, 2009). Since, tau is a microtubule-associated protein, it was hypothesized that tau over-expression confers resistance to TNFα signaling

through stabilization of microtubules. It was, therefore, reasoned that overexpression of a mutant tau (N-terminal tau), lacking microtubule binding capability would not confer TNFα resistance. Using an alternate approach, cells with taxol-stabilized microtubules were exposed to TNFα. Data indicated that microtubule stabilization by taxol was unable to confer TNFα resistance in breast cancer cells.

After proving the hypothesis wrong, it was asked whether N-terminal tau overexpression could still confer TNFα-resistance in breast cancer cells in order to better understand the underlying mechanism. Through site-directed mutagenesis, the N-terminal tau domain absent in all MTBDs (Figure12A) was generated. It was first noted that stable expression of N-terminal-tau exhibited a punctate pattern of localization in MCF7 cells (Figure 12B). In contrast to, the full-length tau isoform that exhibited cytoplasmic distribution, promoted filamentous process formation with altered cell phenotype, expression of N-terminal tau domain in MCF7 cells did not display such changes in cell morphology (Figure 12B). N-terminal tau was predictably truncated in size compared to full-length tau (Figure 12C a), did not co-localize with tubulin by immunocytochemistry (Figure 12D) and was restricted to the soluble compartment in cells and therefore unbound to tubulin (Figure 12C b).

N-terminal tau domain inhibits caspase activation in MCF7 cells.

Immunocytochemistry result indicated that MCF7 GFP control cells displayed robust caspase-3 activation in presence of TNFα (50 ng/ml) and the protein translational inhibitor cycloheximide (CHX; 15μg/ml)) (Figure 13A). Caspase-3 activation was not evident in cells with N-terminal tau expression when compared to the control cells (Figure 13A). Biochemical

assay to quantify caspase activity, showed significant increase in caspase 3/7 activation in control cells at 4 and 6 hrs of TNFα / CHX administration (Figure 13B). Cells with GFP-Tau2N expression did not indicate such increase in caspase activity. Further, exposure to TNFα and CHX led to the loss of endogenous tau in GFP control cells (Figure 13C). Such loss was not evident with N-terminal tau protein. Taken together, the data indicated that N-terminal tau domain could provide resistance to TNFα induced apoptosis and might not require tau to be bound to tubulin.

N-terminal tau domain is necessary to inhibit apoptosis.

To further confirm that N-terminal tau domain was necessary to suppress apoptosis, RNAi mediated knock down of the microtubule associated protein tau (MAPT) was conducted. Data showed that transient knock down of endogenous tau was achieved in MCF7 cells; however, the N-terminal tau was completely resistant against MAPT siRNA (Figure 14A). Bright field images indicated that tau knocked down GFP control cells exhibited cell apoptotic features characterized by cell rounding and membrane blebbing in presence of TNFα / CHX (Figure 14B). In contrast, tau N-terminal domain expression was sufficient to suppress such apoptotic characteristics and the GFP-Tau2N cells maintained a healthy flattened morphology under identical condition (Figure 14B). When exposed to non-lethal dose of TNFα (10 ng/ml) for 72 hrs, the control cells displayed drastic decrease in cell proliferation as measured by phosphorylated histone H3 amount (Figure 14C). Decrease in phospho H3 amount was not observed in cells with N-terminal tau expression. The data, thus, confirmed that N-terminal tau domain was necessary and

sufficient to inhibit TNFα induced apoptosis and the GFP-Tau2N cells were able to proliferate in presence of the cytokine.

N-terminal tau domain inhibits NFκB nuclear translocation.

In presence of TNFα alone, the pro-survival pathway of this cytokine was further studied in MCF7 cells. GFP cells showed predominant NFκB nuclear translocation after an hour exposure to TNFα (50 ng/ml) (Figure 15A). GFP-Tau2N cells failed to display presence of nuclear NFκB under similar conditions (Figure 15B). Sub-cellular fractionation data further confirmed increased amount of nuclear NFκB in control cells at 30 and 60 mins of TNFα addition in comparison to GFP-Tau2N nuclear extract (Figure 15C). Higher amount of cytoplasmic NFκB was observed in GFP-Tau2N cells. The data indicated that tau N-terminal domain could also attenuate NFκB nuclear translocation.

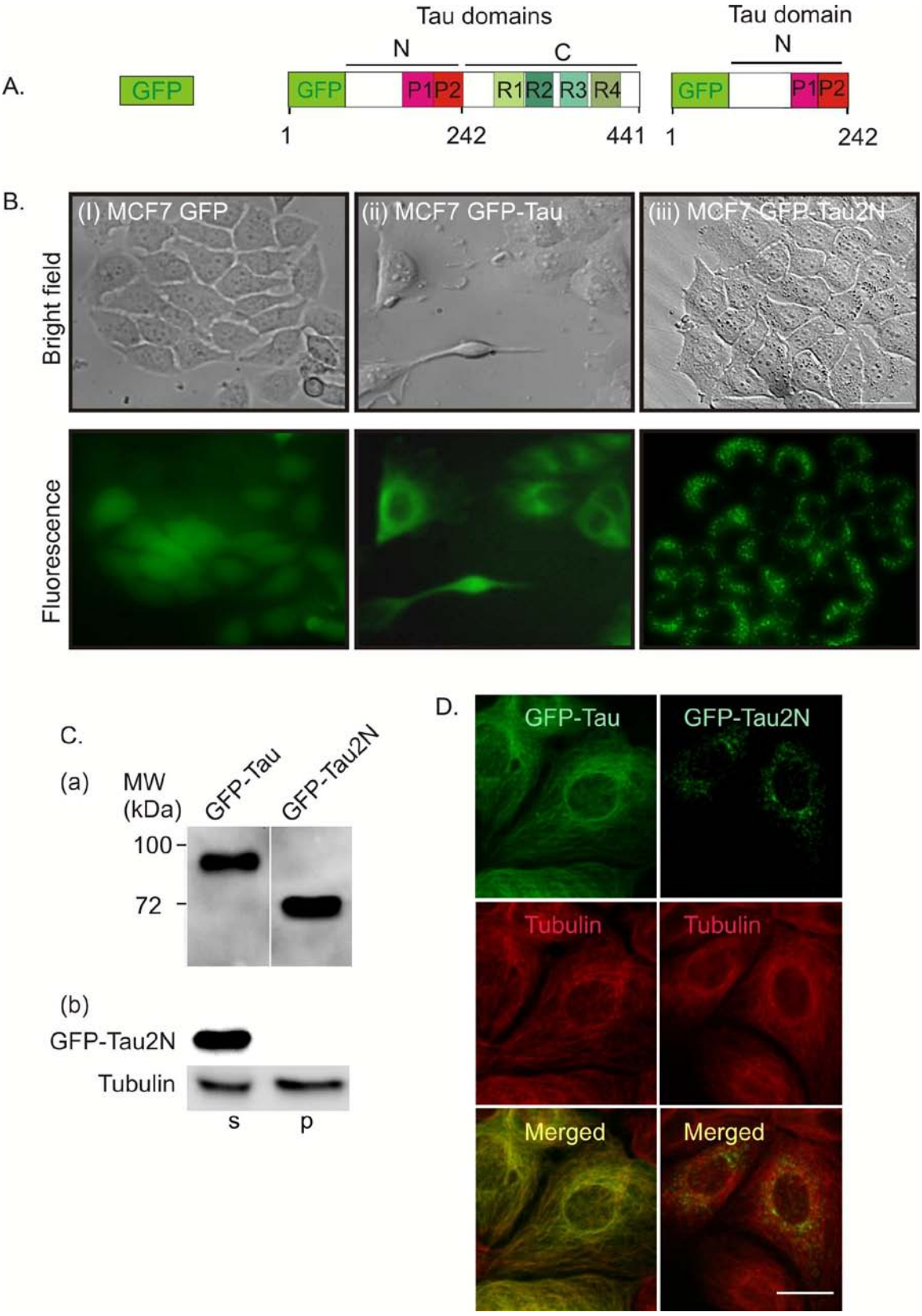

Figure 12: N-terminal tau domain expression in MCF7 cells. (A) Schematic representation of

GFP (left), full length GFP-Tau (middle) and GFP-Tau2N (right) constructs. Amino and carboxy terminals are represented by “N” and “C” respectively. Proline rich (P) and microtubule binding (R) regions are indicated. (B) Live fluorescent microscopy reveals both bright field (top row) and fluorescence (bottom row) of GFP (left), GFP-Tau (middle), and GFP-Tau2N (right) expression patterns in MCF7 cells. Scale bar 35µm. (C) Immunoblot indicates the expected molecular weight of full length GFP-Tau (~100kDa) and GFP-Tau2N (~72kDa) in total cell extract (a). GFP-Tau2N is only detected in the soluble (s) fraction by MtBA, indicating no binding to microtubules (b). (D) Immunocytochemistry of GFP-Tau (left column) and GFP-Tau2N (right column) MCF7 cells indicates GFP-Tau is associated with microtubules while GFP-Tau2N protein is not associated with microtubules. GFP-Tau / Tau2N (green), tubulin (red), co-localization (yellow). Scale bar 12.5µm.

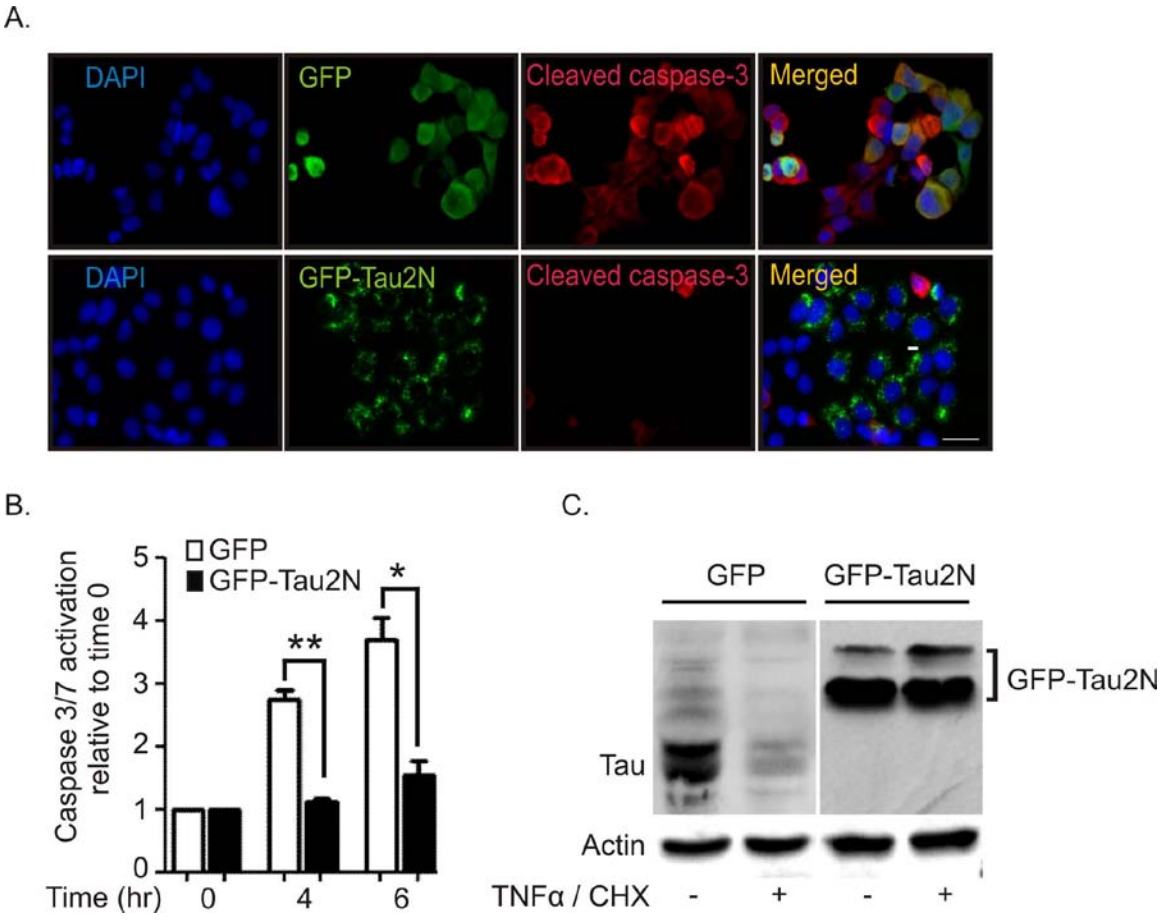

Figure 13: Tau N-terminal domain inhibits caspase-3 activation. (A) Immunocytochemistry of caspase-3 activation (red) in GFP (top row) and GFP-Tau2N MCF7 cells (bottom row) following 6 hrs of exposure to TNFα (50ng/ml)/CHX (15μg/ml) (DAPI (blue), GFP (green), Cleaved caspase-3 (red), overlap of all channels shown as merged) Scale bar 25 μm. (B) Biochemical measurement of caspase-3/7 activity in GFP and GFP-Tau2N MCF7 cells following 0, 4 and 6 hrs of TNFα/CHX exposure reveals significantly less caspase activity at 4 (**$p<0.005$) and 6 hrs (*$p<0.05$) in GFP-Tau2N MCF7 cells (means±SEM; n=3) (Student's t-test). (C) Immunoblot data indicates loss of endogenous tau in GFP control cells post 6 hrs of exposure to TNFα/CHX. Such loss is not evident for GFP-Tau2N protein under similar conditions. Actin used as loading control.

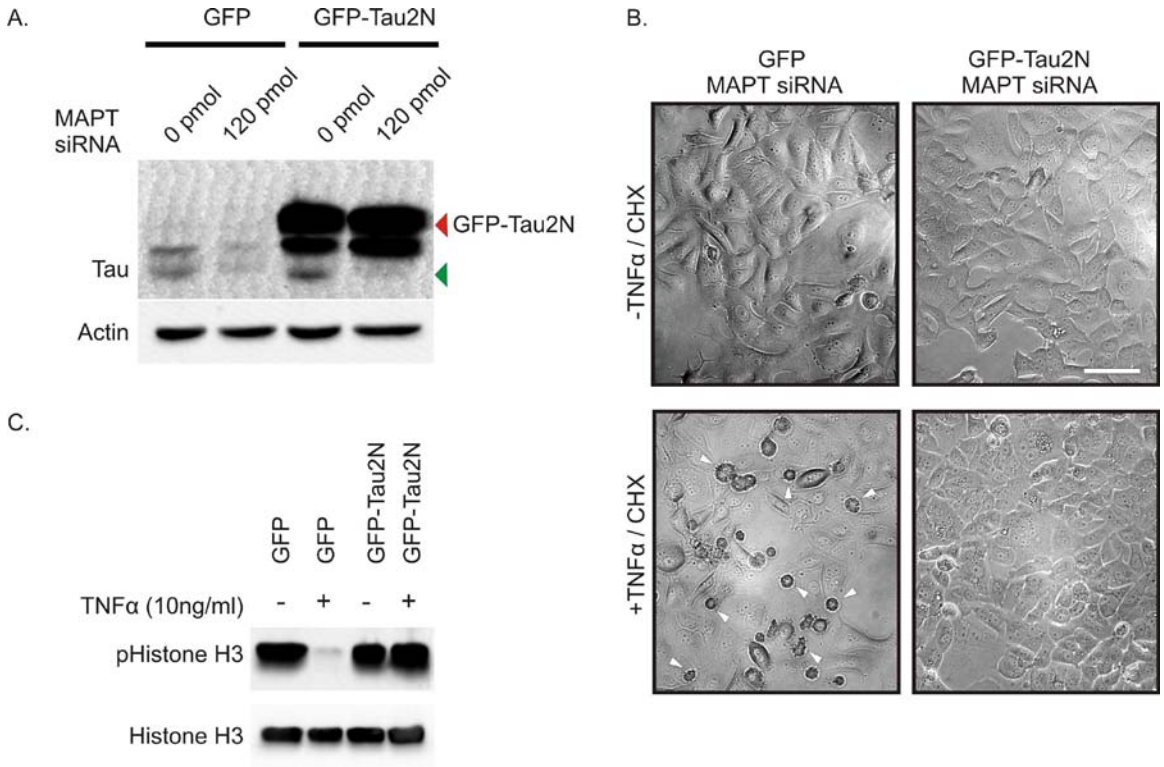

Figure 14: N-terminal tau domain is necessary to inhibit apoptosis. (A) Immnunoblot data of RNAi (0, 120 pmol) mediated knockdown of MAPT in MCF7 GFP and GFP-Tau2N cells. N-terminal tau domain is resistant to MAPT RNAi. (Endogenous tau indicated with green arrow; GFP tagged N-terminal tau indicated with red arrow). Actin used as loading control. (B) Bright field images of MCF7 GFP and GFP-Tau2N cells before (top row) and after (bottom row) exposure to TNFα (50 ng/ml)/CHX (15 µg/ml). The left and right columns were transfected with MAPT siRNA for 48 hrs (arrows = apoptotic cells). Scale bar 50 µm. (C) Cellular proliferation in both GFP and GFP-Tau2N MCF7 cells was measured by phosphorylated histone H3 (phospho-H3) amount in the presence or absence of TNFα (10 ng/ml) for 72 hrs. Total histone H3 amount with ± TNFα is relatively equal in GFP and GFP-Tau2N cells.

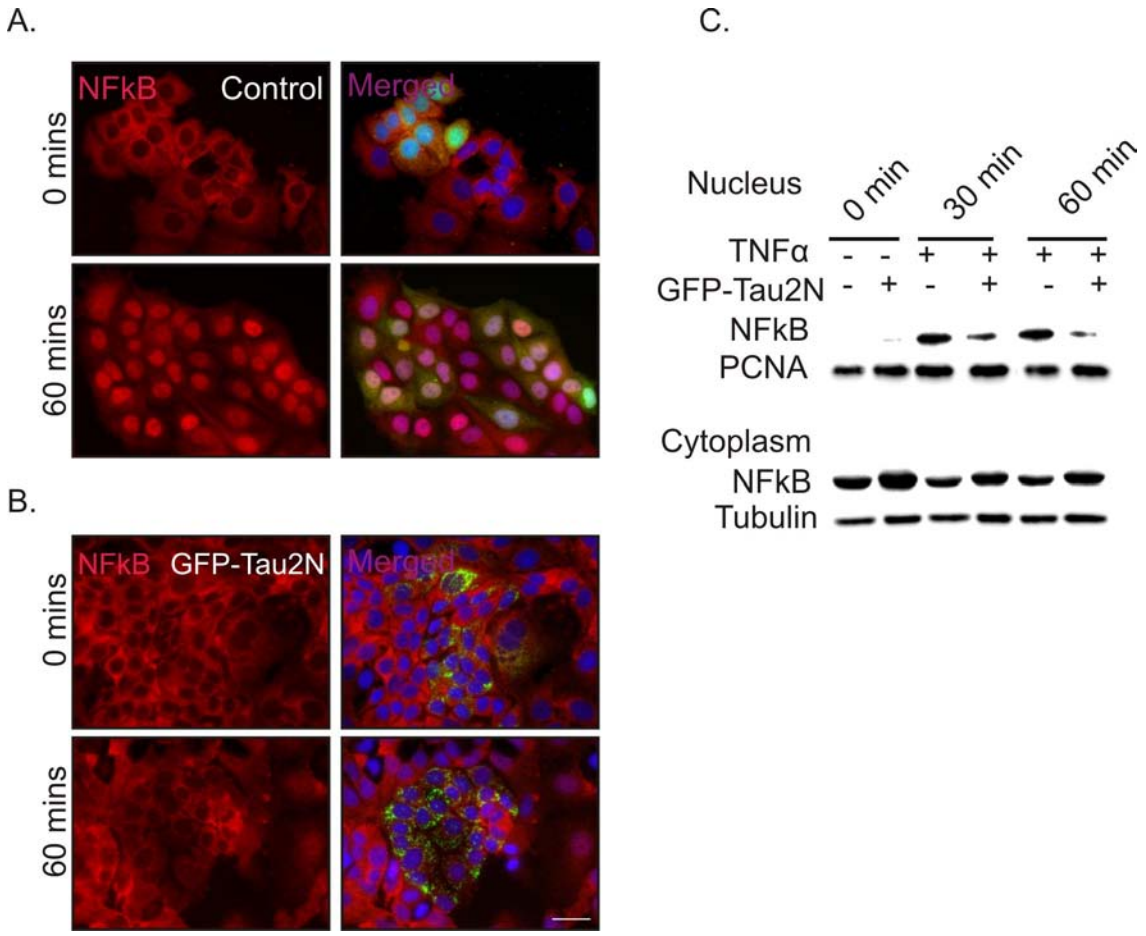

Figure 15: Tau N-terminal domain attenuates NFκB nuclear translocation. Immunostaining data of NFκB in MCF7 GFP control cells (A) and GFP-Tau2N cells (B) at 0 min (top row) and 60 mins (bottom row) of TNFα (50 ng/ml) addition. Data indicates decreased nuclear translocation of NFκB (red) in GFP-Tau2N MCF7 cell lines. NFκB (red), overlap of blue (DAPI), green (GFP) and red (NFκB) channels shown as merged. Scale bar 25 μm (C) Immunoblot analysis was performed to detect nuclear versus cytoplasmic NFκB in MCF7 GFP and GFP-Tau2N cells at 0, 30 and 60 min after TNFα (50 ng/ml) exposure. PCNA used as loading control for nuclear fraction and tubulin for cytoplasmic fraction.

Future direction:

Tau N-terminal proline rich region has been reported to interact with SH3 homology domains of several proteins (Lee et al., 1998; Reynolds et al., 2008). In this study, it has been shown that N-terminal tau domain is able to inhibit TNFα responses in MCF7 breast cancer cells. We were further interested to investigate the effect on TNFα signaling after removal of the proline rich regions from the N-terminal tau domain. Two proline rich sites (P1 and P2) are present in N-terminal tau region, which begin at amino acid residue 151 for P1 and 198 for P2 (Figure 16A). Two mutants of tau N-terminal region, which contain partial deletion of the proline rich regions (removal of P2) and complete deletion of the proline rich sites (removal of both P1 and P2) were generated. Through site directed mutagenesis, tau mutants expressing tau N terminal region with 151 (GFP-Tau151; P1 and P2 absent) and 198 (GFP-Tau198; P1 present) amino acid residues (Figure 16A) were made.

Immunoblot data indicates the expression of GFP-Tau151 and GFP-Tau198 mutated tau proteins and the protein bands display a molecular weight close to 70 kDa (Figure 16B). In contrast to full length N-terminal tau, that exhibits a punctate pattern of localization, stable expression of both GFP-Tau151 and GFP-Tau198 display an even pattern of distribution through out MCF7 transfected cells as revealed by fluorescence microscopy (Figure 16C). Further, preliminary data shows robust caspase-3 activity in both GFP-Tau151 and GFP-Tau198 expressing MCF7 cells when exposed to TNFα (50 ng/ml) and CHX (15μg/ml) (Figure 16D). The data suggests that partial or complete deletion of the proline rich sites in N-terminal tau region fails to inhibit TNFα mediated apoptotic pathway and thus, may play a role in regulation of TNF-responses. The data will be further strengthened, when truncation of the proline rich sites

from the full-length tau, will also exhibit failure to suppress TNF-induced apoptosis in breast cancer cells.

This data endures at initial stage of investigation and further work is required to confirm whether proline rich region of N-terminal tau domain is indeed involved in regulation of TNFα signaling.

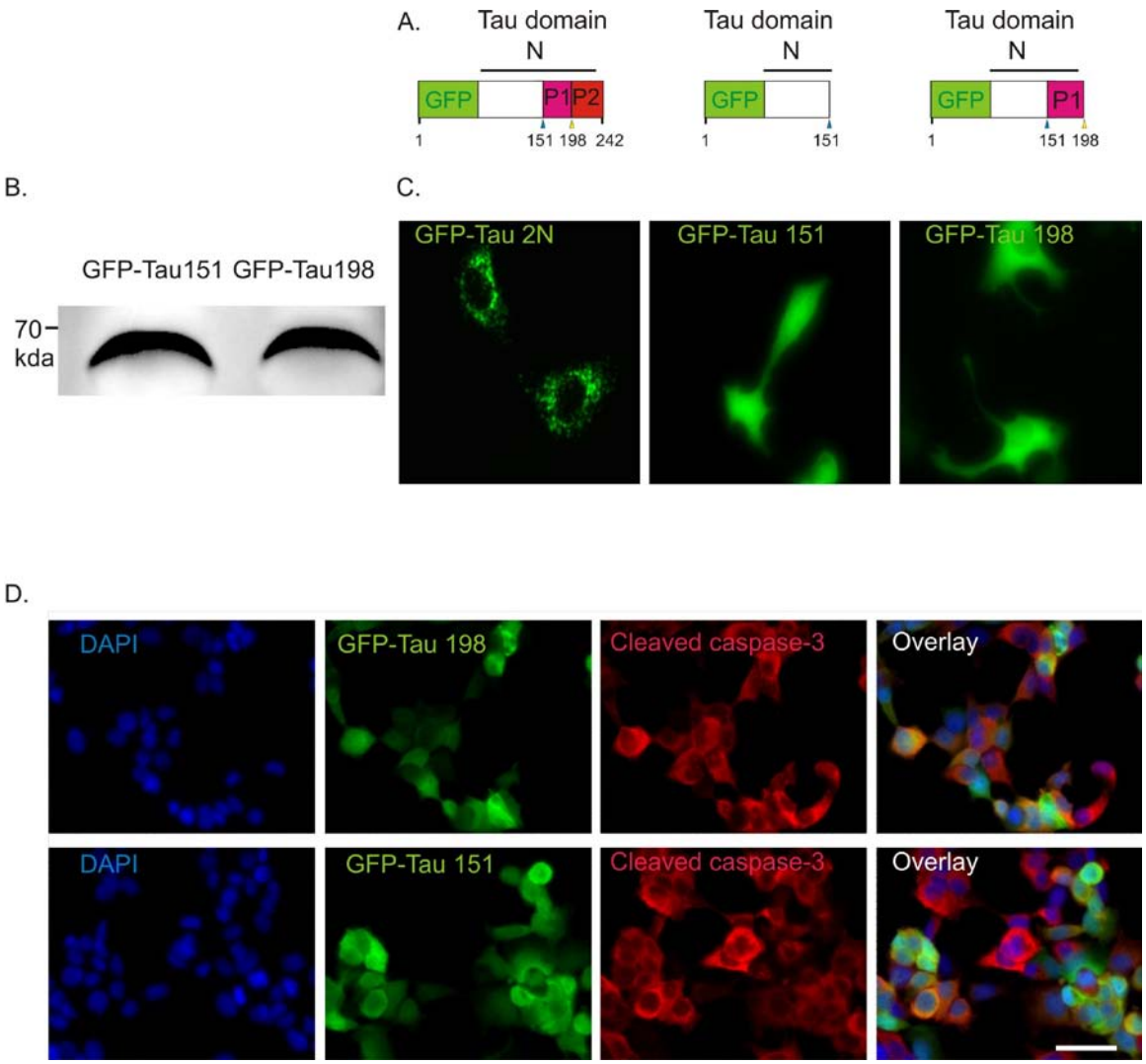

Figure 16: Expression of Tau mutants in MCF7 cells. (A) Schematic representation of the N-terminal tau mutants. Complete N-terminal tau domain (left), N-terminal tau with 151 amino acid residue (middle), N-terminal tau with198 amino acid residue (right). P1 and P2 are the proline rich sites. (B) Immunoblot data indicates protein expression of GFP tagged N terminal tau domain with 151 (GFP-Tau151) and 198 (GFP-Tau198) amino acid residues. Molecular weight of the two protein bands is close to 70kDa. (C) Fluorescent images display expression patterns of GFP-Tau2N (left), GFP-Tau151 (middle), and GFP-Tau198 (right). (D) Caspase-3 activation in GFP-Tau151 and GFP-Tau198 stably transfected MCF7 cells after 8 hrs of exposure to TNFα (50 ng/ml)/CHX (15 µg/ml). (DAPI (blue), GFP (green), Cleaved caspase-3 (red), overlap of all channels shown as merged). Scale bar 50 µm. This data is provided by Peter Hannon.

Evaluation of TNFR1trimerization

TNFα induces cellular signaling upon binding to one of two cell surface receptors (TNFR1 and TNFR2). It has been shown that TNFα binds as a homotrimer to preassembled TNF receptors and this interaction causes the receptor to trimerize and induce downstream signaling. Therefore, disruption of ligand binding with the receptor or interference with receptor trimerization will inhibit TNFα induced downstream signaling. It has been previously shown that tau over-expression in breast cancer cells inhibits TNFα mediated caspase and NFκB activation. Since, ligand-receptor interactions and subsequent receptor trimerization are critical for TNFα signaling, it was hypothesized that tau expression may attenuate one if not both of these processes. In this section, it has been evaluated whether tau can affect TNFα induced trimerization of TNFR1.

Tau inhibits TNFR1 trimerization.

It was previously showed that both full-length tau and N-terminal tau were able to suppress TNF-mediated caspase activation and NFκB nuclear translocation. It was hypothesized that tau mediated TNF-signal regulation lies upstream of the signaling pathway. It was first examined if tau expression affected total TNFR1 level in the transfected cells. Data indicated no significant alteration of total TNFR1 protein in tau expressing cells (Figure 17A). It was also evaluated if TNFR1 was functional in these cells. Biochemical assay was performed to determine the amount of trimerized TNFR1 after MCF7 cells were exposed to TNFα (50 ng/ml) for 1 hour. In control cells, TNFα ligand immediately induced cell surface TNFR1 trimerization similar to previous reports (Figure 17B a) (Chan et al., 2000a). In contrast, overexpression of tau

significantly abrogated an induction of TNFR1 trimerization (Figure 17B a and b). The position of the monomers (M) and trimers (T) are indicated in the immunoblot (Figure 17B a). This experiment was performed three times, and in each independent experiment the control GFP cells displayed increased receptor trimers in presence of TNFα. Immunocytochemistry revealed that control cells when exposed to TNFα ligand display immediate and extensive TNF-receptor clustering, evident by punctate localization (Figure 17C). In stark contrast, cells over-expressing N-terminal tau failed to cluster TNF-receptor in response to TNFα ligand (Figure 17C). These results indicated that in presence of full-length tau and N-terminal tau, TNFR1 failed to trimerize and cluster on the cell surface, respectively.

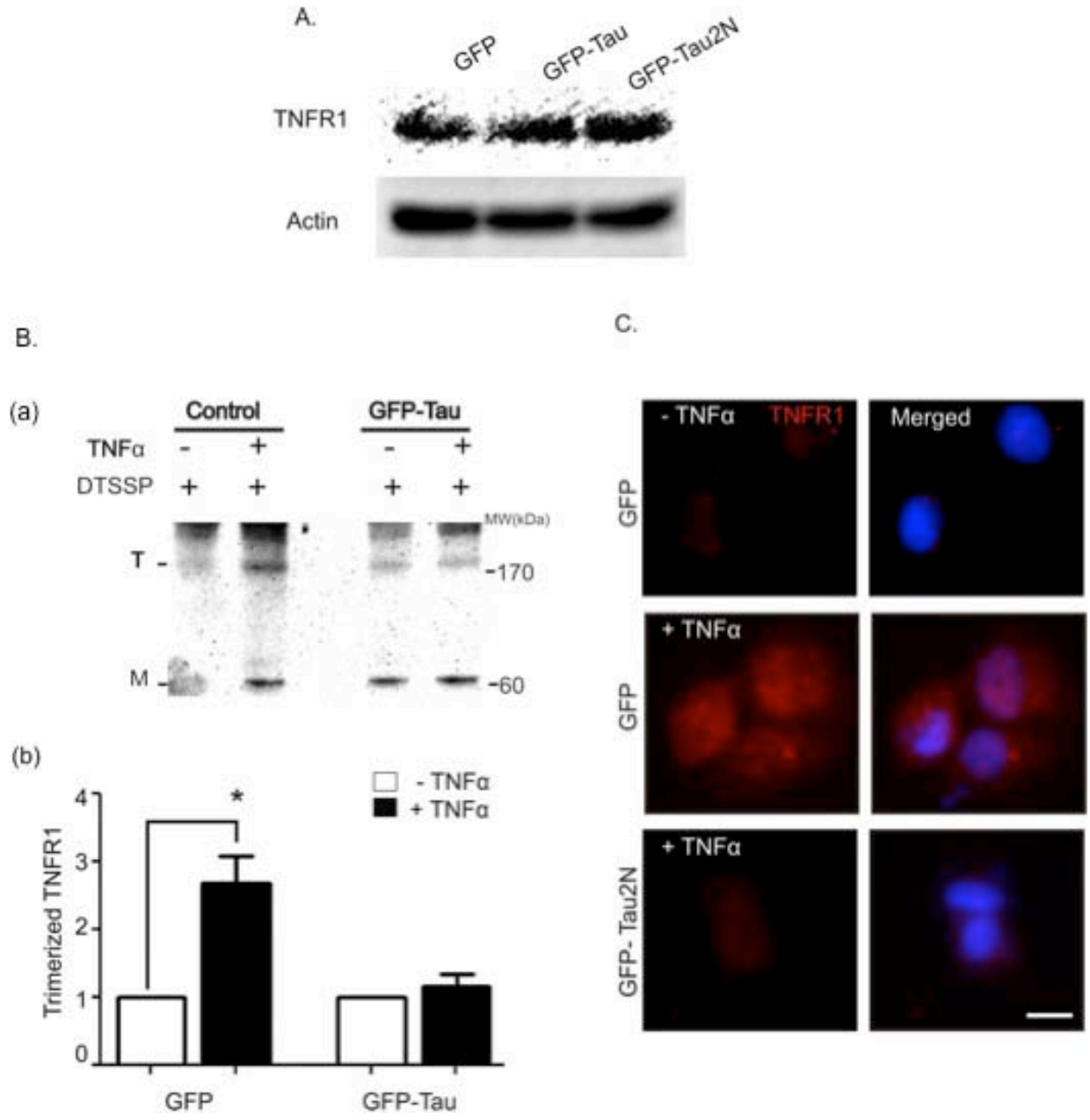

Figure 17: Evaluation of TNFR1 in tau transfected cells. (A) Immunoblot data of total TNFR1 in MCF7 GFP, GFP-Tau and GFP-Tau2N cells. Actin used as loading control. The data is provided by Samantha A. Ni. (B) Immunoblot of trimeric TNFR1 complexes isolated from GFP and GFP-Tau MCF7 cells exposed to TNFα (50ng/ml) for 1hr. The position of trimers (T) and monomers (M) are indicated (a). Quantification of immunoblots for trimerized TNFR1 indicates significant receptor trimerization in GFP (*$p<0.05$), but not GFP-Tau MCF7 cells following TNFα exposure (means±SEM; n=3) (b). (C) Immunocytochemistry of TNFR1 (red) indicates receptor clustering (punctate) in response to TNFα in GFP, but not GFP-Tau2N MCF7 cells. Nuclei stained with DAPI. Scale bar 12µm.

Discussion:

In this study, it is shown that upregulation of tau expression is required for the human breast cancer cell line MCF7 to acquire TNFα resistance. Only a handful of molecular studies have uncovered the key factors associated with tumor cells as they transit from TNFα sensitive to TNFα-resistance. As mentioned before, changes in expression of TNFR1 are found in MCF7 cells as they acquire TNFα-resistance (Antoon et al., 2012). Others have found that TNFα selection in murine fibrosarcoma L929 cells generates two clonal variants each showing TNFα resistance, but at different degrees of sensitivity (Vanhaesebroeck et al., 1991). This finding emphasizes that although TNFα resistance is generated from the same cell line, discrete mechanisms may operate when a sub-population of cells acquire this resistance. In other studies, continual exposure of cells to TNFα induces expression of mitochondrial manganous superoxide dismutase (MnSOD) mRNA level (Wong and Goeddel, 1988). The over expression of MnSOD contributes to TNFα resistance and its specific down regulation reverses the cell sensitivity to this cytokine (Wong et al., 1989). Our findings now add the microtubule associated protein tau to this small list of key factors that are associated with and necessary for breast cancer cells acquiring TNFα resistance.

Extensive research has been done on tau in neurons, yet little is known about its functional significance in non-neuronal disease systems. Increasing similarities between cancer and AD creates a hot spot for this molecule to be explored in the field of cancer. Recently, this protein has evoked new attention in cancer because of its association with drug resistance. Specifically, tau has been found associated with Paclitaxel drug resistance in breast cancer patients (Rouzier et al., 2005). *In vitro* studies have demonstrated that pre-incubation of tubulin with tau leads to a dose-dependent reduction in paclitaxel binding and microtubule stability. The proposed

mechanism for tau inhibition of Paclitaxel response is thought to involve tau competing with Paclitaxel in binding to microtubules. Other studies indicate expression of tau in prostate cancer cells (Souter and Lee, 2009) and that it shows correlation with resistance to anti-mitotic drugs in gastric cancer (Mimori et al., 2006) as well as in pancreatic cancer (Jimeno et al., 2007). Our findings have shown that Tau overexpression in breast cancer cells can inhibit TNFα-induced cytotoxicity and cell apoptosis. This suggests that in breast tumors, ectopic expression of tau could be an important biomarker indicating TNFα resistance similar to it being recognized as a biomarker indicating Paclitaxel resistance. The data also indicates that taxol stabilized microtubules fail to suppress TNF-induced signaling in MCF7 cells (Figure 11). This implies that, in this system, microtubule stability may not be the deciding factor to regulate TNFα signaling in comparison to previous studies which indicate microtubule stability to alter TNF-function (Jackman et al., 2009; Shivanna and Srinivas, 2009). In contrast to the Paclitaxel findings, our results imply that tau mediated stabilization of microtubules may not be involved in order to inhibit TNFα signaling suggesting that multiple mechanisms of tau induced drug resistance may occur in tumor cells.

Evidence shows that tau is a substrate for caspases 3, 6 and 7(Guillozet-Bongaarts et al., 2006; Guo et al., 2004; Horowitz et al., 2004). Caspases cleave tau preferentially at Asp421 (D421), which creates a truncated tau molecule (Rissman et al., 2004; Zhang et al., 2009). Incubation of human tau40 with recombinant caspase-3 in COS kidney cells has been shown to produce fragmentation of tau DNA (Fasulo et al., 2000). Recent study implies that in transgenic mice (Tg4510 strain) caspase activation cleaves tau that leads to tangle formation (de Calignon et al., 2010). Here, the data is consistent with these reports and indicates that activation of caspase-3/7 in presence of TNFα and CHX leads to loss of the endogenous tau in MCF7 control cells

(Figure 5D). However, in contrast to these findings, such loss is not observed in the over-expressed GFP-Tau protein, which emphasizes that caspase activation is not predominant in these cells. This further strengthens the finding that tau over-expression impedes over TNF-induced caspase activation.

Tau protein isoforms have been shown to determine taxane sensitivity in breast cancer cells (Ikeda et al., 2010). These findings have indicated that RNAi mediated specific knockdown of tau protein isoforms of less than 70 kDa in MCF7 and ZR75-1 cell lines increases sensitivity to Paclitaxel. In contrast, HCC3153 cells which express tau of a molecular weight 70 kDa fails to show increase in taxane sensitivity with tau knockdown, indicating that expression of tau isoforms of less than 70 kDa correlates with poor taxane response in breast cancer cells. In this study, the over-expressed full-length human tau isoform has a molecular weight of 60 kDa and this isoform displays TNFα resistivity. Importantly, overexpression of this isoform confers resistance in the non-breast cancer cell line PC12, indicating tau inhibition of TNFα signaling may be a generalized phenomena across all cells. The data also suggests that significant elevation in tau amount may be necessary to confer resistance, since physiological endogenous tau protein in MCF7 and PC12 control cells fails to elicit such effect on TNFα signaling. Taken together, both tau amount and its different types of isoforms become an important consideration, which needs to be explored in the future.

The role of inflammation is important in the pathogenesis of Alzheimer's disease and TNFα is a potent neurotoxic cytokine in Alzheimer's (Alkam et al., 2008; Perini et al., 2002; Takeuchi et al., 2006) where its elevated level is a reflection of disease severity (Paganelli et al., 2002) Evidence elucidates role of TNFα to induce tau aggregation at the neurites of primary cultured neurons and this process gets abrogated upon TNFα neutralization (Gorlovoy et al.,

2009). Further, data shows that administration of antibody against TNFα on AD pathological features in APP/PS1 transgenic mouse brains causes a reduction of TNFα levels, amyloid plaques and tau phosphorylation (Shi et al., 2011). These findings suggest that tau and its function can be affected by TNFα. In contrast, this study investigates the opposite scenario, and asks whether tau can affect TNFα signaling, specifically in cancer.

A potential role of tau in cellular signaling has been evaluated in various studies. Tau has been co-purified with PLCγ in human neuroblastoma SH-SH5Y cells (Jenkins and Johnson, 1998). PLCγ is normally activated through receptor induced tyrosine phosphorylation. Data indicates that tau is able to activate PLCγ in presence of arachidonic acid and higher amount of tau is sufficient to activate PLCγ in absence of this fatty acid (Hwang et al., 1996). *In vivo* studies in mice have shown that tau can inhibit enzyme activity of histone deacetylase-6 (HDA6) (Perez et al., 2009). Furthermore, tau is also involved in cellular response to heat shock. Evidence suggests that deletion of tau in primary cultures of cortical neurons allows recovery of neurons from heat shock induced cell injury and tau knocked out neurons displays a delayed and prolonged activation of Akt and its downstream target GSK3β (Miao et al., 2010). This study adds to this growing list of pathways affected by tau by indicating tau as a novel regulator of TNFα signaling in breast cancer cells.

As discussed earlier, the N-terminal tau domain has been shown to be involved in signal transduction. The PXXP motif of N-terminal tau domain interacts with SH3 domain of fyn and src tyrosine kinases. In support of this, tau can be co-immunoprecipitated with fyn in neuroblastoma cells and both fyn and tau have been shown to co-localize in NIH3T3 cells (Lee et al., 1998). Furthermore, phosphorylation in or around the proline rich domain regulates tau interaction with SH3 domains of various proteins like phospholipase Cγ1, Grb2, PI3 kinase

(Reynolds et al., 2008). Recent studies also emphasize that tau N-terminal domain is able to prevent premature death and memory loss in Aβ forming APP23 mice (Ittner et al., 2010). Here, the data is consistent with these findings and it is shown that the N-terminal domain of tau is involved in regulation of TNFα signaling in breast cancer cells. Tau N-terminal domain has been shown to associate with neural plasma membrane in PC12 cells where it is speculated to be a part of the membrane associated complex (Brandt et al., 1995). It is thought that tau localization to the plasma membrane is mediated through tau projection domain and the event is dependant on tau phosphorylation status (Pooler and Hanger, 2010). It is possible that in MCF7 breast cancer cells the N-terminal tau region associates with the plasma membrane and interacts with TNF-receptor complexes to alter the signaling pathway. A detailed insight to investigate this possibility will be required to determine how tau N-terminal domain is involved in TNF-signal regulation. To summarize our findings, this study indicates that the N-terminal tau domain, which harbors no microtubule binding regions, is sufficient to suppress TNFα signaling.

There are two prevailing hypotheses of how TNF receptor undergoes trimerization. The first involves TNFα ligand-induced trimerization (Tartaglia and Goeddel, 1992) and the second more recent involves a pre-ligand binding assembly domain (PLAD) in the extracellular region of the TNF receptor that mediates ligand independent assembly of receptor trimers (Chan et al., 2000a). Although, receptor trimerization is crucial for TNF signaling, it has been demonstrated that TNF receptor intracellular domain clustering is also necessary and can be sufficient to induce signaling (Vandevoorde and Fiers, 1997). In this study, it seems unlikely that tau would interact with the PLAD region of the receptor, as it is restricted to the extracellular space. Instead, the proposed mechanism suggests that tau could interfere with TNF receptor clustering since the N-terminal domain of tau has been shown to be associated with the plasma membrane

(Brandt et al., 1995). Here, the findings indicate that full-length tau and N-terminal tau is affecting receptor trimerization and receptor clustering, which probably explains how subsequent TNF-mediated signaling is suppressed in tau transfected cells. Evidence shows that the proline rich sequences of N-terminal tau region interact with SH3 domain of several proteins including fyn and src non-receptor tyrosine kinases (Lee et al., 1998; Reynolds et al., 2008)). In this study, it is possible that N-terminal tau interacts with the cytoplasmic portion of TNFR1 and prevents it to undergo conformational change, which is necessary to either bind with the ligand or recruit the signaling complexes. Further studies are necessary to elucidate this possibility. To strengthen these findings, current investigation is underway to determine if tau has direct association with TNFR1 and whether there is perturbation in the formation of the death initiation signal complex (DISC) in presence of the ligand in the tau transfected cells. An insight to such molecular details will be able to depict a complete picture of how tau mediates TNFα signaling.

To summarize, our findings provide a mechanistic explanation of how breast cancer cells may escape high levels of TNFα in their microenvironment. The study indicates that expression levels of soluble tau can determine the extent of TNF-receptor trimerization and therefore alter TNFα-induced downstream signaling.

Over the last few decades, several strategies have been developed to reduce the systemic toxicity of TNFα, as well as to potentiate its powerful anti-tumor activity. Cancer gene therapy using TNFα (TNFerade) together with radiation has demonstrated enhanced anti-cancer efficacy and is currently in advanced Phase II/III clinical studies (Rasmussen et al., 2002; Weibo Cai, 2008). A fusion protein of TNFα and anti-HER2 scFv fragment (scFv23/TNFα) has been shown to increase apoptosis in HER2 expressing cancer cells and is under consideration to be introduced into the clinics (Rosenblum et al., 2000). TNFα is currently used to treat isolated

limb perfusion of sarcoma and melanoma patients. Local administration of TNFα in combination with cytostatic drug Melphalan synergistically accelerates its antitumor and antivasculature properties causing dramatic decrease of the tumor size (van Horssen et al., 2006). Additionally, studies indicate TRAIL molecule (TNF-related apoptosis inducing ligand) which is a member of TNF superfamily, can induce apoptosis in a vast range of tumor cells irrespective of the p53 status without signs of toxicity in normal cells (Ashkenazi et al., 1999; Walczak et al., 1999). Here, the results suggest that down-regulation of tau expression should also be considered as a means for sensitizing breast cancer cells to the anti-cancer properties of TNFα.

Finally, these findings could explain why some breast tumors display resistance to an immune cell attack or why TNFα anti-cancer therapy may prove to be ineffective given breast cancer cells can acquire tau-induced TNFα resistance. Taken together, tau expression becomes an important consideration for when analyzing the TNFα pathway or considering TNFα-directed therapies.

Chapter II

Down regulation of tau affects estradiol mediated cyclin D1 activation in MCF7 breast cancer cells.

Abstract: Estrogen receptor signaling plays an important role in mammary gland development as well as in breast cancer progression. Estrogen receptor (ER) belongs to the nuclear receptor superfamily and is a ligand inducible transcriptional factor. Binding of estradiol to ER activates several genes including the cell cycle regulator cyclin D1. Cyclin D1 plays role in the growth of normal mammary epithelial cells and is considered as an important determinant of estrogen signaling in mammary gland. Studies also indicate that both estrogen addition and ER level can affect tau expression in breast cancer cells. Furthermore, clinical studies in breast cancer have proposed that tau levels are a bifunctional predictor of both endocrine and chemotherapy sensitivity. Given these findings, it was hypothesized that tau may affect estradiol signaling in breast cancer cells. In this study, the role of tau in regulating cyclin D1 activation in response to estradiol exposure has been investigated. In doing so, stable tau knockdown MCF7 cells has been generated to analyze cyclin D1 activation in these cells. The preliminary findings indicate that tau knockdown cells show a decreased amount of nuclear cyclin D1 in response to estradiol stimulation. This suggests a potential role of tau in regulating hormone-induced cyclin D1 activation.

Introduction:

Breast cancer is the most frequently diagnosed cancer and the second leading cause of cancer death in women. Breast cancer is often hormone dependant and therefore hormonal drugs are an important therapy to treat the disease. The female sex steroid hormone 17β-estradiol (E2) mediates multifunctional roles like proliferation, maturation, differentiation, inflammation, apoptosis and plays a key role on growth and development of mammary carcinogenesis (Edwards, 2005; Song et al., 2004; Yager, 2000). Natural estrogens such as E2, estrone and estrogen antagonists such as tamoxifen are widely used for hormone replacement therapy and as anti-cancer agents to treat breast cancer (Bai and Gust, 2009; Cosman and Lindsay, 1999).

Biological functions of estrogen are mediated upon binding with estrogen receptor (ER). ER discovered in the early 1960s, belongs to nuclear receptor superfamily and is a ligand induced transcription factor, which executes its function in a dimeric form (Bai and Gust, 2009; Jensen et al., 1962). The two types of estrogen receptor ERα and ERβ are often expressed together in various tissues like cardiovascular system, urogenital tract, central nervous system, and the mammary gland. However, ERα is predominantly expressed than ERβ in the uterus and breast tissues (Bai and Gust, 2009). In an inactive stage, ER exists in a heterocomplex form with heat shock protein 90 (HSP90) and immunophilin-FK binding protein 52 (FKBP52) (Pratt and Toft, 1997; White and Parker, 1998) and can shuttle freely between the nucleus and the cytoplasm (Maruvada et al., 2003; Monje et al., 2001). In the classic pathway, binding of E2 to ER promotes dissociation of HSP90 and FKBP52 and induces conformational changes in the receptor, which adopts an active dimerized state inside the nucleus that binds with the estrogen response element of the target gene and recruits co-regulators to induce gene transcription (Bai and Gust, 2009; McDonnell and Norris, 2002). In presence of E2, ERα is downregulated through

the ubiquitin / proteasome (Ub/26s) pathway (Alarid et al., 1999). Studies indicate that ligand bound ERα undergoes enzyme mediated polyubiquitination and is directed for proteasomal degradation (Callige et al., 2005; Nawaz et al., 1999). Evidence suggests that E2 mediated degradation of ERα is important to accentuate its ability to activate rapid gene transcription (Jensen et al., 1969).

Several genes are activated in response to estrogen including the cell cycle regulator cyclin D1. Altucci et. al., first noted that Simvastatin treated growth arrested MCF7 cells showed transient induction in cyclin D1 level within initial hours of stimulation with E2 (Altucci et al., 1996). Further, a positive co-relation of increased cyclin D1 mRNA level with ER overexpression is also observed in breast tumor biopsies (Buckley et al., 1993). Estrogen induced cyclin D1activation plays important role in growth of normal and malignant mammary epithelial cells. *In vivo* studies have shown that cyclin D1 deficient mice fail to undergo proliferation in the mammary epithelium compartment during pregnancy (Sicinski et al., 1995) and recent *in vivo* findings highlight cyclin D1 as an important determinant of estrogen signaling in mammary gland (Casimiro et al., 2013).

Studies have also shown that estrogen has effects on tau expression. Data shows that rat pituitary prolactin cells when treated with estrogen causes an increase in tau protein levels (Locksley et al., 2001) (Matsuno et al., 1997). Consistent with this finding, estrogen stimulation is also shown to increase tau levels in neurons and promotes neurite outgrowth (Ferreira and Caceres, 1991). Estrogen mediated effects on tau have also been evaluated in breast cancer. Tau gene contains an imperfect estrogen receptor response element which is present upstream of its promoter and microarray analysis reveals that MCF7 breast cancer cells exhibit an increase in tau mRNA level in response to estrogen (Frasor et al., 2004). Clinical studies in breast cancer

indicate tau to be a predictor of both endocrine and chemotherapy sensitivity. Other findings have indicated that ER positive breast cancer show higher tau mRNA level with a possible outcome of endocrine sensitivity and chemotherapy resistivity (Andre et al., 2007). Further, tau gene expression has been proposed to be predictive in response to endocrine therapy in high-risk early breast cancer patients (Pentheroudakis et al., 2009). Studies have also highlighted that ER can influence tau protein levels. These finding indicate that siRNA mediated ER knock down results in decrease tau levels in MCF7 and ZR75-1 breast cancer cell lines (Ikeda et al., 2010). This growing list of findings implies that estrogen mediated tau expression may have important outcomes in breast cancer.

Based on these reports which show that estrogen can cause cyclin D1 induction and increase tau levels, we were interested to investigate if tau lies upstream of estrogen signaling and therefore plays a role in cyclin D1 activation in breast cancer cells. Therefore, stable tau knockdown MCF7 cells were generated to analyze cyclin D1 activation in response to E2 addition. The following data indicates that tau knockdown cells show decreased amount of nuclear cyclin D1 level in presence of E2, suggesting a potential role of tau in cyclin D1 activation.

Materials and methods:

Cell lines and culture: Human breast cancer cell lines MCF7 was obtained from American Type Culture Collection (ATCC). MCF7 cells were cultured in basal media (High Glucose Dulbecco's Modified Eagle's Medium (Lonza), 10 units/ml Penicillin and 10 ug/ml Streptomycin (Hyclone)) with 10% (v/v) fetal calf serum (FCS). Cells were maintained at 37°C with 5% CO_2 in 10cm culture dishes (BD Bioscienes). Media was changed regularly at 2-3 day intervals. Cells were passaged with 0.25% Trypsin (Cellgro) once they reached a confluency of 70-80%.

Generation of stable tau knockdown MCF7 cells: MCF 7 cells were grown in 6 well plate. MAPT (microtubule associated protein tau) shRNA was ordered and purchased from Thermo Scientific Open Biosystem. Cells were transduced with pGIPZ lentiviral vector (multiplicity of infection 10) suspended in a serum free medium according to the instruction manual. Media was added after 24 hrs. Cells were selected with puromycin (Acros Organics; AC 22742-0500) (2μg/ml) after 72 hrs of infection. Selection with puromycin drug was continued for 10 days. MAPT protein was detected with immunoblotting (described in chapter 1) and the blot was probed with Tau13 (1:5000) or DA9 (1:2000) mouse monoclonal antibody. Anti-β-actin rabbit polyclonal antibody (Cell signaling # 4967, 1:2000) was used a loading control.

Microtubule binding assay (MtBA) of MCF7 cells: The MtBA was performed with MAPT downregulated MCF7 cells grown in 4 well glass chamber slides as described in chapter I. Tubulin was probed with DM1A mouse monoclonal antibody (Milipore -5-829; 1:1000).

Cell fractionation and immunoblotting: MCF7 control and tau knockdown cells of equal density were seeded in a 6 well plate (BD Falcon) and cultured in presence of phenol red free

medium (Cellgro; 17-205CV) supplemented with 5% charcoal stripped FBS (csFCBS) (Invitrogen# 2017-08). Cells were serum starved with 0.5% csFCS for 36 - 48 hrs. Cells were washed twice with plain medium and exposed to 10nM 17β-estradiol (Sigma) diluted in serum free medium. Fresh solution of estradiol was prepared each time before use. To detect ERα nuclear accumulation cells were harvested after 0, 1, 2 or 3 hrs of estradiol addition. For Cyclin D1, cells were extracted after 0, 2, 5 or 8 hrs of estradiol treatment. Cells were fractionated with sub-cellular fractionation buffer as described in chapter I. Protein samples were resolved with 10% SDS-PAGE (described in chapter 1). Blots were probed with anti-cyclin D1 rabbit polyclonal antibody (Milipore# 06-137 (1:1000). Nuclear Lamin A/C was used as loading control (Cell signaling # 4777; 1:2000). ER was detected with rabbit monoclonal anti- ERα antibody (Cell Signaling # 8644, 1:1000).

Microtubules: MCF7 cells were seeded at a density of 20×10^3 cells/well in a 8 well chamber (BD Falcon) and were cultured for 2 days before being fixed with pre-chilled (-20°C) Cytoskelfix™ cell fixative (Cytoskeleton # CSK01) for 4 mins at -20°C. Tubulin was detected with mouse monoclonal DM1A antibody (Milipore, 05-829) (1:200) and Alexa Fluor 594 goat anti-mouse IgG secondary antibody (Invitrogen).

Cyclin D1 and ERα detection: MCF7 control and tau knockdown cells of equal density were seeded in 8well plate (BD Falcon) and cultured in presence of phenol red free medium (Cellgro) supplemented with 5% charcoal stripped FCS (csFCS) (Invitrogen). Cells were serum starved with 0.5% csFCS for 36 hrs. Cells were washed twice with plain medium and exposed to 10nM 17β-estradiol (Sigma) diluted in serum free medium for 0, 5 and 8 hrs. Cells were fixed with 4% PFA for 15 mins at room temperature and immunocytochemistry was performed as described in

chapter 2. Cyclin D1 was detected with anti-cyclin D1 rabbit polyclonal antibody (Milipore# 06-137 (1:200). ERα was detected in cells after 1 hr of exposure to estradiol. Cells were washed twice with plain medium, fixed with 4% PFA and incubated overnight at 4°C with anti-ERα antibody used at dilution of 1: 3000 (Cell Signaling # 8644). Nuclei were counterstained with Hoechst (Invitrogen).

Statistics: Statistical analysis was performed with GraphPad Prism (Version 5) software. We performed unpaired t-test (2 tail) Statistical significance was achieved when $p < 0.05$.

Results:

Characterization of tau knock down MCF7 cells

To investigate if tau plays a role in cyclin D1 activation, stable tau knockdown MCF7 cells (tau protein reduced by 85%) were generated. Data indicated a presence of endogenous tau both in the nuclear and cytoplasmic fractions (Figure 18A). Stable tau knockdown cells displayed reduced levels of tau protein for both higher and lower molecular weight tau isoforms present in MCF7 cells (Figure 18B). Bright field images indicated that tau knockdown was not lethal to the cells (Figure 18C), however the cells exhibited diminished cell proliferation (data not shown). The cell phenotype was not drastically altered in comparison to the control. Microtubule binding assay indicated increase in soluble tubulin fraction in tau knockdown cells (Figure 18D a and b). However, the increase in soluble tubulin was not significant. Further, tubulin immunostaining did not show significant effect on microtubule architecture in tau knocked down cells when compared to control (Figure 18E).

Tau knockdown MCF7 cells display reduced cyclin D1 in response to estradiol addition.

To investigate the effect of tau knockdown on the cell cycle regulator cyclin D1, cells were stimulated with 10 nM 17β-estradiol (E2) and sub-cellular fractionation was performed at various time points (0, 2, 5 and 8 hrs) to extract the nuclear component (Figure 19A). Immunoblot result indicated increased cyclin D1 amount in the control at 2, 5 and 8 hrs of E2 addition. In contrast to control, tau knockdown nuclear fractions did not indicate robust cyclin D1 amount on E2 addition. When quantified, data revealed that control cells displayed a time dependant increase in cyclin D1 amount (Figure 19B). In stark contrast, cyclin D1 amount was relatively similar in tau knocked down cells at various time points of E2 addition. The amount of

cyclin D1 was significantly lower in tau knockdown cells than the control after 8 hrs of E2 addition. Similar results were obtained when probed for the cell proliferation marker phosho-histone H3 (p-H3) (Figure 19C). Data indicated increased levels of p-H3 at 5 and 8 hrs of E2 addition in the control cells compared to knockdown population. To complement immunoblot results, E2 (10nM) treated MCF7 cells were further immunostained to detect cyclin D1 (Figure 19D and E). Immunostaining data was consistent to our previous finding. Data indicated predominant nuclear presence of cyclin D1 after 5 and 8 hrs of E2 stimulation in control cells (Figure 19D). In contrast, tau knockdown cells did not display such increase in nuclear cyclin D1 under similar condition (Figure 19E).

Taken together, the preliminary finding indicates that tau knockdown in MCF7 breast cancer cells impairs E2 mediated activation of cyclin D1. These results suggest that tau can play an important role in hormone-induced cell cycle regulation in cancer.

Estradiol treated ERα nuclear accumulation in MCF7 cells.

It was hypothesized that the reduced amount of cyclin D1 in response to E2 in tau knockdown MCF7 cells is due to decrease in ERα nuclear accumulation. We have characterized E2 stimulated ERα nuclear accumulation in control cells (Figure 20). Data indicates increased amount of nuclear ERα post one hour of E2 addition (Figure 20A and B). This data is also consistent with immunostaining result. Similar to published reports (Kocanova et al., 2010), E2 treated MCF7 cells display accumulation of ERα at numerous foci, which is scattered throughout the nucleus (Figure 20C). In untreated cells, the ERα staining is faint and is evenly distributed throughout the nucleus.

Currently, E2 induced ERα nuclear translocation in tau knockdown MCF7 cells is investigated and the experiments are in progress.

Conclusions / Future direction:

The preliminary data indicates that tau knockdown cells show decreased cyclin D1 in response to E2 addition. One possible reason for such event includes decreased accumulation of ERα inside the nuclei of tau knock down cells, which causes reduced cyclin D1 activation. Based on other reports which indicate that both estrogen and ER affect tau level in breast cancer cells (Frasor et al., 2004), it will be important to investigate if the endogenous ERα amount in tau knockdown cells is affected. Significant alteration in ERα will probably explain decrease in cyclin D1 activation in these cells. Further, studies of ERα accumulation in the nuclei of E2 treated tau knock down cells is necessary to elucidate the functionality of the ER signaling pathway in these cells. This will have important consequences since ERα signaling plays an important role in mammary development and breast cancer progression.

A role of tau on cyclin D1 activation, independent of ER signaling, can be a separate phenomenon. Cyclin D1 is well-established oncogene and its aberrant expression is linked with several types of cancers. Evidence indicates that amplification and or overexpression of cyclin D1 is responsible for 13 to 20% incidence of breast cancer (Arnold and Papanikolaou, 2005). Cyclin D1 over-expression in mammary cells of transgenic mice has been shown to promote abnormal cell proliferation, which results in mammary adenocarcinomas (Wang et al., 1994). In general, cyclin D1 function in cell cycle regulation includes formation of cyclin D1-cdk complexes, followed by cyclin E complex formation that results in phosphorylation of the

retinoblastoma protein (Rb) and release of the G1 phase (Arnold and Papanikolaou, 2005; Sherr, 1996). However, emerging new data in this field suggest that besides, being a cdk activator, which regulates cell cycle, cyclin D1 can also act as a modulator of transcriptional factors (Coqueret, 2002). This includes cyclin D1 mediated regulation of ERα activation. Although it is generally accepted that cyclin D1 activation is downstream of ERα (Altucci et al., 1996; Musgrove et al., 1993), overexpressed cyclin D1 in breast cancer cells has been shown to directly bind to and activate ERα (Neuman et al., 1997; Zwijsen et al., 1997). Subsequent studies have further highlighted that cyclin D1 interacts with ER and acts as a bridging factor to recruit co-activators to ER in absence of the ligand (McMahon et al., 1999; Zwijsen et al., 1998). Given the fact that cyclin D1 is a pathogenetic cornerstone in a large number of breast cancers, a better understanding of its regulation will be important to design successful anti-cyclin D1 therapy. Therefore, we believe that further elucidation of how tau is involved in cyclin D1 activation will create a significant impact in this field.

The data indicates that tau down regulation affects cyclin D1 activation in response to E2. It is possible that tau interferes with cyclin D1 activation. Several findings have indicated nuclear presence of tau. Isolated nuclei of human brains report presence of tau protein (Brady et al., 1995). Similar finding indicates that a portion of tau exists inside the nuclei of LA-N-5 neuroblastoma cells specifically associated with the chromatin fraction containing DNA and associated proteins, which implicates tau to have functional role in the nucleus (Greenwood and Johnson, 1995). Chromatin immunoprecipitation data further shows endogenous tau interaction with neuronal DNA, which is necessary to protect neurons against heat shock (Sultan et al., 2011). Further, in this study, nuclear presence of endogenous tau in MCF7 cells (Figure 1A) is also observed. Therefore, it may be possible that tau nuclear component interacts with and or

interferes with cyclin D1 activation. Co-imunoprecipitation for tau and cyclin D1 will be able to highlight whether tau interacts with cyclin D1.

To summarize, the role of tau in cyclin D1 activation is an important query and we believe further elucidation of this relationship will make a significant contribution in the field of breast cancer.

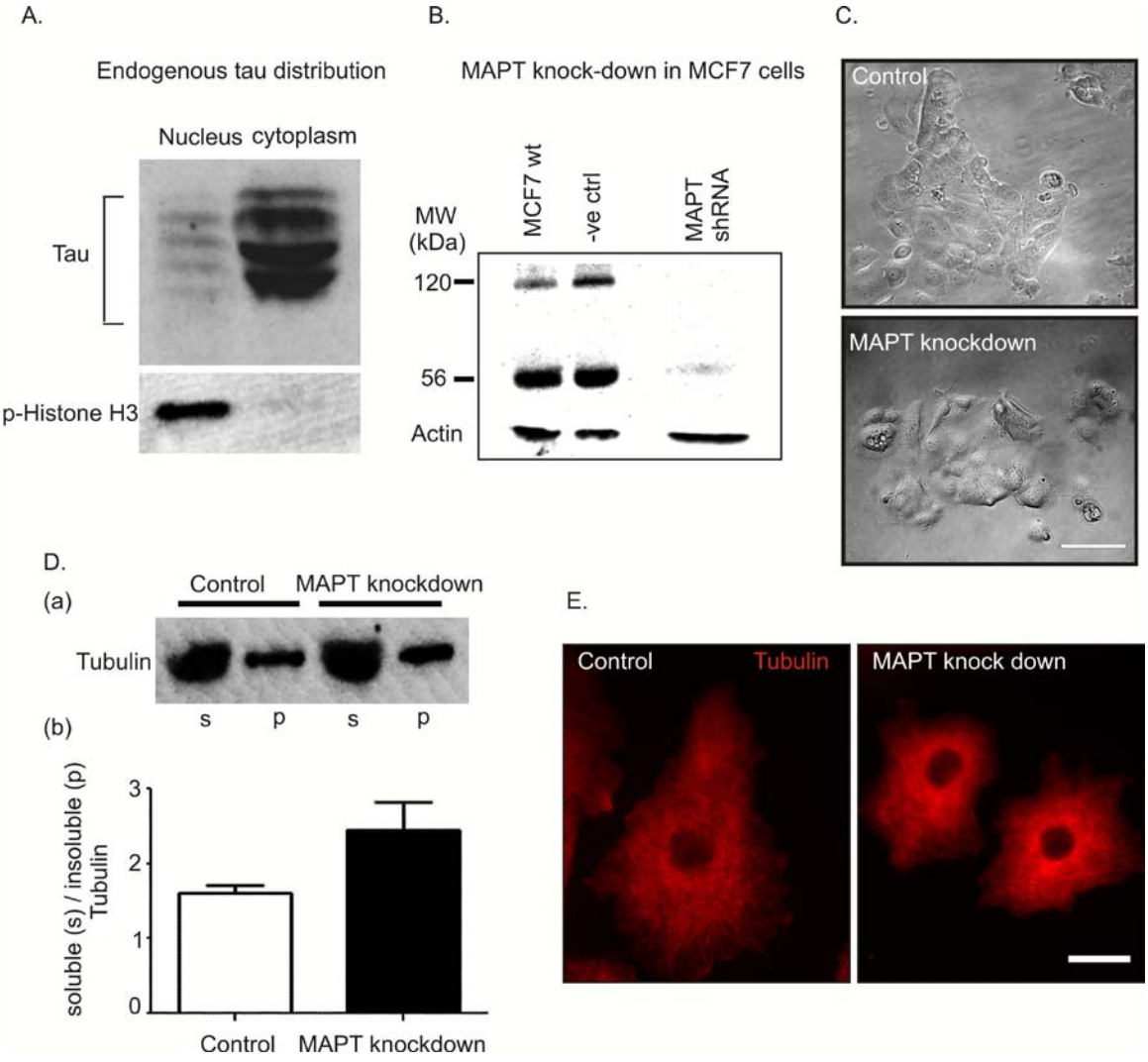

Figure 18: Characterization of tau knockdown MCF7 cells. (A) Sub-cellular fractionation of MCF7 endogenous tau indicates presence of tau in the nucleus and cytoplasm. Phospho Histone H3 is used to indicate the purity of the nuclear isolation. (B) Immunoblot assay indicates shRNA-mediated knockdown of MAPT (microtubule associated protein tau) in MCF7 cells. Actin used as loading control. (C) Bright field images of MCF7 control (top) and MAPT knockdown cells (bottom). Scale bar 50μm. (D) Immunoblot data of the MtBA performed with MAPT knockdown cells. Tubulin distribution is shown in the soluble (s) and insoluble (p) fractions (a). Ratio of soluble to insoluble tubulin is quantified from immunloblot results (means ±SEM; n=2). (E) Immunostaining of tubulin (red) in control and MAPT knockdown MCF7 cells. Scale bar 10μm.

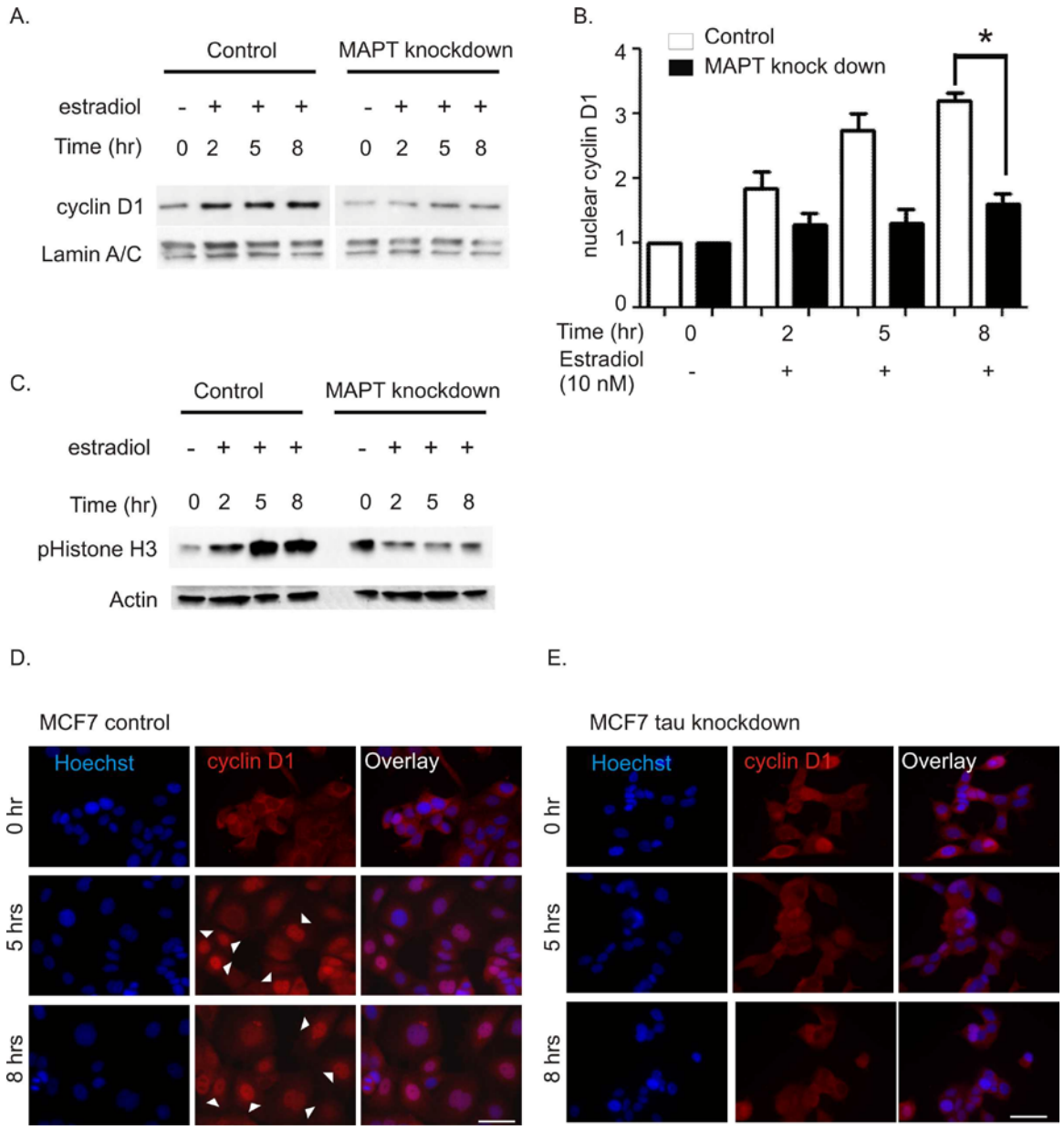

Figure 19: Estradiol mediated cyclin D1 activation in MCF7 MAPT knockdown cells. (A) Immunoblot assay with nuclear fractions of MCF7 cells shows the amount of cyclin D1 at 0, 2, 5 and 8 hrs following stimulation with 17-β estradiol (E2)(10 nM). Data indicates increased amount of cyclin D1 at 2, 5, and 8 hrs in the control compared to the MAPT knockdown fractions. Nuclear lamin A/C used a loading control. (B) When quantified, increase in cyclin D1 (fold-difference) is observed in control cells over time. Data shows significant reduced amount of cyclin D1 (*$p<0.05$; Student's t-test) in MAPT knockdown cells in comparison to control after 8 hrs of E2 addition. Values are relative to time 0 (means± SEM; n=2). (C) Immunoblot data of phospho histone H3 (p-H3) performed with control and MAPT knockdown cell extract, shows amount of p-H3 at 0, 2, 5 and 8 hrs of E2addition (10nM). Actin used as loading control. (D) Immunostaining of cyclin D1 in MCF7 control cells at 0 (top), 5 (middle), and 8 hrs (bottom) of

E2 (10nM) treatment. Presence of nuclear cyclin D1 at 5 and 8 hrs is indicated with arrows. Nuclei shown in blue, cyclin D1 in red, blue and red channels are overlaid. Scale bar 50μm. (E) Cyclin D1 staining in MAPT knockdown MCF7 cells does not indicate predominant cyclin D1 nuclear presence at 5 (middle) and 8 hrs (bottom) of E2 addition. Data of both D and E are provided by Samantha A. Ni.

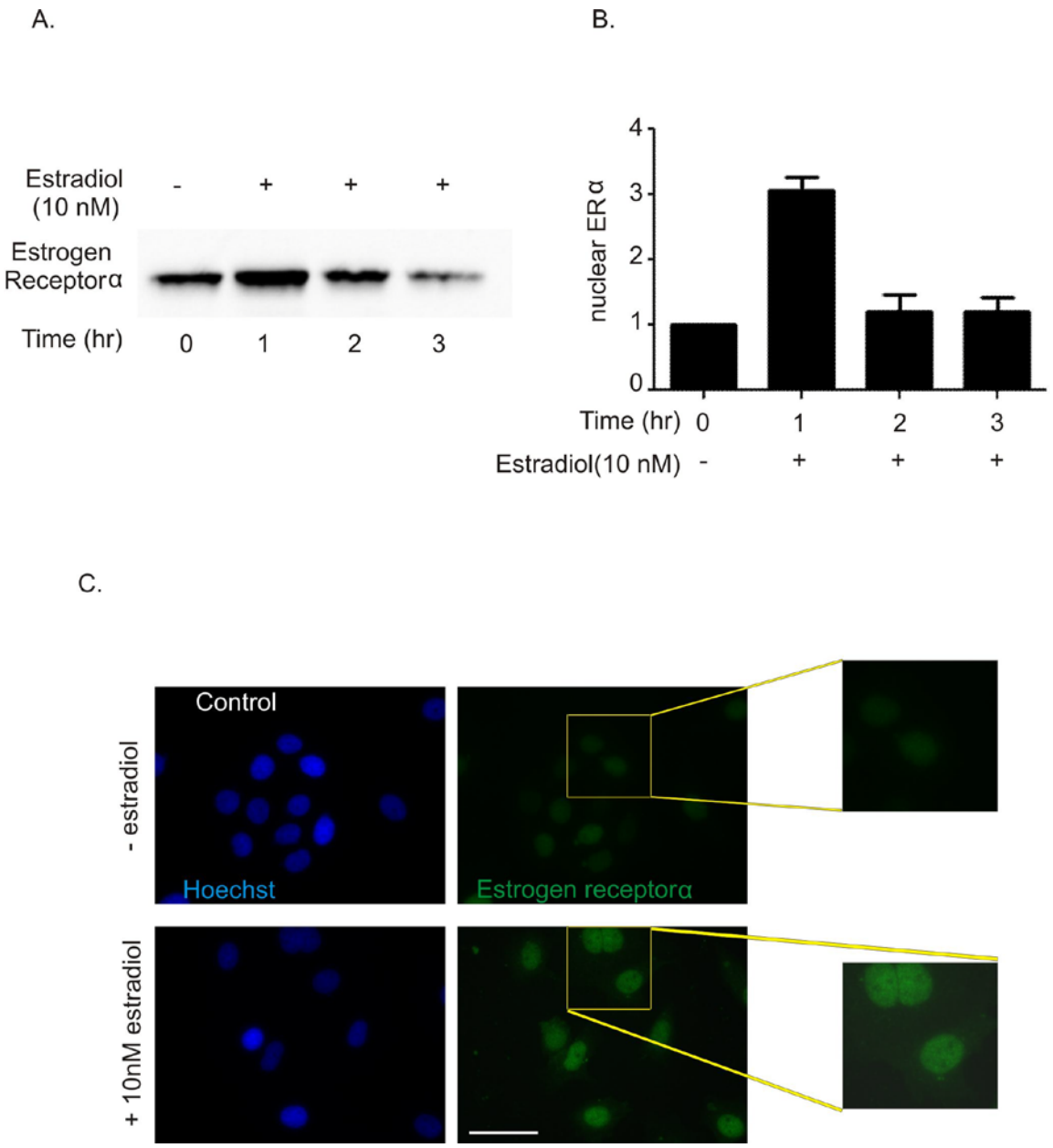

Figure 20: Effect on estrogen receptor-alpha (ERα) in response to estradiol addition. (A) Immunoblot data indicates the amount of nuclear ERα present in MCF7 control cells at 0, 1, 2 and 3 hrs of stimulation with 17-β estradiol (E2)(10nM). (B) Quantification data shows that nuclear ERα amount peaks at 1 hr of E2 addition (means ± SEM; n=3). (C) Immunostaining data of ERα in MCF7 control cells in absence (top) and presence (bottom) of E2 (10nM). Regions of the images marked in yellow boxes are magnified. Nuclei shown in blue, ERα in green. Scale bar 50μm.

Concluding remarks:

Tumor Necrosis Factor-alpha (TNFα) is a multifunctional pro-inflammatory cytokine. The mechanisms and factors associated with how a tumor cell responds to a microenvironment rich in TNFα have not been fully resolved. In this thesis, it has been shown that tau protein is a novel regulator of the cellular response to this key cytokine TNFα. Evidence indicates that Tau inhibits TNFα signaling through its N-terminal projection domain. Tau interferes with TNFR-1 receptor clustering and trimerization that impedes TNFα downstream signaling.

It is also shown that tau N-terminal projection domain is sufficient to provide resistance to TNFα. The preliminary findings also suggest that deletion of the proline rich regions from N-terminal tau results in failure to provide TNFα resistance. In the future, to strengthen this data, it will be important to delete the proline rich region from full-length tau and investigate its relation to TNFα. We have not studied the C-terminal tau domain, but it may be an important consideration to be explored further in relation to this cytokine signaling in breast cancer since, it is directly involved in tubulin binding.

The mechanistic approach indicates that tau interferes with TNFR1 trimerization and clustering. A molecular insight to how tau mediates interference with the receptor functioning is necessary. As mentioned before, it is possible that tau N-terminal domain is associated with plasma membrane where it is associated with TNF-receptor complexes. Co-immunoprecipitation studies of tau and TNFR-1 will be able to highlight this further. Moreover, studies involving ligand binding with the receptor is also required to illustrate whether tau affects TNFα-TNFR1 binding. Analyzing the formation of death initiation complex in response to TNFα addition through high-resolution microscopy or immunoprecipitation techniques will emphasize the

mechanism. This will probably explain how and why tau overexpression suppresses the downstream signaling pathways.

Appendix

Dendrimer-curcumin conjugate: A water soluble and effective cytotoxic agent against breast cancer cell lines.

Send Orders for Reprints to reprints@benthamscience.net

Anti-Cancer Agents in Medicinal Chemistry, **2013***, 13,* **000-000**

Dendrimer-Curcumin Conjugate: A Water Soluble and Effective Cytotoxic Agent Against Breast Cancer Cell Lines

Shawon Debnath[a,d], Darin Saloum[c], Sukanta Dolai[b], Chong Sun[b,d], Saadyah Averick[b], Krishnaswami Raja[b,d] and Jimmie E. Fata[a,c,d,*]

Department of Biology[a] and Chemistry[b], College of Staten Island, 2800 Victory Blvd., Staten Island, NY, 10314, [c]Biology or [d]Biochemistry Doctoral Program, City University of New York Graduate Center, 365 Fifth Ave., NY, NY, 10016

Abstract: Curcumin, which is derived from the plant *Curcuma longa*, has received considerable attention as a possible anti-cancer agent. In cell culture, curcumin is capable of inducing apoptosis in cancer cells at concentrations that do not affect normal cells. One draw-back holding curcumin back from being an effective anti-cancer agent in humans is that it is almost completely insoluble in water and therefore has poor absorption and subsequently poor bioavailability. Here we have generated a number of curcumin derivatives (tetrahydro-curcumin, curcumin mono-carboxylic acid, curcumin mono-galactose, curcumin mono-alkyne and dendrimer-curcumin conjugate) to test whether any of them display both cytotoxicity and water solubility. Of those tested only dendrimer-curcumin conjugate exhibited both water solubility and cytotoxicity against SKBr3 and BT549 breast cancer cells. When compared to curcumin dissolved in DMSO, dendrimer-curcumin conjugate dissolved in water was significantly more effective in inducing cytotoxicity, as measured by the MTT assay and effectively induced cellular apoptosis measured by caspase-3 activation. Since dendrimer-curcumin conjugate is water soluble and capable of inducing potent cytotoxic effects on breast cancer cell lines, it may prove to be an effective anti-cancer therapy to be used in humans.

Keywords: Curcumin, solubility, breast cancer, apoptosis, dendrimer.

DENDRIMER-CURCUMIN CONJUGATEINTRODUCTION

Curcumin is the bioactive component extracted from the rhizome of the perennial herb *Curcuma longa*. It is a lipophilic fluorescent molecule having phenolic groups with conjugated double bonds. Besides its traditional use as a spice and a coloring agent in food, curcumin has shown broad spectrum applications as a therapeutic agent. Moreover, the low intrinsic toxicity of curcumin has promoted its successful application as an antioxidant, anticancer, antimicrobial, anti-inflammatory agent without any adverse side-effects.

The cytotoxic effect of curcumin has been observed in different types of cancer cells including colon [1], breast [2], and prostate [3]. *In vivo* studies, with rat mammary tumors, have shown that curcumin is capable of decreasing tumor initiation and growth [4, 5]. Curcumin has also been shown to be anti-angiogenic by down regulating two major angiogenesis factors, VEGF (vascular endothelial growth factor) and b-FGF (basic fibroblast growth factor) [6], in MDA-MB 231 breast cancer cells. Curcumin added to the diet has been reported to reverse tumor exosome mediated inhibition of Natural Killer cell activation 21a mechanism commonly used by tumor cells to overcome surveillance of the immune system [7]. Evidence also indicates that curcumin decreases the mRNA and protein levels of certain inflammatory cytokines and thereby inhibits the metastatic potentiality of cancer cells [8]. Furthermore, it has been successfully used in combination with different chemotherapeutic drugs like Bortezomib [9], 5-fluorouracil [10]; Gemcitabine [11] for more effective treatment of several types of tumors. Despite the broad spectrum bioactivity against cancer, its application as a successful drug candidate is confronted by its poor water/plasma solubility resulting in low bioavailability and absorption [12].

*Address correspondence to this author at the Department of Biology and Chemistry, College of Staten Island, 2800 Victory Blvd., Staten Island, NY, 10314, Biology or Biochemistry Doctoral Program, City University of New York Graduate Center, 365 Fifth Ave., NY, NY, 10016; Tel: (718) 982-3862; E-mail: jimmie.fata@csi.cuny.edu

The poor bioavailability of curcumin has been accounted by several factors like inadequate absorption, high rate of metabolic degradation and rapid elimination out of the body. This is evident in experiments where high doses of curcumin were administered to both humans and rats but only extremely low levels were subsequently found in the serum [13, 14]. Intraperitoneal and intravenous curcumin administration did not make any impressive contribution to serum level increase of curcumin [15, 16]. Curcumin also displays limited tissue distribution, which is another major issue limiting its potent bioefficacy [12, 14]. Limited tissue distribution is often due to the fact that curcumin undergoes rapid biotransformation into metabolites like curcumin-sulfates and curcumin-glucuronides prior to absorption [17-19].

To overcome these problems several strategies have been designed. Curcumin encapsulation in liposomes, phospholipid-curcumin complexes, and nano-particles bound with curcumin have all been formulated to increase drug delivery, prolonged circulation, enhanced permeability and resistance to metabolic conversion [20-24]. However, improving the water solubility of curcumin has received limited research. Here we screened a number of curcumin derivatives to determine whether they retain both water solubility and cytotoxicity. Our findings have uncovered one novel curcumin derivative that is both water soluble and cytotoxic to breast cancer cell lines.

RESULTS

Determination of IC_{50} Values for Curcumin and Curcumin Derivatives

Two breast cancer cell lines (SKBr3 and BT549) were used to screen the cytotoxicity of curcumin and curcumin derivatives outlined in Fig. (**1**). An MTT assay was used to determine the IC_{50} value for each curcumin derivative, which were compared to the parental compound curcumin (Fig. **2**). In general, SKBr3 breast cancer cells were more resistant to the cytotoxic effects of curcumin and curcumin derivatives when compared to BT549 breast cancer cells. The parental compound curcumin had an IC_{50} value of 47.9 ± 21.5 μM in SKBr3 cells and 35.8 ± 18.4 μM in BT549 cells. Only

1871-5206/13 $58.00+.00

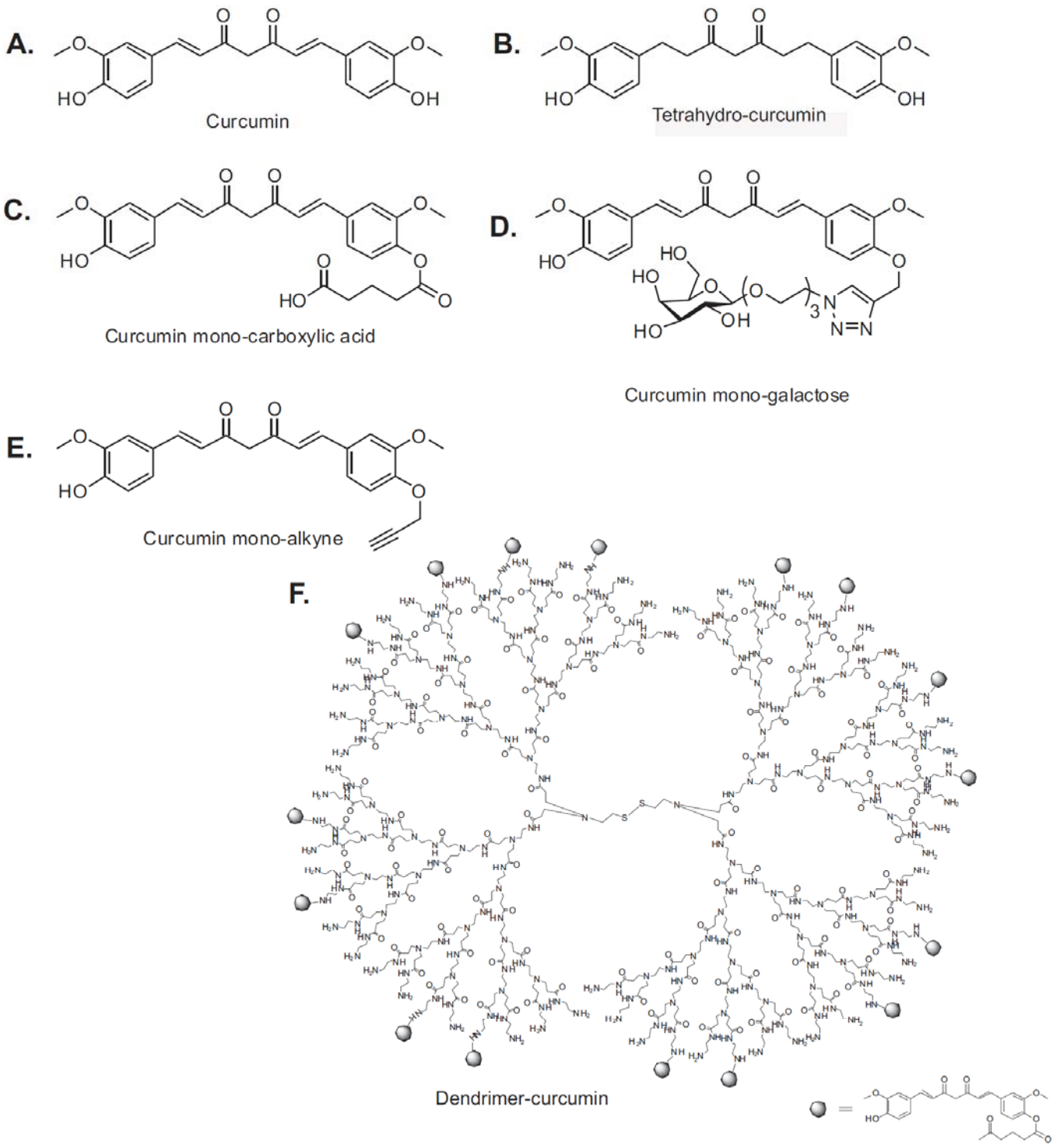

Fig. (1). Chemical structure of A) Curcumin, B) Tetrahydro-curcumin, C) Curcumin mono-carboxylic acid, D) Curcumin mono-galactose E) Curcumin mono-alkyne, and F) Dendrimer-curcumin conjugate.

one other compound, dendrimer-curcumin conjugate (also called dendrimer-curcumin), exhibited IC_{50} values significantly less than curcumin. The IC_{50} values for dendrimer-curcumin were 12.7 ± 7.5 μM for SKBr3 cells (3.77 fold less than curcumin) and 3.3 ± 2.1 μM for BT549 cells (10.8 fold less than curcumin). All other curcumin derivatives (tetrahydro-curcumin, curcumin mono-carboxylic acid, curcumin mono-alkyne, and curcumin mono-galactose) failed to induce any significant cytotoxicity on both breast cancer cell lines at the concentrations examined (0, 2, 5, 10, 25, 50, 100 μM). Curcumin mono-galactose failed to show any cytotoxicity at any concentration but instead appeared to increase cellular metabolism in both cell lines.

Solubility of Curcumin and Dendrimer-Curcumin in DMSO and Water

Curcumin solubility in DMSO was evident by eye as a yellow haze without precipitate when dissolved at 5 μM (Fig. **3A**). However, when added to water, curcumin fails to solubilize and

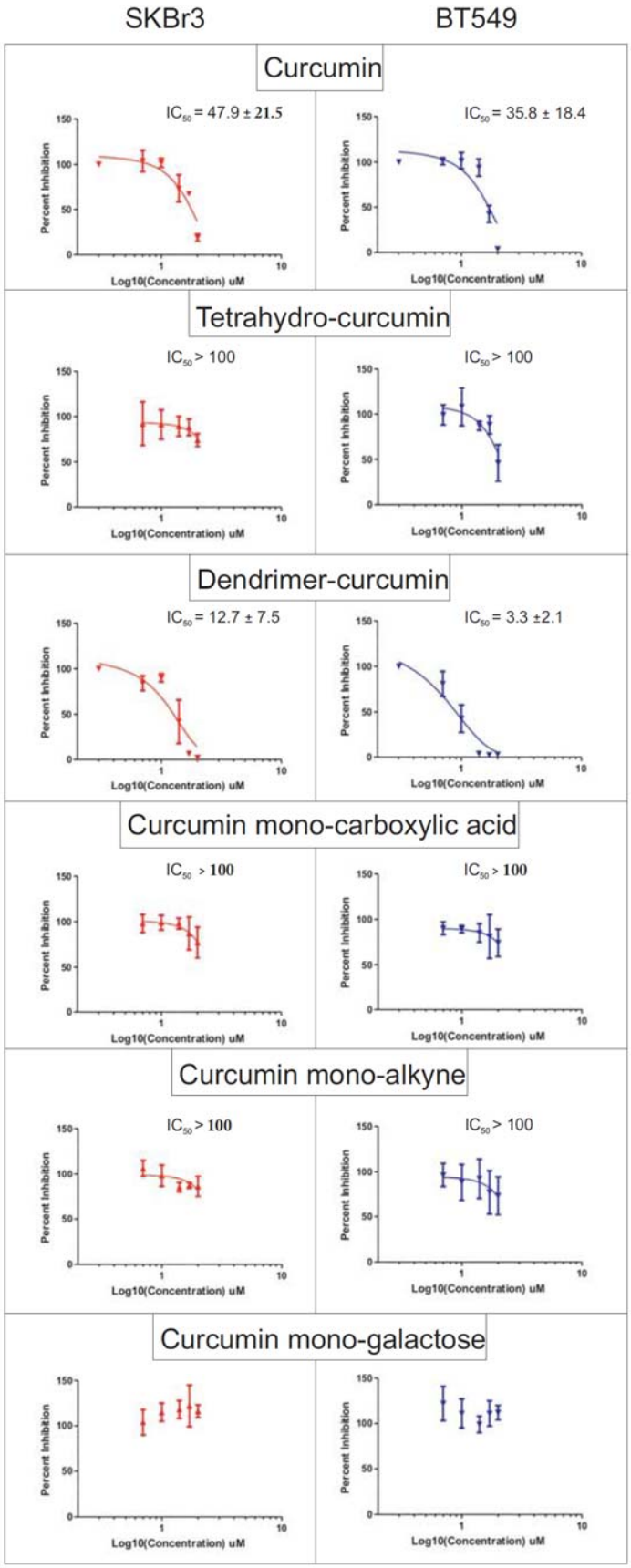

Fig. (2). IC_{50} values for curcumin derivatives on breast cancer cells. SKBr3 (left column - red) and BT549 (right column - blue) were exposed to increasing concentrations of curcumin and curcumin derivatives. IC_{50} values ± 95% confidence intervals were established for all derivatives except curcumin mono-galactose, which did not display any cytotoxic effect. Only curcumin and dendrimer-curcumin conjugate display potent cytotoxic effect on both cancer cell lines.

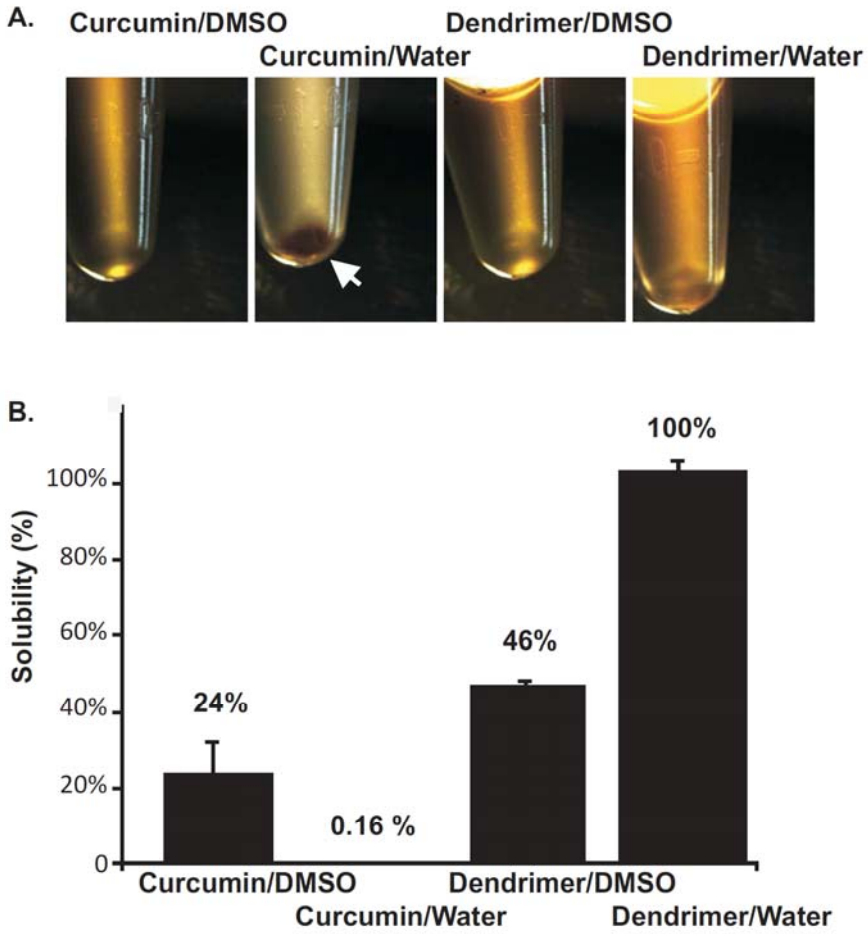

Fig. (3). Solubility of curcumin and dendrimer-curcumin conjugate in DMSO and water. A) Curcumin appears visibly soluble in DMSO (first panel - yellow color) but precipitates out in water (second panel - arrow points to pellet). Dendrimer-curcumin conjugate is soluble in both DMSO (third panel) and water (fourth panel). B) Solubility, measured by absorbance at 430 nm, indicates curcumin is 24% soluble in DMSO and not soluble in water. Using the same measurements Dendrimer-curcumin conjugate is approximately 46% soluble in DMSO and 100% soluble in water.

instead precipitates out (Fig. **3A**). Dendrimer-curcumin also dissolves well in DMSO (Fig. **3A**) but unlike curcumin, is freely soluble in water without any evidence of precipitate (Fig. **3A**). To accurately determine solubility of curcumin and dendrimer-curcumin in DMSO and in water, we measured the absorbance of each condition at 430 nm with a spectrophotometer. The molar concentration of each solution was then determined by the standard equation $A = \varepsilon cl$ (A = absorbance, $\varepsilon = 55 \times 10^3$, which is the molar extinction co-efficient of curcumin, c = concentration; l = length of the light path) as outlined in the Materials and Methods section. Applying this formula to the absorbance readings we found that when 5 μM of curcumin was dissolved in DMSO, 1.2 μM (30%) became completely soluble, while virtually no curcumin became soluble when added to water. In contrast, when a 5 μM solution of dendrimer-curcumin was added to DMSO and water, approximately 2.3 μM (45%) and 5.1 μM (100%) became solubilized, respectfully. These results clearly indicate that dendrimer-curcumin conjugate is highly soluble in water, while the parental curcumin compound is virtually insoluble in water. These findings were extended to show that dendrimer-curcumin still remains 100% soluble at 50 μM (data not shown).

Cellular Accumulation of Curcumin and Dendrimer-Curcumin Conjugate

After excitation at 450 nm, both curcumin and dendrimer-curcumin conjugate exhibit fluorescence. Using a microplate florescence reader we measured the fluorescent intensity of each compound, dissolved in DMSO or water at 5 μM (Fig. **4A**). Fluorescent intensity was highest in curcumin dissolved in DMSO (0.068 ± 0.003; arbitrary units) and lowest in curcumin added to water (0.003 ± 0.002). Dendrimer-curcumin dissolved in DMSO and in water had fluorescent intensities of 0.036 ± 0.003 and 0.011 ± 0.002, respectively. The inherent fluorescence of curcumin and dendrimer-curcumin conjugate allowed an analysis of cell entry and accumulation of each compound/solvent (Fig. **4B**). This involved exposing BT549 breast cancer cells to 5 μM solutions of each condition outlined in Fig. (**4A**) followed one hour later by a measurement of fluorescent intensity. Results from these experiments indicate that curcumin in DMSO, dendrimer-curcumin conjugate in DMSO, and dendrimer-curcumin conjugate in water all enter and accumulate in cells (Fig. **4B** (bottom panel)) and, relative to each other, exhibited fluorescent intensities similar to those measured in solution (Compare Fig. **4A** with Fig. **4C**).

Comparison of IC_{50} Values for Curcumin and Dendrimer-Curcumin Conjugate Dissolved in DMSO or Water

An MTT assay on SKBr3 and BT549 breast cancer cell lines was used to determine the IC_{50} values for curcumin and dendrimer-curcumin conjugate dissolved in either DMSO or water. As noted before in Fig. (**2**), dendrimer-curcumin conjugate (blue) dissolved in DMSO is more effective at inducing cytotoxicity in both breast cancer cell lines when compared to curcumin (red) dissolved in DMSO (Fig. **5** (top panels)). Significant differences are evident when dendrimer-curcumin conjugate dissolved in water is compared

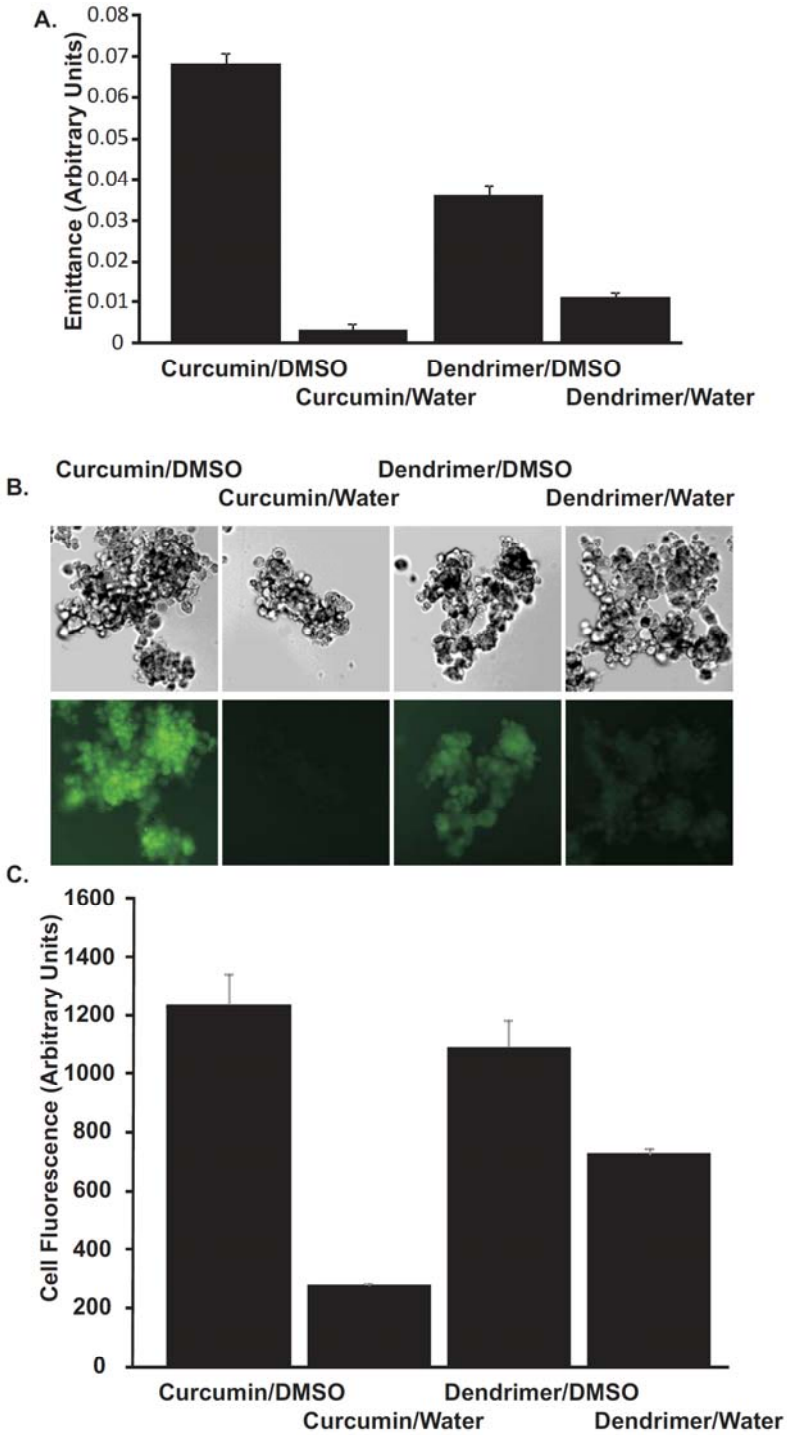

Fig. (4). Fluorescent emittance of curcumin and dendrimer-curcumin conjugate in solution and *in vitro*. Curcumin dissolved in DMSO exhibits fluorescence in solution (A) and when it accumulates in BT549 (SKBr3) cells at 40 minutes (B - bottom panel). Since curcumin in water fails to dissolve it emits minimal fluorescence in solution and *in vitro* (A,B). Dendrimer-curcumin conjugate dissolved in DMSO and water emits fluorescence in solution (A) and *in vitro* after accumulating in cells (B - bottom panel) but at intensities lower than curcumin in DMSO. C) Quantification of fluorescent intensities in B. All solutions are 5 μM.

to curcumin added to water. The latter mixture fails to induce any significant cytotoxic effect on both breast cancer cell lines (Fig. **5** (red in bottom panels)). In contrast, dendrimer-curcumin conjugate dissolved in water is capable of inducing cell cytotoxicity (Fig. **5** (blue in bottom panels). The IC_{50} values of dendrimer-curcumin conjugate dissolved in DMSO and dendrimer-curcumin conjugate dissolved in water were not significantly different from each other. Importantly, dendrimer-curcumin conjugate dissolved in water is significantly different than curcumin dissolved in either DMSO or water, indicating it is a better formulation for inducing cell cytotoxicity.

Induction of Apoptosis and Caspase-3 Activation by Curcumin and Dendrimer-Curcumin Conjugate

To determine whether curcumin and dendrimer-curcumin conjugate can induce cellular apoptosis, detection of activated caspase-3 by immunofluorescence was performed (Fig. **6A**). BT549 cells exposed to 5 μM of each formulation for 10 hours were

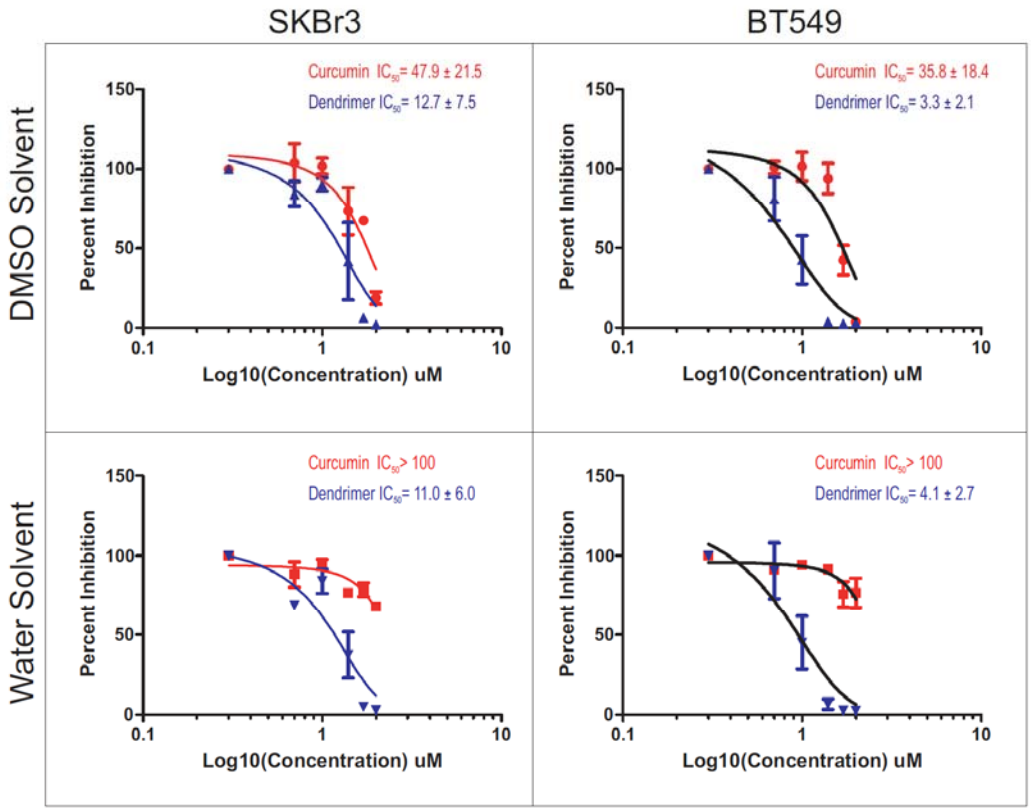

Fig. (5). IC_{50} values for curcumin and dendrimer-curcumin conjugate dissolved in DMSO and water. SKBr3 (left column) and BT549 (right column) were exposed to increasing concentrations of curcumin and dendrimer-curcumin conjugate dissolved in DMSO or water. IC_{50} values ± 95% confidence intervals were established for all conditions. Dendrimer-curcumin conjugate (blue) had lower IC_{50} values compared to curcumin (red) when both were dissolved in DMSO (top panels). Dendrimer-curcumin conjugate also exhibits cytotoxic effects on breast cancer cells when dissolved in water (bottom panels-blue). Since curcumin does not dissolve in water it fails to elicit any cytotoxic effect on breast cancer cell lines (bottom panels-red).

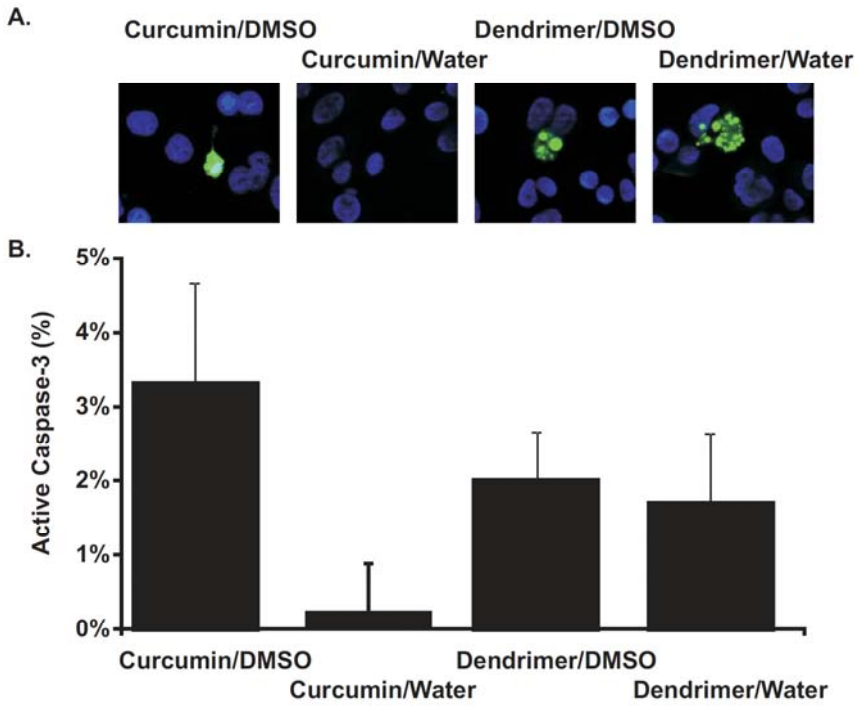

Fig. (6). Curcumin and dendrimer-curcumin conjugate induces caspase-3 activation in breast cancer cells. Caspase-3 activation was evident when BT549 cells were exposed for 10 hours to curcumin dissolved in DMSO, dendrimer-curcumin conjugate dissolved in DMSO, and dendrimer-curcumin conjugate dissolved in water. The inability of curcumin to dissolve in water led to an absence of any substantial caspase-3 activation when this mixture is administered to cells. Cells were exposed to solutions for 10 hours at a concentration of 5 μM.

examined and scored for caspase-3 activation (Fig. **6B**). Curcumin dissolved in DMSO (3.31 ± 1.37 percent caspase-3 activation) and dendrimer-curcumin dissolved in DMSO (2.02 ± 0.65) or water (1.72 ± 0.93) all induced a measureable amount of positive cells having activated caspase-3, even when administered at low concentrations (5 μM). As expected curcumin added to water (0.23 ± 0.46) did not induce any detectable amount of caspase-3 activation which was similar to cells in presence of media or DMSO alone (data not shown).

DISCUSSION

The therapeutic application of curcumin as an anti-cancer agent is confronted by its poor systemic bioavailability. Extensive research and preclinical development is focused on overcoming this challenge and involves such approaches as novel curcumin delivery systems and design of various curcumin derivatives. Previously, our collaborators reported synthesis of mono-functional curcumin derivatives (curcumin mono-galactose, curcumin mono-alkyne, curcumin mono-carboxylic acid, and curcumin mono-azide) to produce better water soluble curcumin conjugates [25, 26]. They have also demonstrated in mouse *in vivo* studies, that curcumin coupled with a cancer cell specific antibody is able to suppress the growth of B16F10 brain tumors [27]. Importantly, this synthesized curcumin-antibody adduct is water-soluble and rapidly targets cancer tissue. Other groups have found that curcumin when loaded with magnetic nanoparticles (MNP) shows concentration dependant accumulation in triple negative MDA-MB 231 breast cancer cell lines through endocytosis [28]. The MNP-curcumin conjugate displays specific targeting and strong anti-cancer properties compared to free curcumin. Together, these findings point toward the fact that improved delivery systems of curcumin ensures increased bioactivity against cancer treatment.

Poly amido amine (PAMAM) dendrimers are well defined high molecular weight macromolecules ideally suited for drug delivery. They are water soluble molecules that have an exquisite degree of molecular uniformity, narrow molecular weight distribution with specific size and highly functionalized terminal surface polyvalently displaying amine groups. They are excellent transfection reagents and therefore are well suited for controlled drug delivery [29-32]. A generation 4 cystamine core PAMAM dendrimer displays 64 amine groups, making it highly soluble in water. During the synthesis of dendrimer-curcumin conjugates, we coupled 37 amine groups to curcumin mono-carboxylic acid to produce a biomimetic polyphenol, which polyvalently displays multiple copies of curcumin [25]. The free amine groups of the dendrimers facilitate efficient water solubility and cell entry. Moreover, this synthesized curcumin conjugate also acts like a pro-drug. The presence of acid labile phenolic ester group of curcumin mono-carboxylic acid could facilitate the release of curcumin under physiological acidic environments [27]. Another advantage of dendrimer drug conjugate arises from the fact that the vasculature in tumor is leaky. This Enhanced Permeability and Retention (EPR) effect will target the dendrimer-curcumin conjugate selectively to tumor cells. Here, our findings have addressed the issue of poor water solubility of curcumin by synthesizing a readily water soluble dendrimer-curcumin conjugate. Furthermore, our evaluation of the cytotoxicity of the water soluble dendrimer-curcumin conjugate indicates that it is a potent anti-cancer agent against breast cancer cells. We noted that entry of dendrimer-curcumin conjugate dissolved in water occurred as early as 15 minutes following treatment of cells (data not shown) and that it has a significantly lower IC_{50} value on breast cancer cells compared to cells accumulating curcumin dissolved in DMSO. Importantly, dendrimer curcumin can induce apoptotic cell death *via* caspase-3 activation.

Currently, curcumin has shown successful anti-carcinogenic effects in a Phase IIa clinical trial against colorectal neoplasia [33]. A phase II clinical trial of curcumin in combination with docetaxel drug is currently underway to treat advanced and metastatic breast cancer patients after its encouraging efficacy results in a Phase I trial [34]. Our findings that dendrimer-curcumin conjugate is water soluble, cytotoxic and induces apoptosis in breast tumor cells suggest it may provide better efficacy compared to the parent compound, curcumin, in the treatment against breast cancer. We believe that improved derivatives of curcumin (like dendrimer-curcumin conjugate) that can specifically target tumor cells will ultimately serve as a convenient and highly efficient platform toward a potent, less toxic treatment of cancer.

MATERIALS AND METHODS

Synthesis of Curcumin and Curcumin Derivatives

Curcumin and tetrahydro-curcumin were purchased from commercially available sources (Sigma). Curcumin mono-alkyne, curcumin mono-carboxylic acid and dendrimer-curcumin conjugate were synthesized according to the previously published procedure [25]. Sugar-curcumin conjugate was synthesized following the referenced article [26].

Solubility Test for Curcumin and Dendrimer-Curcumin Conjugates

Both curcumin and dendrimer-curcumin conjugate were each dissolved in water and DMSO to prepare a stock concentration of 5 μM. The solutions were all briefly spun at 13,000 rpm using a micro-centrifuge to remove the undissolved portion of the solution as precipitate. Effective curcumin concentration was determined my measuring absorbance of each solution at 430 nm in a spectrophotometer (Cary Bio 100 UV-Visible Spectrophotometer). The molar concentration was subsequently determined by the standard equation $A = \varepsilon cl$ (A = absorbance, $\varepsilon = 55 \times 10^3$ which is the molar extinction co-efficient of curcumin, c = concentration; l = length of the light path).

Fluorescence of Curcumin/Dendrimer-Curcumin Conjugates in Solution

The fluorescence of 5 μM curcumin/ dendrimer-curcumin conjugate dissolved in water and DMSO was measured using an excitation wavelength of 450 nm with a FL_X 800 Microplate Fluorescence reader (Biotek Instruments, Vermont).

Cell Lines and Culture

Human breast cancer cell lines SKBr3 and BT549 were obtained from The American Type Culture Collection. The SKBr3 cell line was cultured in DMEM/F-12 (1:1) (Invitrogen) supplemented with 10% (v/v) FCS, 10 units/ml Penicillin and 10 μg/ml Streptomycin (Hyclone). The BT549 cell line was grown in RPMI+Glutamax 1640 medium (InVitrogen) with 10% FCS. The cell lines were maintained at 37°C in an atmosphere of 5% CO_2. Media was replaced every 2-3 days and cells were sub-cultured with 0.05% Trypsin (Cellgro) once they reached a confluency of 80%.

Live Cell Imaging for Uptake of Curcumin Derivatives in Human Breast Cancer Cell Lines

A cell density of 10×10^3 cells/well was plated in a 8 well chamber and incubated for 24 hrs at 37°C supplemented with 5% CO_2. Cells were washed twice with plain medium prior to any treatment. The stock solution of curcumin and dendrimer-curcumin conjugate were briefly spun at 13,000 rpm and the clear supernatant was only used to make subsequent dilutions. A 5 μM working concentration was used for both curcumin and dendrimer-curcumin conjugate to treat the cells. The final DMSO concentration in the treated cells was kept below the accepted toxicity level of 1%. Both bright field and fluorescent images were captured simultaneously

after immediate drug addition to cells with a Zeiss Live Imaging microscope (Zeiss Axio Vision CD29A, Göttingen Germany) for 1 hour at an interval of 10 minutes. Drug uptake by cells was assessed by measuring the increase in fluorescence intensity within cells using Image J software. The data represents average fluorescence value of multiple positions (n = 6) under each condition; means ± SEM.

MTT Assay

Equal density of cells was plated and incubated for 24 hrs in a 96 well plate. Prior to treatment, cells were washed twice with plain medium. A serial drug dilution of 100, 50, 25, 10, 5 and 2μM was prepared in serum free media for curcumin and dendrimer-curcumin conjugate each dissolved in both water and DMSO. The molar concentration of dendrimer-curcumin conjugate reflect the combined molecular weight of the dendrimer and its' attached 37 molecules of curcumin. MTT assay was performed after 24 hrs of treatment with different drug concentrations. Absorbance was measured at 570 nm and 690 nm using Spectra Max 340 PC microplate spectrophotometer (Molecular Device, CA) and was blanked against the control, which contained media alone. The data represents an average of three independent experiments carried out in triplicates, means ± SEM. Data was plotted with a Least Squares Fit of the Log (inhibitor) versus response using GraphPad Prism Software. This model assumes that the dose response curves has a standard slope, equal to a Hill slope (or slope factor) of -1.0. Statistical significance was determined when IC_{50} confidence intervals did not overlap.

Measurement of Caspase-3 Activity

Cells were grown in an 8 well chamber for 24 hrs prior to exposure to curcumin derivatives. Cell apoptosis was determined by caspase-3 activation following treatment with curcumin and dendrimer-curcumin conjugate. The DMSO concentration in the treated cells did not exceed 1%. Cells were fixed post 10 hrs of treatment with 4% paraformaldehyde for 15 minutes at room temperature, blocked for an hour with immunoblocker buffer (IB) solution (2% BSA, 10% horse serum, 0.5% Triton-X 100 in PBS) and incubated overnight at 4°C with cleaved caspase-3 (D175) rabbit polyclonal antibody (Cell Signaling # 9661) at a dilution of 1:200. Cells were washed 3 times with PBS+0.5% Triton X-100 and incubated for 1 hr with Alexa fluor 488 goat anti-rabbit IgG secondary antibody (InVitrogen) diluted to 1:2000 in the IB buffer solution. Nuclei were counterstained with DAPI (400 nM). Images were captured by Zeiss Live Imaging microscope (Zeiss Axio Vision CD29A, Göttingen Germany) and were later processed using Image J software. The data represents percentage of cells that were positive for caspase activation calculated from the captured images.

CONFLICT OF INTEREST

The author(s) confirm that this article content has no conflict of interest.

ACKNOWLEDGEMENTS

We would like to thank the following for monetary support of the project: A CUNY Doctoral Student Grant to SD, a Staten Island Breast Cancer Research Initiative Grant to JEF and a PSC-CUNY Collaborative Grant to KR. We also are grateful to Deepak Menon and Ashley Mathai for technical assistance and Edmund C. Jenkins help with imaging and reading of the manuscript.

REFERENCES

[1] Chen, H.; Zhang, Z.S.; Zhang, Y.L.; Zhou, D.Y. Curcumin inhibits cell proliferation by interfering with the cell cycle and inducing apoptosis in colon carcinoma cells. *Anticancer Res.*, **1999**, *19*(5A), 3675-3680.

[2] Squires, M.S.; Hudson, E.A.; Howells, L.; Sale, S.; Houghton, C.E.; Jones, J.L.; Fox, L.H.; Dickens, M.; Prigent, S.A.; Manson, M.M. Relevance of mitogen activated protein kinase (MAPK) and phosphotidylinositol-3-kinase/protein kinase B (PI3K/PKB) pathways to induction of apoptosis by curcumin in breast cells. *Biochem Pharmacol.*, **2003**, *65*(3), 361-376.

[3] Teiten, M.H.; Gaascht, F.; Eifes, S.; Dicato, M.; Diederich, M. Chemopreventive potential of curcumin in prostate cancer. *Genes Nutr.*, **2010**, *5*, (1), 61-74.

[4] Inano, H.; Onoda, M.; Inafuku, N.; Kubota, M.; Kamada, Y.; Osawa, T.; Kobayashi, H.; Wakabayashi, K. Chemoprevention by curcumin during the promotion stage of tumorigenesis of mammary gland in rats irradiated with gamma-rays. *Carcinogenesis*, **1999**, *20*(6), 1011-1018.

[5] Inano, H.; Onoda, M. Prevention of radiation-induced mammary tumors. *Int. J. Radiat. Oncol. Biol. Phys.*, **2002**, *52*(1), 212-223.

[6] Shao, Z. M.; Shen, Z. Z.; Liu, C. H.; Sartippour, M. R.; Go, V. L.; Heber, D.; Nguyen, M. Curcumin exerts multiple suppressive effects on human breast carcinoma cells. *Int. J. Cancer*, **2002**, *98*(2), 234-240.

[7] Zhang, H.G.; Kim, H.; Liu, C.; Yu, S.; Wang, J.; Grizzle, W.E.; Kimberly, R.P.; Barnes, S. Curcumin reverses breast tumor exosomes mediated immune suppression of NK cell tumor cytotoxicity. *Biochim. Biophys. Acta*, **2007**, *1773*(7), 1116-1123.

[8] Bachmeier, B.E.; Mohrenz, I.V.; Mirisola, V.; Schleicher, E.; Romeo, F.; Hohneke, C.; Jochum, M.; Nerlich, A.G.; Pfeffer, U. Curcumin downregulates the inflammatory cytokines CXCL1 and -2 in breast cancer cells *via* NFkappaB. *Carcinogenesis*, **2008**, *29*(4), 779-789.

[9] Park, J.; Ayyappan, V.; Bae, E.K.; Lee, C.; Kim, B.S.; Kim, B.K.; Lee, Y.Y.; Ahn, K.S.; Yoon, S.S. Curcumin in combination with bortezomib synergistically induced apoptosis in human multiple myeloma U266 cells. *Mol. Oncol.*, **2008**, *2*(4), 317-326.

[10] Du, B.; Jiang, L.; Xia, Q.; Zhong, L. Synergistic inhibitory effects of curcumin and 5-fluorouracil on the growth of the human colon cancer cell line HT-29. *Chemotherapy*, **2006**, *52*(1), 23-28.

[11] Kunnumakkara, A.B.; Guha, S.; Krishnan, S.; Diagaradjane, P.; Gelovani, J.; Aggarwal, B.B. Curcumin potentiates antitumor activity of gemcitabine in an orthotopic model of pancreatic cancer through suppression of proliferation, angiogenesis, and inhibition of nuclear factor-kappaB-regulated gene products. *Cancer Res.*, **2007**, *67*(8), 3853-3861.

[12] Anand, P.; Kunnumakkara, A.B.; Newman, R.A.; Aggarwal, B.B. Bioavailability of curcumin: problems and promises. *Mol Pharm* **2007**, *4*(6), 807-818.

[13] Wahlstrom, B.; Blennow, G. A study on the fate of curcumin in the rat. *Acta Pharmacol. Toxicol. (Copenh)*, **1978**, *43*(2), 86-92.

[14] Ravindranath, V.; Chandrasekhara, N. Absorption and tissue distribution of curcumin in rats. *Toxicology*, **1980**, *16*(3), 259-265.

[15] Perkins, S.; Verschoyle, R.D.; Hill, K.; Parveen, I.; Threadgill, M.D.; Sharma, R.A.; Williams, M.L.; Steward, W. P.; Gescher, A.J. Chemopreventive efficacy and pharmacokinetics of curcumin in the min/+ mouse, a model of familial adenomatous polyposis. *Cancer Epidemiol. Biomarkers Prev.*, **2002**, *11*(6), 535-540.

[16] Yang, K.Y.; Lin, L.C.; Tseng, T.Y.; Wang, S.C.; Tsai, T.H. Oral bioavailability of curcumin in rat and the herbal analysis from Curcuma longa by LC-MS/MS. *J. Chromatogr. B Analyt. Technol. Biomed. Life Sci.*, **2007**, *853*(1-2), 183-189.

[17] Garcea, G.; Jones, D.J.; Singh, R.; Dennison, A.R.; Farmer, P.B.; Sharma, R.A.; Steward, W.P.; Gescher, A.J.; Berry, D.P. Detection of curcumin and its metabolites in hepatic tissue and portal blood of patients following oral administration. *Br. J. Cancer*, **2004**, *90*(5), 1011-1015.

[18] Pan, M.H.; Huang, T.M.; Lin, J.K. Biotransformation of curcumin through reduction and glucuronidation in mice. *Drug Metab. Dispos.*, **1999**, *27*(4), 486-494.

[19] Asai, A.; Miyazawa, T. Occurrence of orally administered curcuminoid as glucuronide and glucuronide/sulfate conjugates in rat plasma. *Life Sci.*, **2000**, *67*(23), 2785-2793.

[20] Wu, W.; Shen, J.; Banerjee, P.; Zhou, S. Water-dispersible multifunctional hybrid nanogels for combined curcumin and photothermal therapy. *Biomaterials*, **2011**, *32*(2), 598-609.

[21] Li, L.; Braiteh, F. S.; Kurzrock, R., Liposome-encapsulated curcumin: *In vitro* and *in vivo* effects on proliferation, apoptosis, signaling, and angiogenesis. *Cancer*, **2005**, *104*(6), 1322-1331.

[22] Liu, A.; Lou, H.; Zhao, L.; Fan, P., Validated LC/MS/MS assay for curcumin and tetrahydrocurcumin in rat plasma and application to pharmacokinetic study of phospholipid complex of curcumin. *J. Pharm. Biomed. Anal.*, **2006**, *40*(3), 720-727.

[23] Li, L.; Ahmed, B.; Mehta, K.; Kurzrock, R. Liposomal curcumin with and without oxaliplatin: effects on cell growth, apoptosis, and angiogenesis in colorectal cancer. *Mol. Cancer Ther.*, **2007**, *6*(4), 1276-1282.

[24] Tiyaboonchai, W.; Tungpradit, W.; Plianbangchang, P. Formulation and characterization of curcuminoids loaded solid lipid nanoparticles. *Int. J. Pharm.*, **2007**, *337*(1-2), 299-306.

[25] Shi, W.; Dolai, S.; Rizk, S.; Hussain, A.; Tariq, H.; Averick, S.; L'Amoreaux, W.; El ldrissi, A.; Banerjee, P.; Raja, K., Synthesis of monofunctional curcumin derivatives, clicked curcumin dimer, and a PAMAM dendrimer curcumin conjugate for therapeutic applications. *Org. Lett.*, **2007**, *9*(26), 5461-5464.

[26] Dolai, S.; Shi, W.; Corbo, C.; Sun, C.; Averick, S.; Obeysekera, D.; Farid, M.; Alonso, A.; Banerjee, P.; Raja, K.S. "Clicked" Sugar-Curcumin Conjugate: Modulator of Amyloid-beta and Tau Peptide Aggregation at Ultra-low Concentrations. *ACS Chemical; Neuroscience*, **2011**, *2 (12)*, 694-699.

[27] Langone, P.; Debata, P.R.; Dolai, S.; Curcio, G.M.; Inigo, J.D.; Raja, K.; Banerjee, P. Coupling to a cancer cell-specific antibody potentiates tumoricidal properties of curcumin. *Int. J. Cancer*, **2011**, *131* (4), 10.

[28] Yallapu, M.M.; Othman, S.F.; Curtis, E.T.; Bauer, N.A.; Chauhan, N.; Kumar, D.; Jaggi, M.; Chauhan, S. C. Curcumin-loaded magnetic nanoparticles for breast cancer therapeutics and imaging applications. *Int. J. Nanomed.*, **2012**, *7*, 1761-1779.

[29] Wu, P.; Feldman, A.K.; Nugent, A. K.; Hawker, C.J.; Scheel, A.; Voit, B.; Pyun, J.; Frechet, J.M.; Sharpless, K.B.; Fokin, V.V. Efficiency and fidelity in a click-chemistry route to triazole dendrimers by the copper(i)-catalyzed ligation of azides and alkynes. *Angew Chem. Int. Ed. Engl.*, **2004**, *43*(30), 3928-3932.

[30] Svenson, S.; Tomalia, D.A. Dendrimers in biomedical applications--reflections on the field. *Adv. Drug Deliv. Rev.*, **2005**, *57*(15), 2106-2129.

[31] Majoros, I.J.; Myc, A.; Thomas, T.; Mehta, C.B.; Baker, J.R., Jr. PAMAM dendrimer-based multifunctional conjugate for cancer therapy: Synthesis, characterization, and functionality. *Biomacromolecules*, **2006**, *7*(2), 572-579.

[32] Balogh, L.P. Dendrimer 101. *Adv. Exp. Med. Biol.*, **2007**, *620*, 136-155.

[33] Carroll, R.E.; Benya, R.V.; Turgeon, D.K.; Vareed, S.; Neuman, M.; Rodriguez, L.; Kakarala, M.; Carpenter, P.M.; McLaren, C.; Meyskens, F.L., Jr.; Brenner, D.E. Phase IIa clinical trial of curcumin for the prevention of colorectal neoplasia. *Cancer Prev. Res. (Phila)*, **2011**, *4* (3), 354-364.

[34] Bayet-Robert, M.; Kwiatkowski, F.; Leheurteur, M.; Gachon, F.; Planchat, E.; Abrial, C.; Mouret-Reynier, M.A.; Durando, X.; Barthomeuf, C.; Chollet, P. Phase I dose escalation trial of docetaxel plus curcumin in patients with advanced and metastatic breast cancer. *Cancer Biol. Ther.*, **2010**, *9* (1), 8-14.

Received: July 12, 2012 **Revised: January 07, 2013** **Accepted: May 06, 2013**

Manuscripts submitted and published:

1. **Debnath S**, Hannon P, Jenkins EC Jr, Toropova K, Rodriguez NN, Alonso A, Fata JE*. Tau Renders Tumor Cell Resistance to TNFα-Mediated Cytotoxicity by Inhibiting TNF-Receptor Trimerization. (*under revision*).

2. **Debnath S**, Saloum D, Dolai S, Sun C, Averick S, Raja K, Fata JE*. Dendrimer-curcumin Conjugate: A Water Soluble and Effective Cytotoxic agent against Breast Cancer cell lines. Anticancer Agents in Med Chem (Epub 2013 Jan 24).

3. Jenkins EC Jr, **Debnath S**, Gundry S, Gundry S, Uyar U, Fata JE*. Intracellular pH regulation by Na+/H+ exchanger-1 (NHE1) is required for growth factor-induced mammary branchingmorphogenesis. Dev Biol. 2012 May 1;365(1):71-81. Epub 2012 Feb 17.

4. Jenkins EC Jr, **Debnath S**, Varriano S, Gundry S, Fata JE*. Na+/H+ Exchanger 1 (NHE1) Function is Necessary for Maintaining Mammary Tissue Architecture.

Dev Dynamics. (Epub 2013 July 23).

5. Sun C, Nirmalananda S, Jenkins EC Jr, **Debnath S**, Balambika R, Fata JE, Raja KS*. First Ayurvedic Approach towards Green Drugs: Anti Cervical Cancer-Cell Properties of

Clerodendrum viscosum Root Extract. Anticancer Agents Med Chem. 2013 Jan 24. [Epub ahead of print]

6. Fata JE, **Debnath S**, Jenkins EC Jr, Fournier MV. Nongenomic Mechanisms of PTEN Regulation. Int J Cell Biol. 2012;2012:379685. Epub 2012 Mar 25.

Manuscript in preparation:

The development of a novel plant-derived pharmaceutical composition that has anti-viral and anti-tumor effects. (Work done in collaboration with Dr. Probal Banerjee from CSI, CUNY and Dr. Mario R. Castellanos from Staten Island University Hospital).

Patent:

Preparation of curcumin triazolyl galactosides via click chemistry as antioxidants" (Principal inventor Dr. Krishnaswami Raja, CUNY Reference No: 10A0023).

References:

Aggarwal, B. B., et al., 2012. Historical perspectives on tumor necrosis factor and its superfamily: 25 years later, a golden journey. Blood. 119**,** 651-65.

Alonso, A. C., et al., 2008. Mechanism of tau-induced neurodegeneration in Alzheimer disease and related tauopathies. Curr Alzheimer Res. 5**,** 375-84.

Antoon, J. W., et al., 2012. Altered death receptor signaling promotes epithelial-to-mesenchymal transition and acquired chemoresistance. Sci Rep. 2**,** 539.

Ashkenazi, A., et al., 1999. Safety and antitumor activity of recombinant soluble Apo2 ligand. J Clin Invest. 104**,** 155-62.

Bai, J., et al., 2005. Predominant Bcl-XL knockdown disables antiapoptotic mechanisms: tumor necrosis factor-related apoptosis-inducing ligand-based triple chemotherapy overcomes chemoresistance in pancreatic cancer cells in vitro. Cancer Res. 65**,** 2344-52.

Balkwill, F., 2002. Tumor necrosis factor or tumor promoting factor? Cytokine Growth Factor Rev. 13**,** 135-41.

Balkwill, F., 2009. Tumour necrosis factor and cancer. Nat Rev Cancer. 9**,** 361-71.

Balkwill, F., Mantovani, A., 2001. Inflammation and cancer: back to Virchow? Lancet. 357**,** 539-45.

Ballatore, C., et al., 2007. Tau-mediated neurodegeneration in Alzheimer's disease and related disorders. Nat Rev Neurosci. 8**,** 663-72.

Beg, A. A., Baltimore, D., 1996. An essential role for NF-kappaB in preventing TNF-alpha-induced cell death. Science. 274**,** 782-4.

Berasain, C., 2009. Inflammation and liver cancer: new molecular links. Ann NY Acad Sci. 1155, 206-21.

Bhat, K. M., Setaluri, V., 2007. Microtubule-associated proteins as targets in cancer chemotherapy. Clin Cancer Res. 13**,** 2849-54.

Burke, F., et al., 1996. A cytokine profile of normal and malignant ovary. Cytokine. 8**,** 578-85.

Coussens, L. M., Werb, Z., 2002. Inflammation and cancer. Nature. 420**,** 860-7.

Dvorak, H. F., 1986. Tumors: wounds that do not heal. Similarities between tumor stroma generation and wound healing. N Engl J Med. 315**,** 1650-9.

Guadagni, F., et al., 2007. Review. TNF/VEGF cross-talk in chronic inflammation-related cancer initiation and progression: an early target in anticancer therapeutic strategy. In Vivo. 21**,** 147-61.

Hanahan, D., Weinberg, R. A., 2011. Hallmarks of cancer: the next generation. Cell. 144**,** 646-74.

Jackman, R. W., et al., 2009. Microtubule-mediated NF-kappaB activation in the TNF-alpha signaling pathway. Exp Cell Res. 315**,** 3242-9.

Krajewski, S., et al., 1999. Prognostic significance of apoptosis regulators in breast cancer. Endocr Relat Cancer. 6**,** 29-40.

LeBlanc, H., et al., 2002. Tumor-cell resistance to death receptor--induced apoptosis through mutational inactivation of the proapoptotic Bcl-2 homolog Bax. Nat Med. 8**,** 274-81.

Lee, G., et al., 1998. Tau interacts with src-family non-receptor tyrosine kinases. J Cell Sci. 111 (Pt 21)**,** 3167-77.

Leek, R. D., et al., 1998. Association of tumour necrosis factor alpha and its receptors with thymidine phosphorylase expression in invasive breast carcinoma. Br J Cancer. 77**,** 2246-51.
Legler, D. F., et al., 2003. Recruitment of TNF receptor 1 to lipid rafts is essential for TNFalpha-mediated NF-kappaB activation. Immunity. 18**,** 655-64.
Magne, N., et al., 2006. NF-kappaB modulation and ionizing radiation: mechanisms and future directions for cancer treatment. Cancer Lett. 231**,** 158-68.
Mantovani, A., et al., 2008. Cancer-related inflammation. Nature. 454**,** 436-44.
Mantovani, A., et al., 1992. The origin and function of tumor-associated macrophages. Immunol Today. 13**,** 265-70.
Rasmussen, H., et al., 2002. TNFerade Biologic: preclinical toxicology of a novel adenovector with a radiation-inducible promoter, carrying the human tumor necrosis factor alpha gene. Cancer Gene Ther. 9**,** 951-7.
Rosenblum, M. G., et al., 2000. A novel recombinant fusion toxin targeting HER-2/NEU-over-expressing cells and containing human tumor necrosis factor. Int J Cancer. 88**,** 267-73.
Rouzier, R., et al., 2005. Microtubule-associated protein tau: a marker of paclitaxel sensitivity in breast cancer. Proc Natl Acad Sci U S A. 102**,** 8315-20.
Sharma, V. M., et al., 2007. Tau impacts on growth-factor-stimulated actin remodeling. J Cell Sci. 120**,** 748-57.
Shivanna, M., Srinivas, S. P., 2009. Microtubule stabilization opposes the (TNF-alpha)-induced loss in the barrier integrity of corneal endothelium. Exp Eye Res. 89**,** 950-9.
Sugarman, B. J., et al., 1985. Recombinant human tumor necrosis factor-alpha: effects on proliferation of normal and transformed cells in vitro. Science. 230**,** 943-5.
Tanaka, S., et al., 2009. Tau expression and efficacy of paclitaxel treatment in metastatic breast cancer. Cancer Chemother Pharmacol. 64**,** 341-6.
Torisu, H., et al., 2000. Macrophage infiltration correlates with tumor stage and angiogenesis in human malignant melanoma: possible involvement of TNFalpha and IL-1alpha. Int J Cancer. 85**,** 182-8.
van Horssen, R., et al., 2006. TNF-alpha in cancer treatment: molecular insights, antitumor effects, and clinical utility. Oncologist. 11**,** 397-408.
Vanhaesebroeck, B., et al., 1991. Two discrete types of tumor necrosis factor-resistant cells derived from the same cell line. Cancer Res. 51**,** 2469-77.
Wagner, P., et al., 2005. Microtubule Associated Protein (MAP)-Tau: a novel mediator of paclitaxel sensitivity in vitro and in vivo. Cell Cycle. 4**,** 1149-52.
Walczak, H., et al., 1999. Tumoricidal activity of tumor necrosis factor-related apoptosis-inducing ligand in vivo. Nat Med. 5**,** 157-63.
Wang, D., et al., 2009. Reduced tumor necrosis factor receptor-associated death domain expression is associated with prostate cancer progression. Cancer Res. 69**,** 9448-56.
Weibo Cai, Z. J. K., Hao Hong, Jiangtao Sun, 2008. Targeted cancer therapy with Tumor Necrosis Factor-Alpha.
Wong, G. H., et al., 1989. Manganous superoxide dismutase is essential for cellular resistance to cytotoxicity of tumor necrosis factor. Cell. 58**,** 923-31.

Wong, G. H., Goeddel, D. V., 1988. Induction of manganous superoxide dismutase by tumor necrosis factor: possible protective mechanism. Science. 242**,** 941-4.
Abraha, A., et al., 2000. C-terminal inhibition of tau assembly in vitro and in Alzheimer's disease. J Cell Sci. 113 Pt 21**,** 3737-45.
Aggarwal, B. B., 2003. Signalling pathways of the TNF superfamily: a double-edged sword. Nat Rev Immunol. 3**,** 745-56.
Alkam, T., et al., 2008. Restraining tumor necrosis factor-alpha by thalidomide prevents the amyloid beta-induced impairment of recognition memory in mice. Behav Brain Res. 189**,** 100-6.
Alonso, A., et al., 2001. Hyperphosphorylation induces self-assembly of tau into tangles of paired helical filaments/straight filaments. Proc Natl Acad Sci U S A. 98**,** 6923-8.
Alonso, A. C., et al., 1996. Alzheimer's disease hyperphosphorylated tau sequesters normal tau into tangles of filaments and disassembles microtubules. Nat Med. 2**,** 783-7.
Alonso, A. C., et al., 2008. Mechanism of tau-induced neurodegeneration in Alzheimer disease and related tauopathies. Curr Alzheimer Res. 5**,** 375-84.
Alonso, A. D., et al., 2010. Phosphorylation of tau at Thr212, Thr231, and Ser262 combined causes neurodegeneration. J Biol Chem. 285**,** 30851-60.
Andreadis, A., et al., 1992. Structure and novel exons of the human tau gene. Biochemistry. 31**,** 10626-33.
Balkwill, F., 2006. TNF-alpha in promotion and progression of cancer. Cancer Metastasis Rev. 25**,** 409-16.
Banner, D. W., et al., 1993. Crystal structure of the soluble human 55 kd TNF receptor-human TNF beta complex: implications for TNF receptor activation. Cell. 73**,** 431-45.
Baud, V., Karin, M., 2001. Signal transduction by tumor necrosis factor and its relatives. Trends Cell Biol. 11**,** 372-7.
Biernat, J., et al., 1993. Phosphorylation of Ser262 strongly reduces binding of tau to microtubules: distinction between PHF-like immunoreactivity and microtubule binding. Neuron. 11**,** 153-63.
Chan, F. K., et al., 2000. A domain in TNF receptors that mediates ligand-independent receptor assembly and signaling. Science. 288**,** 2351-4.
Cho, J. H., Johnson, G. V., 2003. Glycogen synthase kinase 3beta phosphorylates tau at both primed and unprimed sites. Differential impact on microtubule binding. J Biol Chem. 278**,** 187-93.
Cho, J. H., Johnson, G. V., 2004. Primed phosphorylation of tau at Thr231 by glycogen synthase kinase 3beta (GSK3beta) plays a critical role in regulating tau's ability to bind and stabilize microtubules. J Neurochem. 88**,** 349-58.
Cleveland, D. W., et al., 1977. Purification of tau, a microtubule-associated protein that induces assembly of microtubules from purified tubulin. J Mol Biol. 116**,** 207-25.
Crowther, T., et al., 1989. The repeat region of microtubule-associated protein tau forms part of the core of the paired helical filament of Alzheimer's disease. Ann Med. 21**,** 127-32.
de Calignon, A., et al., 2010. Caspase activation precedes and leads to tangles. Nature. 464**,** 1201-4.

De Felice, F. G., et al., 2008. Alzheimer's disease-type neuronal tau hyperphosphorylation induced by A beta oligomers. Neurobiol Aging. 29**,** 1334-47.
Ding, H., et al., 2006. Site-specific phosphorylation and caspase cleavage differentially impact tau-microtubule interactions and tau aggregation. J Biol Chem. 281**,** 19107-14.
Drechsel, D. N., et al., 1992. Modulation of the dynamic instability of tubulin assembly by the microtubule-associated protein tau. Mol Biol Cell. 3**,** 1141-54.
Fasulo, L., et al., 2000. The neuronal microtubule-associated protein tau is a substrate for caspase-3 and an effector of apoptosis. J Neurochem. 75**,** 624-33.
Fellous, A., et al., 1977. Microtubule assembly in vitro. Purification of assembly-promoting factors. Eur J Biochem. 78**,** 167-74.
Ferrari, A., et al., 2003. beta-Amyloid induces paired helical filament-like tau filaments in tissue culture. J Biol Chem. 278**,** 40162-8.
Goedert, M., et al., 1989. Multiple isoforms of human microtubule-associated protein tau: sequences and localization in neurofibrillary tangles of Alzheimer's disease. Neuron. 3**,** 519-26.
Gorlovoy, P., et al., 2009. Accumulation of tau induced in neurites by microglial proinflammatory mediators. FASEB J. 23**,** 2502-13.
Grundke-Iqbal, I., et al., 1986. Microtubule-associated protein tau. A component of Alzheimer paired helical filaments. J Biol Chem. 261**,** 6084-9.
Guillozet-Bongaarts, A. L., et al., 2006. Pseudophosphorylation of tau at serine 422 inhibits caspase cleavage: in vitro evidence and implications for tangle formation in vivo. J Neurochem. 97**,** 1005-14.
Guo, H., et al., 2004. Active caspase-6 and caspase-6-cleaved tau in neuropil threads, neuritic plaques, and neurofibrillary tangles of Alzheimer's disease. Am J Pathol. 165**,** 523-31.
Horowitz, P. M., et al., 2004. Early N-terminal changes and caspase-6 cleavage of tau in Alzheimer's disease. J Neurosci. 24**,** 7895-902.
Hsu, H., et al., 1996a. TNF-dependent recruitment of the protein kinase RIP to the TNF receptor-1 signaling complex. Immunity. 4**,** 387-96.
Hsu, H., et al., 1996b. TRADD-TRAF2 and TRADD-FADD interactions define two distinct TNF receptor 1 signal transduction pathways. Cell. 84**,** 299-308.
Hsu, H., et al., 1995. The TNF receptor 1-associated protein TRADD signals cell death and NF-kappa B activation. Cell. 81**,** 495-504.
Ikeda, H., et al., 2010. The estrogen receptor influences microtubule-associated protein tau (MAPT) expression and the selective estrogen receptor inhibitor fulvestrant downregulates MAPT and increases the sensitivity to taxane in breast cancer cells. Breast Cancer Res. 12**,** R43.
Jackman, R. W., et al., 2009. Microtubule-mediated NF-kappaB activation in the TNF-alpha signaling pathway. Exp Cell Res. 315**,** 3242-9.
Jenkins, E. C., Jr., et al., 2012. Intracellular pH regulation by Na(+)/H(+) exchanger-1 (NHE1) is required for growth factor-induced mammary branching morphogenesis. Dev Biol. 365**,** 71-81.

Jimeno, A., et al., 2007. Development of two novel benzoylphenylurea sulfur analogues and evidence that the microtubule-associated protein tau is predictive of their activity in pancreatic cancer. Mol Cancer Ther. 6**,** 1509-16.
Kar, S., et al., 2003. Repeat motifs of tau bind to the insides of microtubules in the absence of taxol. EMBO J. 22**,** 70-7.
Kondo, J., et al., 1988. The carboxyl third of tau is tightly bound to paired helical filaments. Neuron. 1**,** 827-34.
Lee, V. M., et al., 1991. A68: a major subunit of paired helical filaments and derivatized forms of normal Tau. Science. 251**,** 675-8.
Lee, V. M., et al., 2001. Neurodegenerative tauopathies. Annu Rev Neurosci. 24**,** 1121-59.
Locksley, R. M., et al., 2001. The TNF and TNF receptor superfamilies: integrating mammalian biology. Cell. 104**,** 487-501.
Matrone, M. A., et al., 2010. Metastatic breast tumors express increased tau, which promotes microtentacle formation and the reattachment of detached breast tumor cells. Oncogene. 29**,** 3217-27.
Matsumura, N., et al., 1999. Stable expression in Chinese hamster ovary cells of mutated tau genes causing frontotemporal dementia and parkinsonism linked to chromosome 17 (FTDP-17). Am J Pathol. 154**,** 1649-56.
Matsuo, E. S., et al., 1994. Biopsy-derived adult human brain tau is phosphorylated at many of the same sites as Alzheimer's disease paired helical filament tau. Neuron. 13**,** 989-1002.
McGrogan, B. T., et al., 2008. Taxanes, microtubules and chemoresistant breast cancer. Biochim Biophys Acta. 1785**,** 96-132.
Mimori, K., et al., 2006. Reduced tau expression in gastric cancer can identify candidates for successful Paclitaxel treatment. Br J Cancer. 94**,** 1894-7.
Morris, M., et al., 2011. The many faces of tau. Neuron. 70**,** 410-26.
Muller, U., et al., 1987. Tumour necrosis factor and lymphotoxin genes map close to H-2D in the mouse major histocompatibility complex. Nature. 325**,** 265-7.
Nukina, N., Ihara, Y., 1986. One of the antigenic determinants of paired helical filaments is related to tau protein. J Biochem. 99**,** 1541-4.
Paganelli, R., et al., 2002. Proinflammatory cytokines in sera of elderly patients with dementia: levels in vascular injury are higher than those of mild-moderate Alzheimer's disease patients. Exp Gerontol. 37**,** 257-63.
Perini, G., et al., 2002. Role of p75 neurotrophin receptor in the neurotoxicity by beta-amyloid peptides and synergistic effect of inflammatory cytokines. J Exp Med. 195**,** 907-18.
Rath, P. C., Aggarwal, B. B., 1999. TNF-induced signaling in apoptosis. J Clin Immunol. 19**,** 350-64.
Reynolds, C. H., et al., 1997. Reactivating kinase/p38 phosphorylates tau protein in vitro. J Neurochem. 69**,** 191-8.
Rissman, R. A., et al., 2004. Caspase-cleavage of tau is an early event in Alzheimer disease tangle pathology. J Clin Invest. 114**,** 121-30.
Rouzier, R., et al., 2005. Microtubule-associated protein tau: a marker of paclitaxel sensitivity in breast cancer. Proc Natl Acad Sci U S A. 102**,** 8315-20.

Santarella, R. A., et al., 2004. Surface-decoration of microtubules by human tau. J Mol Biol. 339**,** 539-53.
Senftleben, U., et al., 2001. IKKbeta is essential for protecting T cells from TNFalpha-induced apoptosis. Immunity. 14**,** 217-30.
Shi, J. Q., et al., 2011. Anti-TNF-alpha reduces amyloid plaques and tau phosphorylation and induces CD11c-positive dendritic-like cell in the APP/PS1 transgenic mouse brains. Brain Res. 1368**,** 239-47.
Shivanna, M., Srinivas, S. P., 2009. Microtubule stabilization opposes the (TNF-alpha)-induced loss in the barrier integrity of corneal endothelium. Exp Eye Res. 89**,** 950-9.
Smoter, M., et al., 2011. The role of Tau protein in resistance to paclitaxel. Cancer Chemother Pharmacol. 68**,** 553-7.
Souter, S., Lee, G., 2009. Microtubule-associated protein tau in human prostate cancer cells: isoforms, phosphorylation, and interactions. J Cell Biochem. 108**,** 555-64.
Steinhilb, M. L., et al., 2007. Tau phosphorylation sites work in concert to promote neurotoxicity in vivo. Mol Biol Cell. 18**,** 5060-8.
Stoothoff, W. H., Johnson, G. V., 2005. Tau phosphorylation: physiological and pathological consequences. Biochim Biophys Acta. 1739**,** 280-97.
Takeuchi, H., et al., 2006. Tumor necrosis factor-alpha induces neurotoxicity via glutamate release from hemichannels of activated microglia in an autocrine manner. J Biol Chem. 281**,** 21362-8.
Tanaka, S., et al., 2009. Tau expression and efficacy of paclitaxel treatment in metastatic breast cancer. Cancer Chemother Pharmacol. 64**,** 341-6.
Tartaglia, L. A., et al., 1993. A novel domain within the 55 kd TNF receptor signals cell death. Cell. 74**,** 845-53.
Tartaglia, L. A., Goeddel, D. V., 1992. Tumor necrosis factor receptor signaling. A dominant negative mutation suppresses the activation of the 55-kDa tumor necrosis factor receptor. J Biol Chem. 267**,** 4304-7.
Trojanowski, J. Q., et al., 1989. Distribution of tau proteins in the normal human central and peripheral nervous system. J Histochem Cytochem. 37**,** 209-15.
Vogelsberg-Ragaglia, V., et al., 2000. Distinct FTDP-17 missense mutations in tau produce tau aggregates and other pathological phenotypes in transfected CHO cells. Mol Biol Cell. 11**,** 4093-104.
Wagner, P., et al., 2005. Microtubule Associated Protein (MAP)-Tau: a novel mediator of paclitaxel sensitivity in vitro and in vivo. Cell Cycle. 4**,** 1149-52.
Yu, Y., et al., 2009. Developmental regulation of tau phosphorylation, tau kinases, and tau phosphatases. J Neurochem. 108**,** 1480-94.
Yvon, A. M., et al., 1999. Taxol suppresses dynamics of individual microtubules in living human tumor cells. Mol Biol Cell. 10**,** 947-59.
Zempel, H., et al., 2010. Abeta oligomers cause localized Ca(2+) elevation, missorting of endogenous Tau into dendrites, Tau phosphorylation, and destruction of microtubules and spines. J Neurosci. 30**,** 11938-50.
Zhang, Q., et al., 2009. Truncated tau at D421 is associated with neurodegeneration and tangle formation in the brain of Alzheimer transgenic models. Acta Neuropathol. 117**,** 687-97.

Alonso, A., et al., 2001. Hyperphosphorylation induces self-assembly of tau into tangles of paired helical filaments/straight filaments. Proc Natl Acad Sci U S A. 98**,** 6923-8.
Alonso, A. C., et al., 2008. Mechanism of tau-induced neurodegeneration in Alzheimer disease and related tauopathies. Curr Alzheimer Res. 5**,** 375-84.
Augustinack, J. C., et al., 2002. Specific tau phosphorylation sites correlate with severity of neuronal cytopathology in Alzheimer's disease. Acta Neuropathol. 103**,** 26-35.
Biernat, J., et al., 1992. The switch of tau protein to an Alzheimer-like state includes the phosphorylation of two serine-proline motifs upstream of the microtubule binding region. EMBO J. 11**,** 1593-7.
Brandt, R., et al., 1995. Interaction of tau with the neural plasma membrane mediated by tau's amino-terminal projection domain. J Cell Biol. 131**,** 1327-40.
Fischer, D., et al., 2009. Conformational changes specific for pseudophosphorylation at serine 262 selectively impair binding of tau to microtubules. Biochemistry. 48**,** 10047-55.
Gu, Y., et al., 1996. Tau is widely expressed in rat tissues. J Neurochem. 67**,** 1235-44.
Gustke, N., et al., 1994. Domains of tau protein and interactions with microtubules. Biochemistry. 33**,** 9511-22.
Hwang, S. C., et al., 1996. Activation of phospholipase C-gamma by the concerted action of tau proteins and arachidonic acid. J Biol Chem. 271**,** 18342-9.
Ittner, L. M., et al., 2010. Dendritic function of tau mediates amyloid-beta toxicity in Alzheimer's disease mouse models. Cell. 142**,** 387-97.
Jackman, R. W., et al., 2009. Microtubule-mediated NF-kappaB activation in the TNF-alpha signaling pathway. Exp Cell Res. 315**,** 3242-9.
Jenkins, S. M., Johnson, G. V., 1998. Tau complexes with phospholipase C-gamma in situ. Neuroreport. 9**,** 67-71.
Jho, Y. S., et al., 2010. Monte carlo simulations of tau proteins: effect of phosphorylation. Biophys J. 99**,** 2387-97.
Jimeno, A., et al., 2007. Development of two novel benzoylphenylurea sulfur analogues and evidence that the microtubule-associated protein tau is predictive of their activity in pancreatic cancer. Mol Cancer Ther. 6**,** 1509-16.
Kar, S., et al., 2003. Repeat motifs of tau bind to the insides of microtubules in the absence of taxol. EMBO J. 22**,** 70-7.
Lee, G., et al., 1998. Tau interacts with src-family non-receptor tyrosine kinases. J Cell Sci. 111 (Pt 21)**,** 3167-77.
Lee, V. M., et al., 2001. Neurodegenerative tauopathies. Annu Rev Neurosci. 24**,** 1121-59.
Leugers, C. J., Lee, G., 2010. Tau potentiates nerve growth factor-induced mitogen-activated protein kinase signaling and neurite initiation without a requirement for microtubule binding. J Biol Chem. 285**,** 19125-34.
Maas, T., et al., 2000. Interaction of tau with the neural membrane cortex is regulated by phosphorylation at sites that are modified in paired helical filaments. J Biol Chem. 275**,** 15733-40.
Mandelkow, E. M., et al., 1996. Structure, microtubule interactions, and phosphorylation of tau protein. Ann N Y Acad Sci. 777**,** 96-106.

Miao, Y., et al., 2010. Deletion of tau attenuates heat shock-induced injury in cultured cortical neurons. J Neurosci Res. 88**,** 102-10.
Mimori, K., et al., 2006. Reduced tau expression in gastric cancer can identify candidates for successful Paclitaxel treatment. Br J Cancer. 94**,** 1894-7.
Morris, M., et al., 2011. The many faces of tau. Neuron. 70**,** 410-26.
Perez, M., et al., 2009. Tau--an inhibitor of deacetylase HDAC6 function. J Neurochem. 109**,** 1756-66.
Pooler, A. M., Hanger, D. P., 2010. Functional implications of the association of tau with the plasma membrane. Biochem Soc Trans. 38**,** 1012-5.
Reynolds, C. H., et al., 2008. Phosphorylation regulates tau interactions with Src homology 3 domains of phosphatidylinositol 3-kinase, phospholipase Cgamma1, Grb2, and Src family kinases. J Biol Chem. 283**,** 18177-86.
Rouzier, R., et al., 2005. Microtubule-associated protein tau: a marker of paclitaxel sensitivity in breast cancer. Proc Natl Acad Sci U S A. 102**,** 8315-20.
Santarella, R. A., et al., 2004. Surface-decoration of microtubules by human tau. J Mol Biol. 339**,** 539-53.
Shivanna, M., Srinivas, S. P., 2009. Microtubule stabilization opposes the (TNF-alpha)-induced loss in the barrier integrity of corneal endothelium. Exp Eye Res. 89**,** 950-9.
Souter, S., Lee, G., 2009. Microtubule-associated protein tau in human prostate cancer cells: isoforms, phosphorylation, and interactions. J Cell Biochem. 108**,** 555-64.
Trojanowski, J. Q., et al., 1989. Distribution of tau proteins in the normal human central and peripheral nervous system. J Histochem Cytochem. 37**,** 209-15.
von Bergen, M., et al., 2005. Tau aggregation is driven by a transition from random coil to beta sheet structure. Biochim Biophys Acta. 1739**,** 158-66.
von Bergen, M., et al., 2001. Mutations of tau protein in frontotemporal dementia promote aggregation of paired helical filaments by enhancing local beta-structure. J Biol Chem. 276**,** 48165-74.
Zhu, J. H., et al., 2007. Regulation of autophagy by extracellular signal-regulated protein kinases during 1-methyl-4-phenylpyridinium-induced cell death. Am J Pathol. 170**,** 75-86.
Aggarwal, B. B., et al., 2012. Historical perspectives on tumor necrosis factor and its superfamily: 25 years later, a golden journey. Blood. 119**,** 651-65.
Banner, D. W., et al., 1993. Crystal structure of the soluble human 55 kd TNF receptor-human TNF beta complex: implications for TNF receptor activation. Cell. 73**,** 431-45.
Baud, V., Karin, M., 2001. Signal transduction by tumor necrosis factor and its relatives. Trends Cell Biol. 11**,** 372-7.
Boldin, M. P., et al., 1995. Self-association of the "death domains" of the p55 tumor necrosis factor (TNF) receptor and Fas/APO1 prompts signaling for TNF and Fas/APO1 effects. J Biol Chem. 270**,** 387-91.
Chan, F. K., 2007. Three is better than one: pre-ligand receptor assembly in the regulation of TNF receptor signaling. Cytokine. 37**,** 101-7.
Chan, F. K., et al., 2000a. A domain in TNF receptors that mediates ligand-independent receptor assembly and signaling. Science. 288**,** 2351-4.

Chan, F. K., Lenardo, M. J., 2000. A crucial role for p80 TNF-R2 in amplifying p60 TNF-R1 apoptosis signals in T lymphocytes. Eur J Immunol. 30**,** 652-60.
Chan, F. K., et al., 2003. A role for tumor necrosis factor receptor-2 and receptor-interacting protein in programmed necrosis and antiviral responses. J Biol Chem. 278**,** 51613-21.
Chan, F. K., et al., 2001. Fluorescence resonance energy transfer analysis of cell surface receptor interactions and signaling using spectral variants of the green fluorescent protein. Cytometry. 44**,** 361-8.
Chan, K. F., et al., 2000b. Signaling by the TNF receptor superfamily and T cell homeostasis. Immunity. 13**,** 419-22.
Chen, G., Goeddel, D. V., 2002. TNF-R1 signaling: a beautiful pathway. Science. 296**,** 1634-5.
Declercq, W., et al., 1998. Cooperation of both TNF receptors in inducing apoptosis: involvement of the TNF receptor-associated factor binding domain of the TNF receptor 75. J Immunol. 161**,** 390-9.
Haridas, V., et al., 1998. Overexpression of the p80 TNF receptor leads to TNF-dependent apoptosis, nuclear factor-kappa B activation, and c-Jun kinase activation. J Immunol. 160**,** 3152-62.
Heller, R. A., et al., 1992. The p70 tumor necrosis factor receptor mediates cytotoxicity. Cell. 70**,** 47-56.
Hsu, H., et al., 1996. TRADD-TRAF2 and TRADD-FADD interactions define two distinct TNF receptor 1 signal transduction pathways. Cell. 84**,** 299-308.
Hymowitz, S. G., et al., 1999. Triggering cell death: the crystal structure of Apo2L/TRAIL in a complex with death receptor 5. Mol Cell. 4**,** 563-71.
Leonard, W. J., 2001. Cytokines and immunodeficiency diseases. Nat Rev Immunol. 1**,** 200-8.
Locksley, R. M., et al., 2001. The TNF and TNF receptor superfamilies: integrating mammalian biology. Cell. 104**,** 487-501.
Mongkolsapaya, J., et al., 1999. Structure of the TRAIL-DR5 complex reveals mechanisms conferring specificity in apoptotic initiation. Nat Struct Biol. 6**,** 1048-53.
Naismith, J. H., et al., 1996a. Seeing double: crystal structures of the type I TNF receptor. J Mol Recognit. 9**,** 113-7.
Naismith, J. H., et al., 1995. Crystallographic evidence for dimerization of unliganded tumor necrosis factor receptor. J Biol Chem. 270**,** 13303-7.
Naismith, J. H., et al., 1996b. Structures of the extracellular domain of the type I tumor necrosis factor receptor. Structure. 4**,** 1251-62.
Ozcan, F., et al., 2006. On the nature of low- and high-affinity EGF receptors on living cells. Proc Natl Acad Sci U S A. 103**,** 5735-40.
Papoff, G., et al., 1999. Identification and characterization of a ligand-independent oligomerization domain in the extracellular region of the CD95 death receptor. J Biol Chem. 274**,** 38241-50.
Siegel, R. M., et al., 2000a. The multifaceted role of Fas signaling in immune cell homeostasis and autoimmunity. Nat Immunol. 1**,** 469-74.
Siegel, R. M., et al., 2000b. Fas preassociation required for apoptosis signaling and dominant inhibition by pathogenic mutations. Science. 288**,** 2354-7.

Vandevoorde V., and Fiers W., 1997. Induced expression of trimerized intracellular domains of the human tumor necrosis factor (TNF) p55 receptor elicits TNF effects. J Cell Biol.137(7), 1637-38.
Weiss, T., et al., 1998. TNFR80-dependent enhancement of TNFR60-induced cell death is mediated by TNFR-associated factor 2 and is specific for TNFR60. J Immunol. 161**,** 3136-42.
Alarid, E. T., et al., 1999. Proteasome-mediated proteolysis of estrogen receptor: a novel component in autologous down-regulation. Mol Endocrinol. 13**,** 1522-34.
Altucci, L., et al., 1996. 17beta-Estradiol induces cyclin D1 gene transcription, p36D1-p34cdk4 complex activation and p105Rb phosphorylation during mitogenic stimulation of G(1)-arrested human breast cancer cells. Oncogene. 12**,** 2315-24.
Andre, F., et al., 2007. Microtubule-associated protein-tau is a bifunctional predictor of endocrine sensitivity and chemotherapy resistance in estrogen receptor-positive breast cancer. Clin Cancer Res. 13**,** 2061-7.
Arnold, A., Papanikolaou, A., 2005. Cyclin D1 in breast cancer pathogenesis. J Clin Oncol. 23**,** 4215-24.
Bai, Z., Gust, R., 2009. Breast cancer, estrogen receptor and ligands. Arch Pharm (Weinheim). 342**,** 133-49.
Brady, R. M., et al., 1995. Presence of tau in isolated nuclei from human brain. Neurobiol Aging. 16**,** 479-86.
Buckley, M. F., et al., 1993. Expression and amplification of cyclin genes in human breast cancer. Oncogene. 8**,** 2127-33.
Callige, M., et al., 2005. CSN5/Jab1 is involved in ligand-dependent degradation of estrogen receptor {alpha} by the proteasome. Mol Cell Biol. 25**,** 4349-58.
Casimiro, M. C., et al., 2013. Cyclin D1 Determines Estrogen Signaling in the Mammary Gland in Vivo. Mol Endocrinol.
Coqueret, O., 2002. Linking cyclins to transcriptional control. Gene. 299**,** 35-55.
Cosman, F., Lindsay, R., 1999. Selective estrogen receptor modulators: clinical spectrum. Endocr Rev. 20**,** 418-34.
Edwards, D. P., 2005. Regulation of signal transduction pathways by estrogen and progesterone. Annu Rev Physiol. 67**,** 335-76.
Ferreira, A., Caceres, A., 1991. Estrogen-enhanced neurite growth: evidence for a selective induction of Tau and stable microtubules. J Neurosci. 11**,** 392-400.
Frasor, J., et al., 2004. Selective estrogen receptor modulators: discrimination of agonistic versus antagonistic activities by gene expression profiling in breast cancer cells. Cancer Res. 64**,** 1522-33.
Greenwood, J. A., Johnson, G. V., 1995. Localization and in situ phosphorylation state of nuclear tau. Exp Cell Res. 220**,** 332-7.
Ikeda, H., et al., 2010. The estrogen receptor influences microtubule-associated protein tau (MAPT) expression and the selective estrogen receptor inhibitor fulvestrant downregulates MAPT and increases the sensitivity to taxane in breast cancer cells. Breast Cancer Res. 12**,** R43.
Jensen, E. V., et al., 1969. Estrogen-binding substances of target tissues. Steroids. 13**,** 417-27.
Kocanova, S., et al., 2010. Ligands specify estrogen receptor alpha nuclear localization and degradation. BMC Cell Biol. 11**,** 98.

Locksley, R. M., et al., 2001. The TNF and TNF receptor superfamilies: integrating mammalian biology. Cell. 104**,** 487-501.
Maruvada, P., et al., 2003. Dynamic shuttling and intranuclear mobility of nuclear hormone receptors. J Biol Chem. 278**,** 12425-32.
Matsuno, A., et al., 1997. Modulation of protein kinases and microtubule-associated proteins and changes in ultrastructure in female rat pituitary cells: effects of estrogen and bromocriptine. J Histochem Cytochem. 45**,** 805-13.
McDonnell, D. P., Norris, J. D., 2002. Connections and regulation of the human estrogen receptor. Science. 296**,** 1642-4.
McMahon, C., et al., 1999. P/CAF associates with cyclin D1 and potentiates its activation of the estrogen receptor. Proc Natl Acad Sci U S A. 96**,** 5382-7.
Monje, P., et al., 2001. Differential cellular localization of estrogen receptor alpha in uterine and mammary cells. Mol Cell Endocrinol. 181**,** 117-29.
Musgrove, E. A., et al., 1993. Growth factor, steroid, and steroid antagonist regulation of cyclin gene expression associated with changes in T-47D human breast cancer cell cycle progression. Mol Cell Biol. 13**,** 3577-87.
Nawaz, Z., et al., 1999. Proteasome-dependent degradation of the human estrogen receptor. Proc Natl Acad Sci U S A. 96**,** 1858-62.
Neuman, E., et al., 1997. Cyclin D1 stimulation of estrogen receptor transcriptional activity independent of cdk4. Mol Cell Biol. 17**,** 5338-47.
Pentheroudakis, G., et al., 2009. Gene expression of estrogen receptor, progesterone receptor and microtubule-associated protein Tau in high-risk early breast cancer: a quest for molecular predictors of treatment benefit in the context of a Hellenic Cooperative Oncology Group trial. Breast Cancer Res Treat. 116**,** 131-43.
Pratt, W. B., Toft, D. O., 1997. Steroid receptor interactions with heat shock protein and immunophilin chaperones. Endocr Rev. 18**,** 306-60.
Sherr, C. J., 1996. Cancer cell cycles. Science. 274**,** 1672-7.
Sicinski, P., et al., 1995. Cyclin D1 provides a link between development and oncogenesis in the retina and breast. Cell. 82**,** 621-30.
Song, R. X., et al., 2004. The role of Shc and insulin-like growth factor 1 receptor in mediating the translocation of estrogen receptor alpha to the plasma membrane. Proc Natl Acad Sci U S A. 101**,** 2076-81.
Sultan, A., et al., 2011. Nuclear tau, a key player in neuronal DNA protection. J Biol Chem. 286**,** 4566-75.
Wang, T. C., et al., 1994. Mammary hyperplasia and carcinoma in MMTV-cyclin D1 transgenic mice. Nature. 369**,** 669-71.
White, R., Parker, M. G., 1998. Molecular mechanisms of steroid harmone. Endocr Relat Cancer. 5**,** 1-14.
Yager, J. D., 2000. Endogenous estrogens as carcinogens through metabolic activation. J Natl Cancer Inst Monogr. 67-73.
Zwijsen, R. M., et al., 1998. Ligand-independent recruitment of steroid receptor coactivators to estrogen receptor by cyclin D1. Genes Dev. 12**,** 3488-98.
Zwijsen, R. M., et al., 1997. CDK-independent activation of estrogen receptor by cyclin D1. Cell. 88**,** 405-15.